

**The Biological Functions of miR-122 and its Therapeutic Application in
Liver Cancer**

DISSERTATION

**Presented in Partial Fulfillment of the Requirements for the Degree
Doctor of Philosophy in the Graduate School of The Ohio State
University**

By

Shu-hao Hsu

Graduate Program in Molecular, Cellular and Developmental Biology

The Ohio State University

2012

Dissertation Committee:

Dr. Samson T. Jacob, Advisor

Dr. Kalpana Ghoshal

Dr. Thomas D. Schmittgen

Dr. Robert J. Lee

Dr. David Symer

**Copyright by
Shu-hao Hsu
2012**

Abstract

miR-122, the most abundant liver-specific microRNA (miRNA), is involved in many different biological functions, including cholesterol metabolism, hepatitis C virus replication, and hepatocarcinogenesis. Previous studies have shown that downregulation of miR-122 in hepatocellular carcinoma (HCC) correlates with metastasis and poor prognosis. Deregulated expression of miRNAs in liver resulting from the loss of Dicer1, a critical enzyme involved in miRNA processing, induced spontaneous HCC development. Among the deregulated miRNAs in HCC, miR-122 is drastically reduced in HCC. Based on these observations, our hypothesis is that miR-122 is a liver-specific tumor suppressor and its loss may promote hepatocarcinogenesis.

To test this hypothesis, we generated germ-line (KO) and liver-specific (LKO) miR-122 knockout mice. Both KO and LKO mice exhibited hepatic microsteatosis and hepatic inflammation at early adult stage. Serum analysis showed significantly reduced cholesterol and elevated alkaline phosphatase level. Further, lipid analysis showed accumulated hepatic triglyceride, which correlated with increased *de novo* triglyceride synthesis and reduced triglyceride secretion. These pathological phenotypes became more pronounced with age. By 6 month both KO and LKO mice develop hepatic

steatosis, inflammation, and fibrosis. After twelve months, these mice produce spontaneous liver tumors resembling HCC. The HCC incidences were ~30% and ~50% in LKO and KO mice, respectively. Microarray and realtime RT-PCR analysis attributed these pathological phenotypes to dysregulated expression of signaling pathways involved in triglyceride synthesis, cytokine expression, and oncogenesis. Among the deregulated genes, *Agpat1*, *Cidec* and *Mapre1* were identified for the first time as the direct targets of miR-122. Exploration of the mechanism leading to hepatic inflammation in KO and LKO mice led to the identification of CD11b^{high}Gr-1⁺ subtype of inflammatory cells increased in the liver of KO mice. These cells were determined as the major source of high levels of IL-6 and TNF- α that accumulated in the livers of KO and LKO mice. Ccl2, a reported myeloid chemo-attractant, was induced in hepatocytes of KO and LKO mice and was inversely regulated by miR-122 *in vitro*. Taken together, these results further support tumor suppressor and anti-inflammatory role of miR-122.

To establish further the tumor suppressor role of miR-122, we tested the feasibility of the therapeutic delivery of miR-122 to the liver and tumor cells by lipid-based nanoparticles, which is recognized as a safe delivery method due to its biocompatibility. We developed a novel LNP, designated LNP-DP1, consisting of a conditionally ionizable cationic lipid, 2-dioleoyloxy-N,N-dimethyl-3-aminopropane (DODMA), egg PC, cholesterol (Chol) and Chol-polyethylene glycol (Chol-PEG). Ectopic expression of miR-122 in HCC

cell lines by LNP-DP1 reduced expression of miR-122 targets, such as Adam10, by >95%. The biodistribution analysis revealed that hepatocytes and tumor epithelial cells preferentially took up systemic circulated LNP-DP1 conjugated fluorescence labeled siRNA. Serum profile of treated mice showed that LNP-DP1 did not induce significant liver or kidney damage in mice. Realtime RT-PCR and western blot analysis demonstrated downregulation of several target genes of miR-122 after systemic delivery of LNP-DP1 conjugated miR-122. This result suggested that miR-122 was successfully released from LNP-DP1 and was functional in hepatocytes and tumor cells. Furthermore, intratumoral injection of LNP-DP1 conjugated miR-122 into HCC xenograft developed in *nude* mice resulted in suppression of tumor growth within 30 days of miR-122 delivery, which correlated well with reduced expression of its target genes such as Adam10 and proliferation markers such as Ki67.

In conclusion, these findings revealed critical functions for miR-122 in liver metabolism, hepatic immune response, and in hepatocarcinogenesis. This study underscores the necessity to monitor HCV patients receiving long-term miR-122 inhibition therapy are likely to have increased risk of developing HCC. The application of miR-122 delivery by LNP-DP1 in animal HCC model suggested potential utility of miR-122 therapy for selected HCC patients negative for HCV.

Dedication

Dedicated to my parents, my wife, my son
and all patients suffering from liver cancer

Acknowledgements

I would like to sincerely thank my advisor, Dr. Samson T. Jacob for his mentoring during my graduate study. Dr. Jacob has given me invaluable advice to guide me through the difficulties in pursuing miR-122 project. Dr. Jacob always discussed with me about the ongoing direction of my study and encouraged me to conduct research independently. These six years of training in lab strengthens my confidence and knowledge toward my research life in the future.

I would like to show my gratitude to Dr. Kalpana Ghoshal, my co-advisor. Dr. Ghoshal not only helped me to conduct research in a very organized and efficient way but also showed me that courage and perseverance were the keys to be a good scientist. Without her invaluable insight and constant support, it will be impossible for me to publish the paper on miR-122 knockout mice.

I am indebted to all my colleagues for their help on my research and friendship in my life. I owe my sincere thank to Dr. Huban Kutay for her tremendous help on my graduate study. Also, it is a precious experience working and being friend with my classmate Bo Wang, who always encouraged me during the difficult time of my research. I am also very grateful for the productive collaboration and helpful insights from Drs. Bo Yu

and Xinmei Wang, especially for the development of nanoparticles. I would like to sincerely thank Dr. Yuanzhi Lu for being a good friend and his important guidance on my animal techniques. I would also like to thank Drs. Sarmila Majumder, Tasneem Motiwala and Jharna Datta for invaluable discussion and generous help in my research.

This project would not be possible without all the collaborators: Dr. L. James Lee and Dr. Robert J. Lee, who helped me to conduct the nanoparticle project. Dr. Jianhua Yu, who helped to analyze the inflammation phenotypes in our knockout model. Dr. Gerard Nuovo, who helped with the pathological analysis and immunohistochemistry; Dr. Stefan Costinean, who helped with pathological analysis.

I am deeply grateful to all my committee members, Drs. Thomas D. Schmittgen and Robert J. Lee for their exceptional guidance, critiques and timely help.

Lastly, I would like to sincerely thank my parents, wife, and son. It will be impossible to achieve this without their sacrifice and understanding.

Vita

- 2001 Bachelor of Science, Zoology,
National Taiwan University
- 2003 Master of Science, Anatomy and Cell
Biology, National Taiwan University
- 2006 to present Graduate Research Associate,
Molecular, Cellular and
Developmental Biology, The Ohio
State University

Publications

Hsu SH, Wang B, Kota J, Yu J, Costinean S, Kutay H, Yu L, Bai S, La Perle K, Chivukula RR, Mao H, Wei M, Clark KR, Mendell JR, Caligiuri MA, Jacob ST, Mendell JT, and Ghoshal K. Essential metabolic, anti-inflammatory and anti-tumorigenic functions for miR-122 in mouse liver.

Wang B, **Hsu S**, Frankel W, Ghoshal K, Jacob ST. Stat3-mediated activation of miR-23a suppresses gluconeogenesis in hepatocellular carcinoma by downregulating G6PC and PGC-1 α . *Hepatology*. 2012. (In press)

Tsuei DJ, Lee PH, Peng HY, Lu SL, Su DS, Jeng YM, Hsu HC, **Hsu SH**, Wu JF, Ni YH, Chang MH. Male germ cell-specific RNA binding protein RBMY: a new oncogene explaining male predominance in liver cancer. *PLoS One*. 2011; 6(11)

Wang B, **Hsu SH**, Majumder S, Kutay H, Huang W, Jacob ST, Ghoshal K. TGFbeta-mediated upregulation of hepatic miR-181b promotes hepatocarcinogenesis by targeting TIMP3. *Oncogene*. 2010; 29(12):1787-97.

Bai S, Nasser MW, Wang B, **Hsu SH**, Datta J, Kutay H, Yadav A, Nuovo G, Kumar P, Ghoshal K. MicroRNA-122 inhibits tumorigenic properties of hepatocellular carcinoma cells and sensitizes these cells to sorafenib. *J Biol Chem*. 2009; 284 (46):32015-27.

Hsu SH, Lee MJ, Hsieh SC, Scaravilli F, Hsieh ST. Cutaneous and sympathetic denervation in neonatal rats with a mutation in the delta subunit of the cytosolic chaperonin-containing t-complex peptide-1 gene. *Neurobiol Dis*. 2004 Jul;16(2): 335-45.

Fields of Study

Major Field: Molecular, Cellular and Developmental Biology

Table of Contents

Abstract	ii
Dedication	v
Acknowledgements	vi
Vita	viii
List of Tables	xv
List of Figures	xvii
Chapter 1. Introduction	1
1.1 Hepatocellular carcinoma (HCC)	1
1.2 Epidemiology and risk factors of HCC	2
1.3 Pathological grading of HCC.....	4
1.4 Options and potential challenges of HCC treatment.....	6
1.5 Involvement of miRNAs in hepatocarcinogenesis.....	7
1.5.1 Mechanism of miRNAs biogenesis.....	8
1.5.2 Mechanism of miRNAs silencing gene expression	9
1.5.3 The involvement of miRNAs in cancer	11
1.5.4 The deregulated miRNAs in HCC	13
1.6 Therapeutic research for HCC	15
1.6.1 Mouse models of HCC	16

1.6.2	miRNA based gene therapy for HCC	19
Chapter 2. The loss of miR-122 induces steatohepatitis and spontaneous HCC		
	in miR-122 knockout mice	28
2.1	Abstract.....	28
2.2	Introduction	29
2.3	Materials and Methods	31
2.3.1	Generation of liver specific (LKO) and germline miR-122 knockout (KO) mice	31
2.3.2	Serological, histological and immunohistochemical analysis	31
2.3.3	Transmission Electron Microscopy.....	32
2.3.4	Measurement of hepatic triglyceride synthesis	33
2.3.5	Hepatic triglyceride secretion	33
2.3.6	Microarray analysis of liver RNA	33
2.3.7	Real-time RT-PCR analysis	34
2.3.8	Western blot analysis	34
2.3.9	Microarray analysis of the tumor RNA.....	34
2.3.10	Flow cytometric analysis	35
2.3.11	Generation of liver specific (LKO) and germline miR-122 knockout (KO) mice.	35
2.3.12	Measurement of hepatic triglyceride synthesis.	36
2.3.13	Determination of Triglyceride synthesis in primary mouse	

hepatocytes transfected with siRNA.....	36
2.3.14 Microarray analysis.	37
2.3.15 Microarray analysis of the tumor RNA.....	38
2.3.16 Ingenuity Pathway Analysis.....	39
2.3.17 Plasmid construction	39
2.3.18 Accession numbers	39
2.4 Results	40
2.4.1 Liver specific (LKO) and germ-line (KO) miR-122 loss-of-function results in an altered serum lipid profile	40
2.4.2 LKO mice develop hepatic microsteatosis due to triglyceride accumulation in early adult life	41
2.4.3 Genes involved in lipid metabolism and cellular proliferation and survival are abnormally expressed in livers of LKO mice	42
2.4.4 Recruitment of monocytes and neutrophils to livers of miR-122 LKO/KO mice leads to inflammation and production of pro- tumorigenic cytokines	46
2.4.5 LKO and KO mice develop HCC with age.....	48
2.5 Discussion.....	48
Chapter 3. Liposomal delivery of miR-122 to HCC cell lines and DEN induced HCC animal model.....	92
3.1 Abstract.....	92

3.2 Introduction	93
3.3 Materials and Methods	96
3.3.1 Materials	96
3.3.2 Preparation of miRNA encapsulated LNPs	97
3.3.3 Liver tumor models	98
3.3.4 Antitumor activity of miR-122 encapsulated LNP-DP1 in xenograft model.....	98
3.3.5 Cell culture and transfection study	99
3.3.6 <i>In vivo</i> biodistribution study of LNP-DP1	100
3.3.7 Biological evaluation of LNP-DP1 mediated delivery of miR-122 in miR-122KO model.....	101
3.3.8 Statistical analysis.....	99
3.4 Results	102
3.4.1 Optimization of PEG-lipids for LNPs mediated delivery of miR-122 to HCC cell lines	102
3.4.2 <i>In vivo</i> liver targeting delivery mediated by LNP-DP1	104
3.4.3 Efficacy evaluation of LNP-DP1 mediated delivery to liver tumors	105
3.4.4 LNP-DP1 mediated delivery of miR-122 specifically downregulates miR-122 target genes in liver and tumor tissues	106
3.4.5 Intratumoral delivery of miR-122 containing LNP-DP1 suppresses the growth of HCC xenografts in nude mice.....	108
3.5 Discussion	109

Chapter 4. Conclusion and future development.....	124
Bibliography.....	128

List of Tables

Table 1.1 Deregulated miRNAs identified in HCC.....	27
Table 2.1 Serum profiles of 8-10 week old control and miR-122 LKO mice.	82
Table 2.2 Serum profiles of 5 week old control and miR-122 KO mice	83
Table 2.3 Networks identified by Ingenuity Pathway Analysis among dysregulated genes in livers of miR-122 LKO mice.....	84
Table 2.4. Genes involved in lipid metabolism that are dysregulated in the livers of miR-122 LKO mice.....	85
Table 2.5 Genes related to hepatocarcinogenesis are significantly upregulated in miR-122 LKO livers.....	86
Table 2.6 Genes related to hepatocarcinogenesis are significantly upregulated in miR-122 LKO livers.....	87
Table 2.7 Serum profiles of 6 month old control and miR-122 KO mice.....	88
Table 2.8 Summary of the incidence and characteristics of the tumors that developed in 12-17 month-old LKO mice.....	89
Table 2.9 Summary of the incidence and characteristics of the tumors that developed in 10-15 month old KO mice.....	90
Table 2.10 Summary of the incidence and characteristics of HCC developed in 10-15 month old KO male and female mice.....	91

List of Figures

Figure 1.1 Summary of HCC incidence (red bar) and mortality (blue bar) in males and females worldwide.....	22
Figure 1.2 H&E staining of normal mouse liver sections.....	23
Figure 1.3 H&E staining of tumor sections at different HCC stages.....	24
Figure 1.4 Biogenesis of microRNA in cells.....	25
Figure 1.5 Two models of miRNA mediated translation repression.....	26
Figure 2.1 Generation of conditional and germ-line miR-122 knockout mice.....	54
Figure 2.2 Northern blot analysis of miRNA levels in liver of LKO and KO.....	56
Figure 2.3 Expression of miR-122 target genes in LKO	57
Figure 2.4 Liver morphology, lipid accumulation and glycogen depletion of LKO	59
Figure 2.5 Electronic microscopy (EM) and immunohistochemical analysis of LKO mice.....	60
Figure 2.6 Dysregulated metabolism of triglyceride (TG) and cholesterol in LKO.....	61
Figure 2.7 Sylamer analysis of mRNA expression from miR-122 LKO.....	62
Figure 2.8 RNA and protein expression of genes involved in triglyceride synthesis and storage in LKO livers.....	63

Figure 2.9 miR-122 negatively regulates the expression of genes involved in triglyceride biosynthesis.....	64
Figure 2.10 Agpat1 and Mapre1 are the direct targets of miR-122.....	66
Figure 2.11 TG synthesis was mainly affected by Agpat1 in hepatocytes.....	67
Figure 2.12 The IPA network of Igf2 signaling and downstream effectors.....	68
Figure 2.13 Expression of genes involved in development, cellular proliferation and death, and cancer.....	69
Figure 2.14 Igf2 and H19 are transcriptionally upregulated in miR-122 LKO livers.....	70
Figure 2.15 miR-122 LKO livers do not undergo repopulation with non-recombined miR-122-expressing hepatocytes.....	71
Figure 2.16 miR-122 LKO mice develop hepatitis and fibrosis with age.....	72
Figure 2.17 miR-122 KO mice develop hepatitis and fibrosis with age.....	73
Figure 2.18 miR-122 LKO and KO mice develop hepatitis and fibrosis with age.....	74
Figure 2.19. Infiltration of IL-6-producing CD11b ^{high} Gr1 ⁺ cells in livers of LKO/KO mice.....	75
Figure 2.20 Cytometric analysis of cell types expressing IL6, TNF- α , and CCR2.....	76
Figure 2.21 Loss of miR-122 correlated with Ccl2 expression in primary hepatocytes.....	78
Figure 2.22 Ccl2 is a direct target gene of miR-122.....	79

Figure 2.23 miR-122 LKO mice develop spontaneous HCC with age.....	80
Figure 3.1 LNPs mediated delivery of miRNA122 to HCC cell lines <i>in vitro</i>	113
Figure 3.2 LNP-DP1 mediated delivery of miR-122 to HCC cell line <i>in vitro</i>	115
Figure 3.3 <i>In vivo</i> liver targeting delivery mediated by LNP-DP1.....	116
Figure 3.4 <i>In vivo</i> toxicity analysis of the systemic delivery of LNP-DP1 carrying miR-122.....	117
Figure 3.5 <i>In vivo</i> biodistribution of LNP-DP1 mediated delivery in three liver tumor models.....	118
Figure 3.6 <i>In vivo</i> biodistribution of LNP-DP1 mediated delivery in xenograft and Hep3B orthotopic liver tumor models.....	119
Figure 3.7 LNP-DP1 mediated delivery of miR-122 specifically downregulates target genes in liver and tumor tissues.....	121
Figure 3.8 Intratumoral delivery of miR-122 in LNP-DP1 suppresses the growth of liver tumor xenografts in nude mice.....	122
Figure 3.9 Intratumoral delivery of miR-122 in LNP-DP1 suppresses the growth of liver tumor xenografts in nude mice.....	123

Chapter 1. Introduction

1.1 Hepatocellular carcinoma (HCC)

Hepatocellular carcinoma is the sixth most common malignant cancers and causes 0.69 million deaths each year worldwide according to the GLOBOCAN (2008) and Cancer Incidence in Five Continents databases [1]. In United States, despite the improved survival rate of patients with most malignancies, 5-year survival of patients with HCC has remained less than 10%. The poor outcome of patients with HCC is mainly due to the late stage detection with over two-thirds of patients diagnosed at advanced stages [2], when patients are symptomatic and exhibit different degrees of liver malfunction. For the patients diagnosed at an early stage, there are the options of curable treatments that includes resection, liver transplantation, or percutaneous treatment. However, these treatments can only be applied to 30% of patients under restricted condition [3]. Therefore, to increase the treatment options for patients that are not qualified for existing criteria for surgical removal, it is necessary to develop novel therapeutic strategies for HCC treatment.

1.2 Epidemiology and risk factors of HCC

The incidence of hepatocellular carcinoma varies a lot among different regions worldwide. The incidence and mortality rate of HCC is very high in developing countries, especially those of Southeast Asia and sub-Saharan Africa, whereas it is much lower in developed countries, such as Europe, Japan and North America (**Figure 1.1**). Overall, 80% of HCC cases were diagnosed in developing countries and the rest of 20% were found in the developed countries [1].

The risk factors of HCC vary with different regions. In high-incidence region such as Taiwan, China and sub-Saharan Africa, the major risk factor of HCC is hepatitis B virus (HBV) infection. Cirrhosis developing from chronic HBV infection accounts for 70% to 90% of HBV-related HCC [4]. Since high rate of mother-to-infant transmission (vertical transmission) of HBV is the major cause of chronic HBV infection, the worldwide immunization of infants has been reported to be the most effective method to reduce chronic HBV carrier rates and HCC in population [5-8]. Other than cirrhosis, HBV also induces HCC through the integration of HBV DNA to the genome of hepatocytes. Numerous sites of HBV integration have been reported to closely associate with carcinogenesis [9-12]. Furthermore, it has been shown that HCC patients expressed abundant RNA and protein of Hepatitis B virus X (HBx) in the absence of HBV replication [13, 14]. Many studies based on HBx transgenic mice have shown that HBx overexpression promoted c-myc [15] or carcinogen [16] induced

hepatocarcinogenesis. The oncogenic mechanisms of HBx may be through transactivation of many signaling pathway such involved in hepatocarcinogenesis (see review [17])

In developed countries, such as West and Japan, Hepatitis C virus (HCV) infection is the major cause of HCC. About 50-70% of HCC cases in Europe and North America are associated with HCV infection [18]. The incidence of HCC in HCV infected patients is highly dependent on the degree of hepatic fibrosis. A large cohort study conducted in Japan for 2890 HCV infected patients has shown that patients with severe grade of hepatic fibrosis has higher HCC incidence (~8 fold) than patients with low-grade hepatic fibrosis [18]. Unlike HBV infection, there is no vaccination available to prevent HCV infection [19].

Other major risk factors are Aflatoxin and alcohol. Aflatoxin can be metabolized by specific cytochrome P450 enzymes in liver to form reactive oxygen species (aflatoxin-8, 9-epoxide), which may bind to DNA and cause mutation leading to HCC development [20]. Alcoholism is a serious problem in America and Europe, and it is increasing in Asia. Although alcohol is not a liver carcinogen in murine model [21, 22], alcohol-induced cirrhosis was reported to be major cause of HCC in some region [23, 24], but the detail mechanism is still controversial. The possible mechanisms reported so far include loss of heterozygosity of tumor suppressor genes [25], alcohol derived carcinogenic acetaldehyde [26, 27], and DNA methylation [28, 29].

1.3 Pathological grading of HCC

Due to the rapid enhancement of detection technique, more HCC patients can be diagnosed at early HCC stage. Therefore, characteristic of HCC prognosis from increasing cases at early stage of HCC was documented and reported in a better way. Four key factors are needed to determine the prognosis of patients with HCC [30]: (1) tumor stage at diagnosis; (2) overall health of the patient; (3) hepatic synthetic function; and (4) efficacy of treatment. These standards are particularly useful to define the HCC stage of patients and help to decide the applicable treatment at different stages. From the research point, biopsy of HCC are examined and classified into four grades. Grade I has the mildest level of malignancy whereas grade IV has the severest level. The following are the pathological features used to determine tumor stages according to Edmondson-Steiner's grading system [31]:

- **Normal liver:** Normal liver is composed of hepatocytes arranged in single-cell thick plates separated by vascular sinusoids. From the sectioned tissue, the liver is composed of lobules, which are a hexagonal structure. The center of each lobule is central vein and the single-cell hepatocytes plates radiate from central vein to the perimeter of the lobule. Portal tracts surrounding the lobules are mainly composed of portal veins, bile ducts, and hepatic arteries. Functionally, the blood enters liver from portal veins and hepatic arteries to portal tracts and then flows into vascular sinusoid and finally drains into

central vein, which connect to inferior vena cava (**Figure 1.2 and 1.3A**).

- **Grade I HCC** (well differentiated HCC): the tumor consists of uniformly distributed well-differentiated cancerous tissue showing an irregular thin trabecular pattern without capsule outlining the nodule. Also, portal tracts can be seen in the lesion. Further, the tumor at this grade shows markedly increased cell density (**Figure 1.3B**).
- **Grade II HCC** (moderately differentiated HCC): The tumor cells have abundant eosinophilic cytoplasm with round nuclei and distinct nucleoli. The nucleus to cytoplasm ratio is almost equal to that of a normal hepatocyte. The tumor tissue shows a trabecular pattern consisting of several to tens of layers of cancer cells (**Figure 1.3C**).
- **Grade III HCC** (poorly differentiated HCC): The tumor cells have markedly less cytoplasm with a high nucleus to cytoplasm ratio (**Figure 1.3D**). At this stage, HCC is subdivided into solid type and giant-cell type. Solid type HCC lacks sinusoid-like blood spaces Giant-cell type HCC presents pleomorphism and indistinct trabecular pattern.
- **Grade IV HCC** (undifferentiated or anaplastic HCC): The tumor cells also exhibit less cytoplasm with oval and/or round nuclei. However, due to the lack of specific type of cells or structure at this stage for identification, it is hard to identify Grade IV HCC with the biopsy without surrounding tissues of cirrhosis.

1.4 Options and potential challenges of HCC treatment

Generally, there are many potential options for the HCC patients that are diagnosed at the early stage of HCC. These treatment options include resection, liver transplantation, percutaneous treatment, and transarterial embolization.

- **Percutaneous treatment:** it is usually used as a first-line treatment on early HCC patients. A typical percutaneous treatment is percutaneous ethanol administration, which has advantages of low cost, low technical requirement, and less complication after treatment. For HCC smaller than 3 cm, the percutaneous ethanol injection can suppress the tumor growth with 70%~100% of successful rate [32].
- **Resection:** For HCC patients at advanced stage, surgical resection is considered as the most efficient way to remove tumors. However, strict criteria of selection are applied before the surgery. For example, portal hypertension is considered as a important indicator of patients not suitable for liver resection. Statistically, seventy-four percent 5 years survival rate post-surgery in patients without clinically relevant portal hypertension, whereas there is only 25% of survival rate for patients with portal hypertension [33, 34]. Furthermore, postoperative tumor recurrence occurred in 70% of patients in 5 years [35].
- **Liver transplantation:** HCC patients with cirrhosis and small HCC (maximal diameter < 5cm and < 3 nodules) are usually suggested to receive liver transplantation. The 5-year survival rate reaches about

70% for patients with or without cirrhosis [36, 37]. However, the shortage of liver donation becomes the major obstacle of transplantation [36]. Therefore, under careful selection criteria, liver resection is still considered as first-line treatment for patients who are too critical to wait for transplantation [36].

- **Transarterial embolization (TAE):** TAE is a very common HCC treatment, which is applied to patients with asymptomatic multinodular HCC without curative options according to Barcelona-Clinic Liver Cancer Group staging classification and treatment schedule [38]. The main effect of TAE is to block the hepatic arterial supply of tumor that leads to tumor apoptosis by tumor cells. Many reports have pointed out the improved survival rate of the combination of TAE and percutaneous ethanol ablation [39] or chemotherapy [40], such as Doxorubicin. However, TAE was shown to induce hypoxic tumor microenvironment, which further enhances angiogenesis and stimulates recurrence of HCC [41].

1.5 Involvement of miRNAs in hepatocarcinogenesis

In the past decade, the discovery of miRNAs and its biological function opened up a new page for the gene regulation distinct from transcriptional control. The involvement of miRNAs in cellular functions and cancers will be discussed in the following paragraphs:

1.5.1 Mechanism of miRNAs biogenesis

miRNAs are short noncoding RNAs consisting of about 22 nucleotides that negatively regulate expression of coding genes. The biogenesis of miRNAs were initially determined based on the studies on miRNA-23a~27a~24-2, a 2.2-kb transcript containing three miRNAs [42]. This gene is predominantly transcribed into primary miRNAs (pri-miRNA) by polymerase II (pol II), which starts transcription by binding to a pol II dependent promoter (~600 bp). However, this promoter lacks all typical promoter elements. In fact, identification of the microRNA promoter is still a challenging task [42-44]. Most known miRNAs were found to overlap with fixed transcription units. Some miRNAs in this subset were located within introns of protein-coding genes, while some were found in both introns and exons of 66 mRNA-like noncoding RNAs (miIncRNAs) [45]. Therefore, the majority of miRNAs may be transcribed together with associated mRNAs and processed into pri-miRNA afterward in nucleus.

Figure 1.4 summarizes the processing of miRNA. The pri-miRNA is sequentially processed by microprocessor complex, which is comprised of Drosha, a RNase III ribonucleases, and DGCR8, a cofactor of Drosha [46, 47]. Pri-miRNAs has a specific hairpin-shaped secondary structure that is recognized and asymmetrically cleaved by Drosha to form a 60-70 nucleotide miRNA precursor (pre-miRNA). The pre-miRNA was then transported from nucleus to cytoplasm by the mediation of exportin-5 (Exp-5) in a Ran guanosine triphosphate-dependent manner [48]. Exp-5 mediated export is an

important step to ensure the sequence accuracy since the knockdown of Exp-5 by RNAi greatly affects the yields of mature miRNA and Exp-5 interacts weakly with incorrectly processed pre-miRNAs.

In cytoplasm, Dicer, also a RNase III endonuclease, interacts with TRBP (Tar RNA binding protein) to mediate further processing of pre-miRNA to a ~22 nucleotide long mature miRNA [49]. Pre-miRNA is dimerized with Dicer by binding to the two domains of Dicer, PAZ and dsRBD (double-stranded RNA binding domain) [50]. After cleavage by Dicer, a ~22 nucleotide miRNA duplex is produced and usually one strand of this duplex will be degraded. Mature miRNA harbors a 5' phosphate and a 2-nucleotide 3' overhang and is later incorporated into effector complexes known as miRISC (miRNA-containing RNA-induced silencing complex), the effector of RNA interference system (RNAi). miRISC contains a key component protein, which is Argonaute 2 (Ago2). The Argonaute protein family has a characteristic PAZ domain, which is critical in miRNA binding to miRISC, and a PIWI domain, which resembles the function of RNase H endonuclease to catalyze the cleavage of mRNA [51].

1.5.2 Mechanism of miRNAs silencing gene expression

Generally, miRNAs regulate gene expression in animal cells through two mechanisms: (1) reducing translation of target mRNAs, and (2) targeting mRNAs for increased decay through endonuclease and exonuclease cleavage.

- **Reducing translation of target mRNAs:**

In 1993, Lee et al. found that lin-4 miRNA reduced the expression of lin-14 protein without reducing the amount of lin-14 mRNA [52, 53]. This interesting observation suggests that miRNA may regulate target expression by suppressing translation. For the mechanism, many studies showed that miRNA/RISC complex decrease the rate of translation initiation to inhibit translation. This conclusion was drawn by many observations. First, AGOs, miRNAs, and the matching target genes accumulate in P-bodies [54, 55]. P-bodies are known as a site of mRNA degradation because it contains untranslated mRNAs which are targeted for degradation [56, 57]. Evidence showed that a mutated lin-41 mRNA lacking binding site of let-7 are not transported to P-bodies, which suggested the involvement of miRNA in the suppression of translation by targeting mRNA to P-bodies [58] (**Figure 1.5A**). Interestingly, miR-122 was also found to bind the 3'UTR of Cationic Amino acid Transporter 1 (CAT-1) and induced its translational repression through shifting CAT-1 mRNA to P-bodies [59]. Second, artificial tethering of translation factors to mRNA to start translation can inhibit the miRNA dependent repression [55]. This evidence suggested the effect of miRNA starts before the assembly of translation complex (**Figure 1.5B**). Taken together, it is proposed that miRNA may suppress the translation initiation through the kinetic competition for target mRNAs between translation complex and miRISC

within P-bodies. However, more researches are needed to reveal the detail mechanism.

- **Targeting mRNA to increased decay:**

In addition to the translational repression of target mRNAs, it has been shown that miRNAs may target mRNAs to exonuclease-mediated decay. Studies show that the expression level of miRNAs inversely correlated with the level of target genes [60, 61]. The depletion of essential components of miRNA pathways, such as Dicer or AGOs, also increases the transcript levels of target genes [60, 62]. The mechanisms leading to these observations are quite different between plant and animal cells. In plant cells, miRNA can form fully or nearly complimentary matching to target mRNA and direct the endonucleolytic cleavage on target mRNA [63]. The cleaved mRNA then undergoes exonuclease mediated decay. In contrast, in animal cells, miRNA directly leads their targets to be degraded by exonuclease (5' to 3' mRNA decay pathway). In this pathway, the mRNAs are first deadenylated by the CAF1-CCR4-NOT deadenylase complex and then decapped by DCP2 [64, 65]. The decapped mRNAs are ultimately degraded by the major cytoplasmic exonuclease XRN1.

1.5.3 The involvement of miRNAs in cancer

In the past decade, miRNA based researches have revealed the essential role of miRNA in carcinogenesis. The dysregulated miRNA expression is either the cause or the result of tumor development. Based on

these studies, more novel strategies were designed to treat or diagnose cancer related diseases. In 2002, Calin et al. reported the loss of chromosome 13 in patients with chronic lymphocytic leukemia (CLL) [66]. In this study, they identified two miRNA genes, *miR-15* and *miR-16*, were both absent or downregulated in most CLL patients due to the deletion in chromosome 13. This report was the first one to suggest that the deregulation of miRNA alone can lead to cancer development. Further studies pointed out that many fragile sites on the chromosome that are commonly amplified or deleted in cancer contained miRNA genes [67]. These key findings promoted intensive studies in the following decade to identify many abnormally amplified oncogenic or deleted tumor suppressor miRNAs in cancer cells.

Interestingly, miR-17-92 cluster, usually overexpressed in patients with CLL [68] and lung cancer [69], was also identified in a frequently amplified region on the chromosome 13 in human B-cell lymphoma [70, 71]. To experimentally determine its role in tumorigenesis, miR-17-92 clustered was ectopically expressed in mouse B-cell model. The results showed that miR-17-92 cluster act together with c-Myc overexpression to accelerate the tumor growth in mouse. Similar finding was made in colorectal cancer [72]. miR-17-92 was therefore suggested as the first potential non-coding oncogene. In the following year, many other microRNAs are identified as oncogene, including miR-155 in B-cell malignancy [73] and miR-21 in different types of cancer [74, 75].

In contrast, some miRNAs exhibit tumor suppressor function by the control of oncogenic proteins. For example, let-7 was shown to inhibit RAS protein in lung cancer and its expression is frequently reduced in patients with lung cancer [76]. RAS overexpression was found in many different cancer types [77-79]. The subject miRNA in this thesis, miR-122, was also demonstrated as a tumor suppressor in our previous studies [80, 81]. miR-122 was reduced in rodent HCC models and in human primary HCC. Many targets of miR-122 are critical for cell proliferation and will be discussed in the latter chapters [82].

1.5.4 The deregulated miRNAs in HCC

As in other cancer types, miRNAs are also frequently deregulated in HCC and are involved in many different stages of tumor development, including cell proliferation, resistance to apoptosis, metastasis. These discoveries may shed some light on the development of novel therapy for HCC. **Table.1.1** summarized the deregulated miRNAs that were reported in multiple studies in HCC. Many of these miRNAs such as miR-21 [83], miR221/222 [84], and miR199 [85] were also deregulated in other cancer types,

MiRNAs affect cell proliferation by targeting genes involved in the control of cell cycle. For example, cyclins are targeted by many miRNA related to HCC development. Cyclin D2 and cyclin E2 are direct targets of miR-26a, which is reduced in HCC [86]. Ectopic expression of miR-26a by

viral delivery in c-Myc HCC model was shown to suppress the tumor growth. Also, expression of miR-221 which promotes tumor growth by repressing CDK inhibitor p27 [87] *in vitro*, was shown to closely correlated with HCC. Through indirect effect, miR-21 was shown to induce rapid CyclinD1 expression to promoter liver regeneration and possibly involved in hepatocarcinogenesis[88]. CDK6, a direct target of miR-124, which is reduced in HCC and induces cell cycle arrest at the G1-S transition [89]. Recently, systemic delivery of miR-124 in a carcinogen induced HCC animal model was shown to suppress tumor growth [90].

MiRNAs also regulate apoptotic genes to affect tumor growth. The major protein family involved in the regulation of apoptosis is Bcl-2 protein family, which includes both pro-apoptotic (Bim, Bmf, Bax, Bak, Bid) and anti-apoptotic (Bcl-2, Bcl-W, Bcl-XL, Mcl-1) members. Several miRNAs regulate apoptosis by targeting Bcl-2 protein family. For example, miR-122, the tumor suppressor in HCC [80], targets Bcl-W to block its anti-apoptotic function [91]. In contrast, miR-221 and miR-25 target Bmf and Bim, respectively to help tumor cells escape from apoptosis [92, 93].

A third way by which miRNAs regulate the tumor progression is through regulating target genes involved in tumor invasion and metastasis. MiR-21 is an intensively studied miRNAs promoting tumor metastasis in different types of cancers [94-96]. In HCC patient samples, the expression of the phosphatase and tensin homolog (PTEN) tumor suppressor is increased when miR-21 is decreased [97]. Further ectopic expression of miR-21 in HCC

cell line decreases tumor cell proliferation, migration, and invasion. Cell migration was promoted in normal human hepatocytes transfected with precursor miR-21. PTEN affects cell migration and invasion by dephosphorylating focal adhesion kinase (FAK) and increasing expression of MMP2 and MMP9. Interestingly, miR-221/222 was also shown to enhance HCC cell migration by targeting PTEN [98]. These findings suggested that some key genes involved tumor development are simultaneously regulated by multiple miRNAs in HCC. Furthermore, c-Met, also an important gene involved in tumor metastasis, is a direct target of two miRNAs, miR-34a [99] and miR-23b [100], in HCC models. c-Met is well-studied as the receptor for hepatocyte growth factor (HGF) [101]. The upregulation of c-Met may induce phosphorylation of its downstream effectors such as ERK1/2, the key factors influencing the tumor invasion and migration [102, 103].

1.6 Therapeutic research for HCC

To develop new strategies for HCC, it is important to establish experimental animal models to reveal the molecular pathogenesis of hepatocarcinogenesis. Therefore, it is critical that animal models mimic the characteristics of HCC, including etiology, genetic alteration, tumor types, and physiological similarity. Mouse (*Mus musculus*) is the best model system for HCC study mainly because of the well-established gene targeting method on mice, short lifespan (~3 years) of mice and similar genetic background of mice compared to human [104]. Based on the mouse HCC models, a variety

of therapeutic approaches are developed and tested, including radiation based therapy, chemotherapy, tumor removal surgery, and gene therapy.

1.6.1 Mouse models of HCC

- **Xenograft model:**

This animal tumor model was established at late 60s' by implanting large amount of cultured cells subcutaneously in *nude* mice, which is a type of immunodeficient mice [105]. The wide usage of this model is because of several advantages, including less technical requirement, easier monitoring of the tumor growth, and faster growth of cultured tumor cells. However, later studies revealed that the simplified subcutaneous tumor xenograft model cannot mimic the complexity of tumor microenvironment *in situ*. Specifically, the tumor architecture, vasculature, and genetic heterogeneity are all quite different between subcutaneous xenograft model and *in situ* tumor xenograft, or so called autochthonous tumor, from tumor bearing animals. To improve this problem of subcutaneous model, orthotopic xenograft model is used to transplant *in situ* tumor tissue from human patient or animal model to the target organ immunodeficient *nude* mice [106]. However, as mentioned in the third chapter of this thesis, the tumor structure in orthotopic or xenograft model is still not comparable to the spontaneous liver tumor due to the surrounded fibrotic tissue induced after the transplantation (**Figure 3.6**).

- **Genetically engineered animal models:**

Since more genes were identified as oncogenes and tumor suppressors in many studies, genetic alteration of these genes in mice was utilized to generate spontaneous HCC. Such models are ideal to examine the molecular mechanism leading to cancer development. Generally, genetically engineered animal are categorized as either transgenic or endogenous models [107]. To induce spontaneous tumor, transgenic mice are genetically engineered to overexpress oncogenes or dominant-negative tumor suppressor genes. Briefly, a recombinant DNA was delivered to the pronucleus of a fertilized mouse egg by microinjection [108] or lentiviral infection [109]. However, the ectopic expression in the conventional transgenic model is not tissue dependent and may induce tumor formation in other organs. Therefore, a tissue specific inducible system is established by using a tissue specifically activated promoter to drive target gene expression in the specific organ. For example, albumin promoter is used to activate gene expression in liver [110]. Another type of genetically engineered model is endogenous model, which is either “knockout” the target genes from genome or “knockin” target gene expression under the control of endogenous promoter. Again, the effect of germline mutation is not tissue specific because it is present in all cell types of mice and is constitutively altered. Conditional regulation of gene expression is developed to express gene of interest in specific location or at specific time-point [111]. To achieve this, bi-transgenic mice are

generated by crossing transgenic mice carrying inducible transactivator gene to another transgenic mice carrying engineered genes controlled by transactivator. Cre-Lox system is a well-studied method to conditionally delete tumor suppressor genes. In this system, Cre recombinase catalyzes a site-specific recombination to delete out the gene of interest flanked by two Lox P sites. The promoter that activated the Cre expression is designed to express under the desired condition. For example, the *Albumin-Cre* system functions by inducing or deleting transgene in hepatocytes in early adult stage.

- **Diethylnitrosamine induced HCC model:**

In the chemical carcinogenesis models HCC is initiated by mutations in normal cells followed by promoting the clonal expansion of mutated cells. Therefore, it is necessary to induce liver to DNA damage when liver is at the proliferative stage. One of the most well known models is Diethylnitrosamine (DEN) induced HCC model [112]. In this model, DEN was injected to mice at day postnatal 14 when liver is highly proliferative, and liver tumor will develop at the age of 30 weeks after DEN injection. Cytochrome P450 (CYP) was shown to activate DEN and generated DNA-adducts to cause DNA damage and apoptosis to hepatocytes [113]. A small number of cells will survive from the damage and evolve into dysplastic foci and dysplastic nodules. It has been shown that DEN exposure promotes more HCC in newborn and infant mice than adult mice [114]. To accelerate the progress of

tumorigenesis, liver resections or chemicals are applied after the DEN exposure to promote the clonal expansion of neoplastic cells. Combination of DEN exposure and partial hepatectomy in rat model, which is also known as Solt-Farber method [115], can induce preneoplastic foci within one week after surgery. Similar effect was observed with the combination of DEN exposure and phenobarbital feeding [116]. Phenobarbital was shown to facilitate the growth of proliferative cells and therefore increased HCC incidence.

1.6.2 miRNA based gene therapy for HCC

The main goal of gene therapy is to restore the deregulated gene expression in diseased organism. In the past, gene therapy is not feasible because of the lack of knowledge of molecular mechanism and techniques to deliver genetic material. Today, fast growing discoveries of novel genes involved in carcinogenesis, including miRNAs, greatly highlight the therapeutic potential of gene delivery. The development of vehicle for miRNAs delivery was shifted from *in vitro* cell culture, experimental animal models and recently to clinical applications [117]. The delivery methods can be divided into viral and non-viral method.

- **Viral delivery method**

The advantage of viral delivery is a single administration of low dose yields the long-term expression of miRNA in both dividing and non-dividing cells. The viral vector is constructed with genes encoding the hairpin structure

of miRNA under the control of promoter activated by polymerase II or polymerase III. Adeno-associated virus (AAV) is commonly used to deliver miRNA to prove the therapeutic potential. AAV simultaneously infect dividing and non-dividing cells and stay in an extrachromosomal state without integrating its genes into host's genome. Kota et al. have performed the therapeutic delivery of miR-26a to Myc overexpression induced HCC model and successfully suppress the tumor growth compared to the control group [86]. Although Myc is not the direct target of miR-26a, the tumor growth is suppressed by the miR-26a mediated downregulation of the genes downstream to Myc. Furthermore, adenoviral delivery of let-7a to a xenografted lung cancer model also significantly repressed the tumor growth [118]. The respiratory inhalation of adenovirus encoding let-7a significantly reduces the spontaneous lung tumor growth by 66%. However, the treatment did not completely kill the tumor cells due to the transient expression of let-7 from the adenoviral vector [119].

- **Non-viral delivery method**

Due to the surface negative charge, naked miRNAs are hard to be taken up by cells without delivery vehicle. Therefore, different strategies are developed to deliver miRNA, anti-miRNA, or siRNA *in vitro* and *in vivo*, including stabilization of the anti-miRNA in circulation by modification of anti-miRNA structure [120], modified siRNA with ligands of the receptors expressed on hepatocytes [121], and conditional dissociation of miRNA and vehicles [122]. Rozema et al. have developed a polymer named Dynamic

PolyConjugates (DPC) to conditionally release miRNA in the endosome, which is a subcellular organelle that contains more acidic environment compared to other subcellular structures. [122]. Without the acidic environment, DPC is tightly associated with miRNAs during the whole period of circulation. Another strategy is to increase targeting specificity of the compound conjugated to miRNAs. Because of its biocompatibility and preferential uptake by the liver and jejunum, cholesterol is conjugated to siRNA to specifically downregulate its target, ApoB [123]. Recently, an important advance of siRNA/miRNA delivery to the liver is the development of stable nucleic-acid lipid particles (SNALP), which is a natural cationic lipid nanoparticle. Zimmermann et al. have used SNALP based delivery of siRNA to target APOB mRNA to the liver of non-human primates [124]. Notably, with a single intravenously injection, APOB was downregulated by 90% and the effect lasted for 11 days without causing tissue toxicity. SNALP has been tested in clinical trial and may be developed as a medicine in the near future [125]. These progresses suggest strong therapeutic potential of SNALP conjugated miRNA in cancer.

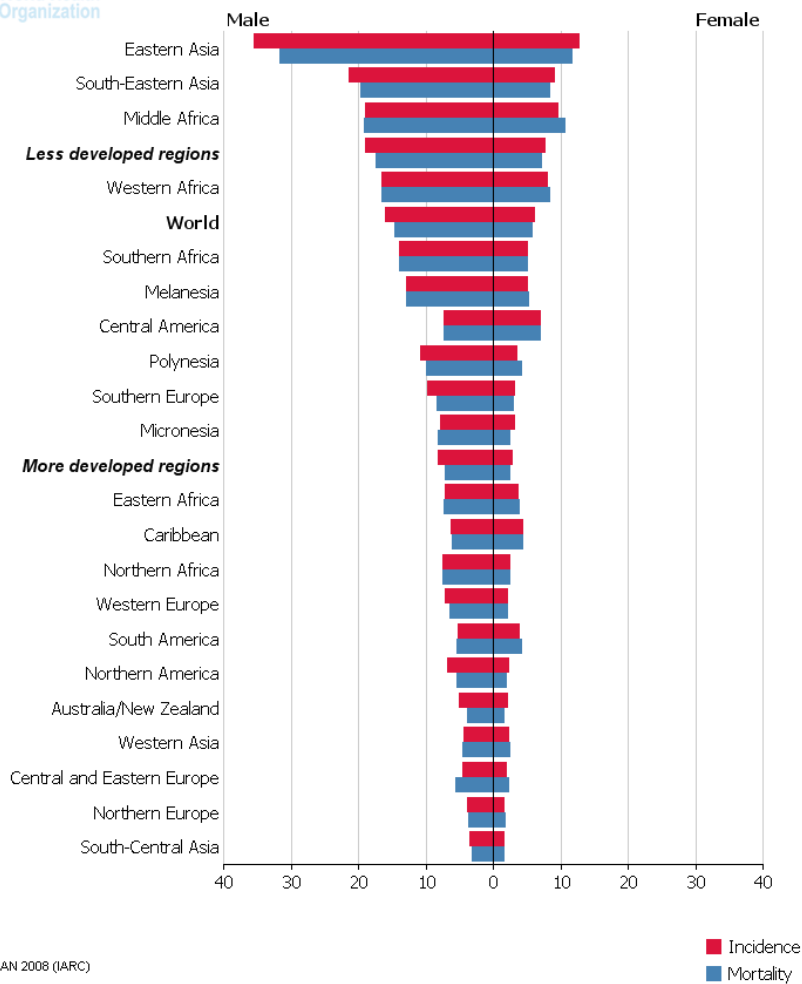


Figure 1.1 Summary of HCC incidence (red bar) and mortality (blue bar) in males and females worldwide

X-axis indicated the cases per 100,000 people and Y-axis indicated the area inspected. This figure is a reprint with permission from Dr. Ferlay [1].

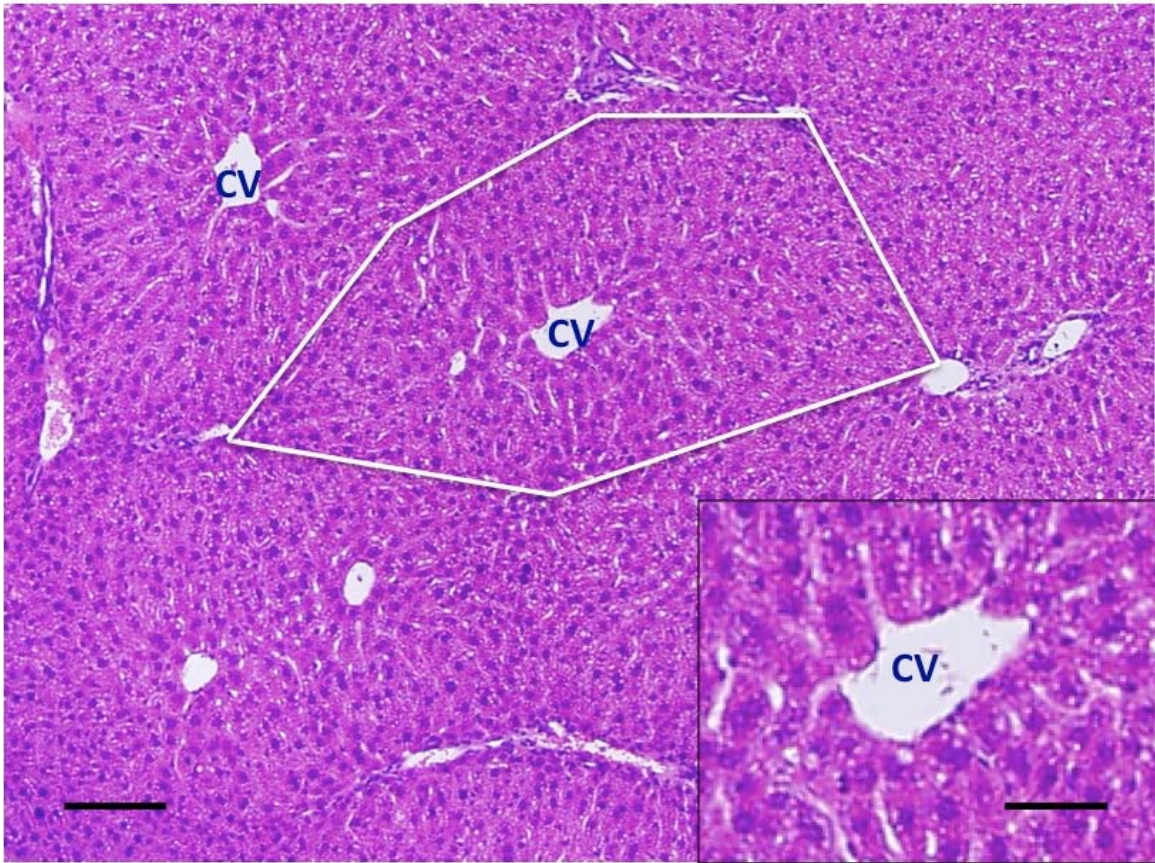


Figure 1.2 H&E staining of normal mouse liver sections.

A hexagonal lobule is surrounded by portal tract (white line) and the single-cell layer of hepatocytes (magnified in inset) radiates from central vein (CV) to portal tract. Scale bar: lower left: 150 μ m; right left: 50 μ m. The picture is taken from the liver section of a six-month old C57/Bl6J mouse [77]

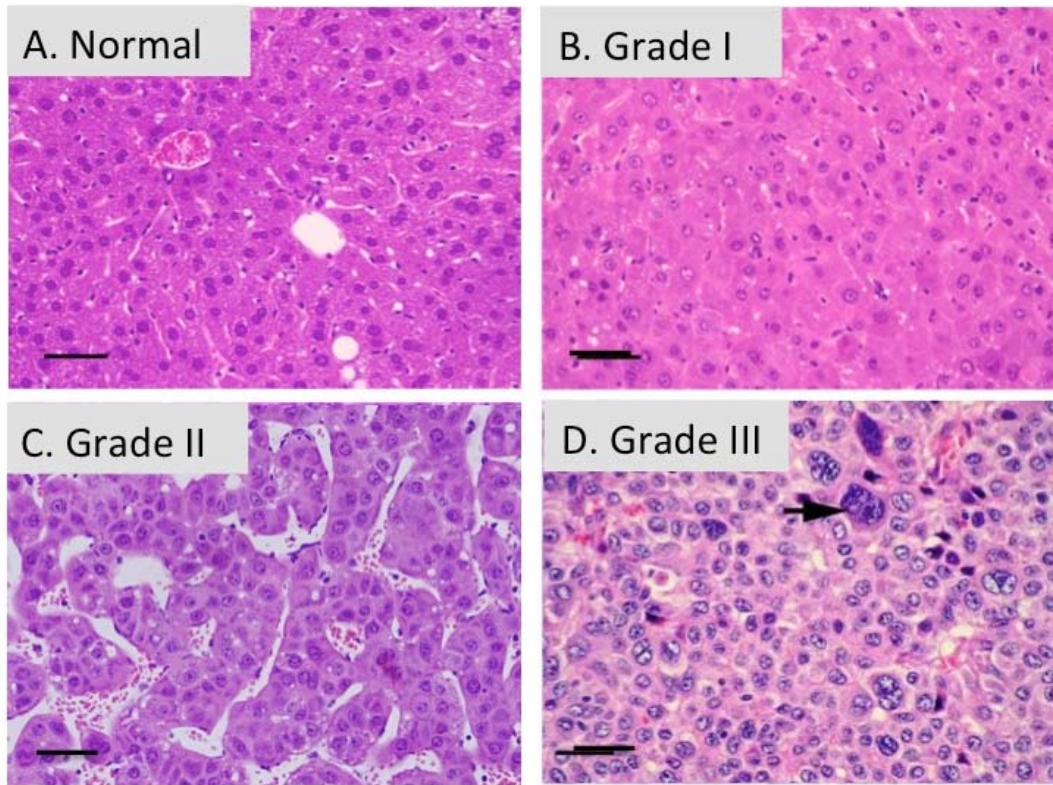


Figure 1.3 H&E staining of tumor sections at different HCC stages

(A) Normal liver. (B) Grade I: well differentiated HCC. (C) Grade II: medially differentiated HCC. (D) Grade III: poorly differentiated HCC (Arrow: Giant cell).

D is a reprint modified from data on Pathpedia.com with permission. Scale bar: 50 μ m.

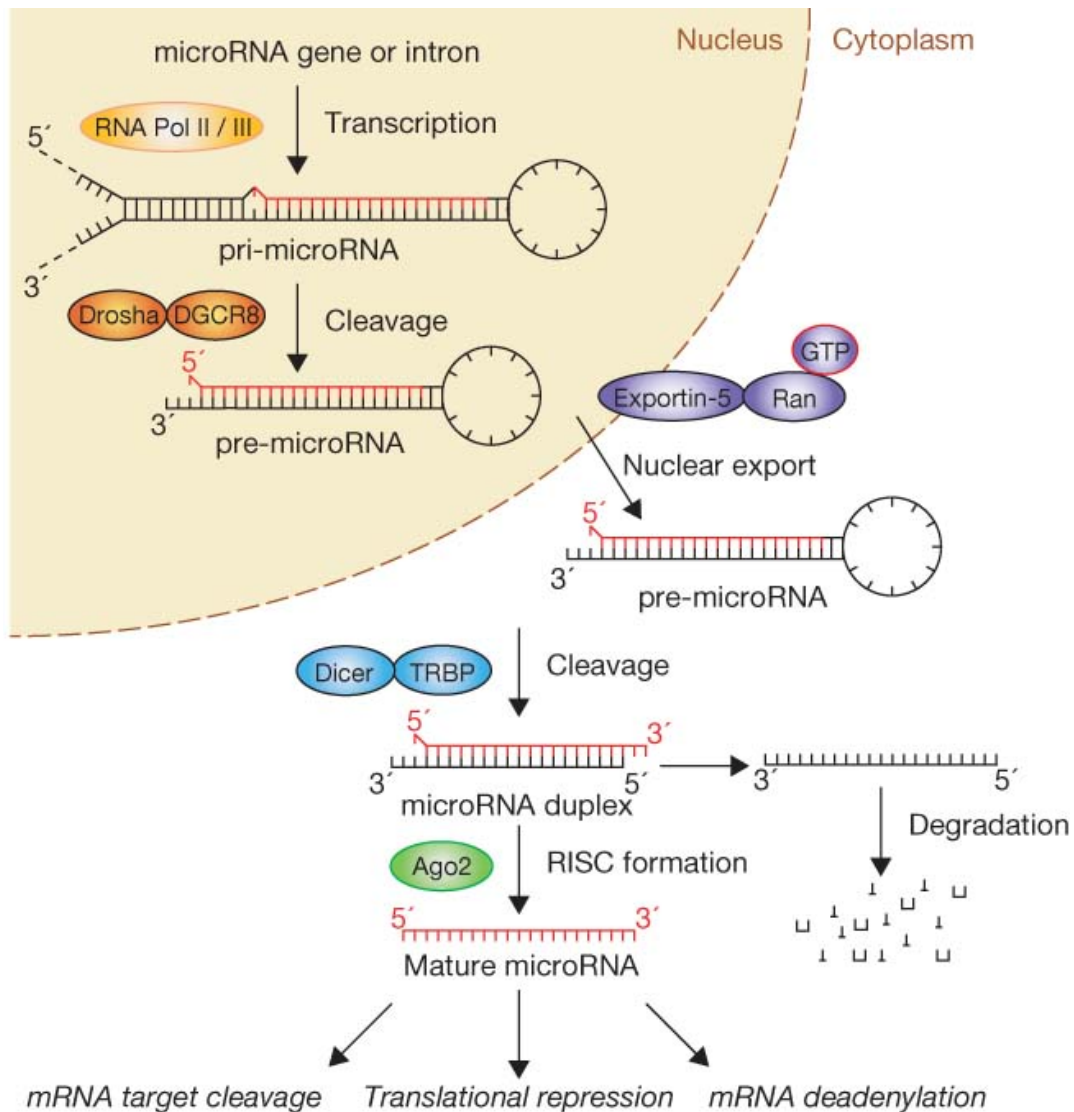


Figure 1.4 Biogenesis of microRNA in cells.

MicroRNA are first transcribed into pri-microRNA through Pol II/III mediated transcription. The pri-microRNA is then cleaved by Drosha/DGCR8 complex to form pre-microRNA and is exported into cytoplasm by Exportin-5. The pre-microRNA is further cleaved by Dicer/TRBP complex to form a microRNA duplex, which gives one strand of mature microRNA that suppresses target gene expression. This figure is a reprint with permission from Dr. Diederichs [126]

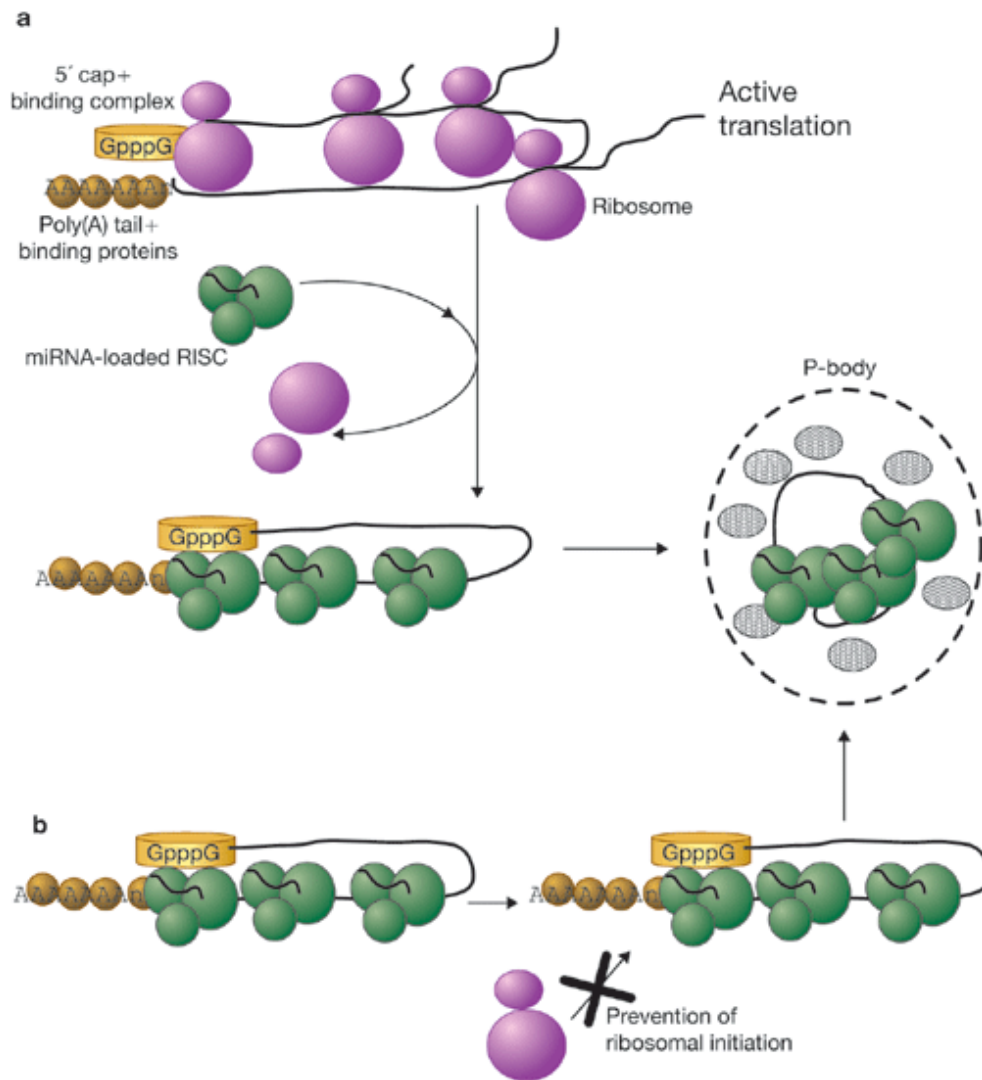


Figure 1.5 Two models of miRNA mediated translation repression

(A) First, miRNA loaded RISC block ongoing translation by binding to 3'UTR of the target mRNA. The mRNA bound by RISC was then targeted to P-bodies for degradation. (B) Second model proposed that RISC suppressed the translation by preventing ribosomal initiation. This figure was adapted with permission [127].

microRNA	Up/Down	miRMA cluster	Cancers other than HCC
miR-18	Up	mir-17–92	No
miR-21	Up	-	Ovarian, glioblastoma, lung, breast
miR-221	Up	mir221/222	Colon, pancreas, stomach, bladder, glioblastoma, thyroid
miR-222	Up	mir221/222	Stomach, pancreas
miR-224	Up	mir224/452	Prostate, Thyroid
miR-122	Down	-	No
miR-125a	Down	mir-99b/let7-e/125a	Breast, Ovarian, Lung
	Down	miR125b-1/let7a-2/miR100	Breast, Ovarian
miR-130a	Down		Breast, Lung
miR-150	Down	-	No
miR-199a-1-5p	Down	-	Ovarian
miR-199a-2-5p	Down	mir-199a2/214	Ovarian
miR-199b	Down	-	Ovarian, Lung
miR-200a	Down	mir-200b/200a/429	No
miR-200b	Down	mir-200b/200a/429	Ovarian

Table 1.1 Deregulated miRNAs identified in HCC

This is a modified reprint modified with permission [128].

Chapter 2. The loss of miR-122 induces steatohepatitis and spontaneous HCC in miR-122 knockout mice

2.1 Abstract

miR-122, a highly abundant liver-specific microRNA (miRNA), regulates cholesterol metabolism and is essential for Hepatitis C Virus (HCV) replication. Reduced miR-122 expression in hepatocellular carcinoma (HCC) correlates with metastasis and poor prognosis. Nevertheless, the consequences of sustained miR-122 loss-of-function *in vivo* have not been determined. Here we demonstrate that germ-line or liver-specific deletion of the mouse *miR-122* locus results in microsteatosis, chronic hepatitis, and the development of tumors resembling HCC. These pathologic manifestations are associated with dysregulated expression of oncogenic pathways and the infiltration of liver parenchyma with inflammatory cells that produce pro-tumorigenic cytokines including IL-6 and TNF- α . These findings reveal critical functions for miR-122 in the maintenance of liver homeostasis and have important therapeutic implications including the potential utility of miR-122 delivery for selected patients with HCC and the need for careful monitoring of patients receiving miR-122 inhibition therapy for HCV.

2.2 Introduction

miR-122 is a highly conserved liver-specific microRNA (miRNA) that constitutes 70% of the cloned hepatic miRNA in adult mouse [129]. Several key observations underscore the importance of miR-122 in liver biology and disease. First, antisense-mediated inhibition of miR-122 in mice leads to the induction of genes that are normally repressed in adult liver [130], suggesting that this miRNA is important for the maintenance of the terminally-differentiated hepatocyte gene expression program. Furthermore, miR-122 inhibition reduces serum cholesterol by causing the downregulation of genes involved in cholesterol biosynthesis including the rate limiting enzyme HMG-CoA reductase (Hmgcr) [130], thereby protecting animals from diet-induced hypercholesterolemia [131]. Additionally, miR-122 plays a non-canonical role in the life-cycle of the Hepatitis C virus (HCV). Through interaction with two seed sequence binding sites located at the 5'-end of the HCV genomic RNA, miR-122 performs an incompletely understood function that is essential for replication of the virus [132]. Accordingly, intravenous administration of locked nucleic acid (LNA) antisense miR-122 oligonucleotides reduces viral load in HCV infected chimpanzees [133], a therapeutic approach that is currently under clinical investigation for HCV in humans.

Hepatocellular carcinoma (HCC) is the fifth most prevalent cancer worldwide and the third leading cause of cancer-related death [134]. HCC often occurs in the setting of underlying liver dysfunction, especially chronic inflammation and cirrhosis. We have previously demonstrated that miR-122

expression is reduced during the initiation and progression of hepatocarcinogenesis in rats fed a diet deficient in folic acid, choline, and methionine that induces nonalcoholic steatohepatitis (NASH) [81]. Downregulation of miR-122 is also prevalent in human NASH patients [135]. Moreover, reduced expression of miR-122 is common in human HCC cell lines and tumors and low expression of this miRNA correlates with poor prognosis and metastasis in HCC patients [reviewed in [136]]. Ectopic expression and depletion studies in HCC cell lines have demonstrated that miR-122 exhibits pleiotropic anti-tumorigenic activities including the inhibition of proliferation and metastasis. Moreover, ectopic expression of miR-122 sensitizes HCC cells to anti-cancer drugs such as doxorubicin [82] and sorafenib [80].

Despite these indications of a critical role for miR-122 in liver physiology and disease, and the potential for this miRNA as a therapeutic target for HCV and perhaps other disease states, the consequences of genetic loss-of-function of this miRNA *in vivo* have yet to be documented. Here we describe the generation and characterization of mice with germ-line knockout (KO) or liver-specific knockout (LKO) of the *miR-122* locus. Both KO and LKO mice develop normally and are viable and, consistent with studies performed using antisense-mediated miR-122 inhibition [130, 131, 137], exhibit reduced serum cholesterol. In contrast to transient inhibition studies, however, miR-122 KO and LKO animals develop microsteatosis, hepatitis, and fibrosis in early adult life and later develop spontaneous tumors

resembling HCC. Hepatocarcinogenesis is likely initiated in these animals through the upregulation of several oncogenic pathways coupled with liver injury associated with the infiltration of inflammatory cells which produce the pro-tumorigenic cytokines IL-6 and TNF- α . These findings provide important insight into the natural functions of this miRNA, establish its role as a tumor suppressor *in vivo*, and underscore the need for caution when implementing miR-122 inhibition therapies.

2.3 Materials and Methods

2.3.1 Generation of liver specific (LKO) and germline miR-122 knockout (KO) mice

miR-122 conditional knockout ($miR-122^{loxP/loxP}$ or floxed) mice were generated as depicted in Figure S1A. $miR-122^{loxP/loxP}$ littermates served as controls in all studies. Animals were housed in a helicobacter-free facility and were handled and euthanized following institutional guidelines.

2.3.2 Serological, histological and immunohistochemical analysis

Serum was isolated from mice by cardiac puncture after CO₂ asphyxiation and cervical dislocation following overnight fasting. Biochemical

analysis of enzymes, and lipids in the sera was performed at the OSU mouse phenotyping core facility using VetAce (Alfa Wassermann system).

For histology, tissues were fixed in 4% paraformaldehyde and frozen in O.C.T. or embedded in paraffin. H&E, Oil-Red-O, PAS, and Masson's Trichrome staining of liver sections were performed as described [138, 139]. For immunohistochemical analysis, the slides were dewaxed, subjected to antigen retrieval at 95°C for 30 minutes followed by incubation with the antibodies and color development by the DAB method. The scoring of inflammation and steatosis were performed on H&E stained sections (100x magnification) using the following criteria: (1) Scoring criteria for inflammation: score=0: no inflammation; score=1: mild lymphocytic infiltration in the portal triad; score=2: severe lymphocytic infiltration in portal triad; score=3: extended infiltration of lymphocytes throughout liver. (2) Scoring criteria for steatosis: score=0: no steatosis; score=1: microsteatosis; score=2: microsteatosis and mild macrosteatosis; score=3: severe macrosteatosis. All scoring was performed by two blinded pathologists.

2.3.3 Transmission Electron Microscopy

For transmission electron microscopy (TEM), animals were perfused through the portal vein with 2.5% glutaraldehyde. The liver was post-fixed in 2% OsO₄, embedded in resin, and sectioned. After locating the periportal area in thick (1µm) toluidine blue (EMS), thin (<90nm) sections were cut on an

ultramicrotome (Leica UC6) and were post-stained with uranyl acetate. Electron micrographs were taken using an FEI Philips Tecnai T-12.

2.3.4 Measurement of hepatic triglyceride synthesis

The *in vivo* triglyceride synthesis rate was determined by measuring $^3\text{H}_1$ - glycerol incorporation into hepatic triglycerides following a published protocol [140, 141].

2.3.5 Hepatic triglyceride secretion

After overnight fasting, mice were injected via the tail vein with Triton WR1339 (Sigma) [142], a lipoprotein lipase inhibitor. Blood was collected from the tail vein and the serum triglyceride levels were measured at 0, 1, and 3 hours post-injection.

2.3.6 Microarray analysis of liver RNA

Total RNA from the livers of male mice was isolated using Trizol (Invitrogen), purified using mini RNeasy columns (Qiagen), and the integrity and quantity of the RNA was assessed using an Agilent Bioanalyzer and Nanodrop RNA 6000, respectively. Total RNA was labeled using the Affymetrix Whole Transcript Sense Labeling kit and hybridized to the Affymetrix Mouse Exon 1.0 ST array following the manufacturer's protocol at the Microarray Shared Resource Facility, Ohio State University

Comprehensive Cancer Center. The microarray data was deposited in the GEO database. Microarray data analysis methodology is described in the Supplementary Methods.

2.3.7 Real-time RT-PCR analysis

Real-time RT-PCR analysis of mRNAs was performed using SYBR Green chemistry. Relative expression was calculated using $\Delta\Delta C_T$ method [143]. The primer sequences are provided in the Supplementary Materials.

2.3.8 Western blot analysis

Mouse liver microsomes were purified following a published protocol [144]. Whole tissue or microsomal extracts were prepared as described [145] and subjected to western blot analysis with specific antibodies using supplier's protocol. The signal was detected using ECL western blotting reagent. Details of the antibodies used are provided in the Supplementary Materials.

2.3.9 Microarray analysis of the tumor RNA

Agilent 4X44 platform was used to assess gene expression in liver tumors from 4 LKO and 4 KO mice and in normal liver from age-matched control mice using manufacturer's protocol. Further details are provided in the Supplementary Methods.

2.3.10 Flow cytometric analysis

Flow analysis of liver immune cells was performed as described [146]. The following antibodies reactive with murine cells were obtained from BD Biosciences: Gr1 (RB6-8c5), CD11b (M1/70), CD3 (145-2C11), CD19 (1D3), NK1.1 (PK136), IL-6 (MP5-20F3), and TNF- α (MP6-XT22). CCR2 mAb (475301) was purchased from R&D Systems.

2.3.11 Generation of liver specific (LKO) and germline miR-122 knockout (KO) mice.

The targeting vector was constructed by amplifying homology arms from 129SvJ genomic DNA and cloning them into pBlueScript SK (pBSK) (Stratagene). *mmu-miR-122* gene with the flanking region (569bp) was PCR amplified and cloned into pFlox-Frt-Neo [147]. Floxed *mmu-miR-122*-neo was subcloned into pBSK flanked by 5'- and 3'-arms (**Figure S1**). Electroporation of mouse ES cells and subsequent generation of chimeric mice from targeted clones were performed at the University of Michigan Knockout Mouse Core Facility. Two of the mutant clones were transmitted through the mouse germ line, which was confirmed by analysis of tail DNA by PCR. *miR-122*^{loxP/loxP} littermates served as controls in all studies. Animals were housed in a helicobacter-free facility and were handled and euthanized following institutional guidelines.

2.3.12 Measurement of hepatic triglyceride synthesis.

The *in vivo* triglyceride synthesis rate was determined by measuring $^3\text{H}_1$ -glycerol incorporation into hepatic triglycerides following a published protocol [140, 141]. Briefly, 8-10 week-old mice were trained to feed during 3h periods from 9 A.M. to 12 noon every day for two weeks. On the day of the experiment, after a 3 hour feeding and subsequent 1h fasting, $^3\text{H}_1$ glycerol (50mCi/150ml) was injected IP. Twenty minutes later, mice were sacrificed and livers were harvested. Total lipid was extracted from 0.3g of liver tissue and separated on a TLC plate. Triglyceride spots were scraped from the plate, suspended in the scintillation cocktail and counted in a scintillation counter. The tritium incorporated into hepatic triglycerides was normalized to serum $^3\text{H}_1$ level in each mouse.

2.3.13 Determination of Triglyceride synthesis in primary mouse hepatocytes transfected with siRNA.

Primary hepatocytes were isolated from LKO or KO mice with collagenase-based method as previously described [148]. The cell viability over 85% was determined by trypan blue staining before seeded onto 12 well plates at 5×10^5 cells per well in culture medium (Williams' Medium E with 10% FBS, 10mM HEPES and 10 nm insulin plus penicillin and streptomycin) and cultured overnight. The hepatocytes were transfected with a mixture of 50nmol/L gene-specific siRNA or scrambled si-RNA (Smartpool si-Genome from Dharmacon) and 2ul/ml lipofectamine 2000 (Invitrogen) in culture

medium without antibiotics. After 6 hours of incubation, the mixture was replaced with culture medium. After 48h the culture medium was replaced with 10uCi/ml [³H₁]-glycerol in FBS free culture medium containing 5% fatty acid free BSA and 0.3mM oleic acid. TG synthesis in transfected mouse hepatocytes was determined by extracting lipids and separating TG on TLC plates followed by counting ³H₁ incorporation in TG in a scintillation counter.

2.3.14 Microarray analysis.

Total RNA from the livers of male mice fasted overnight was isolated using Trizol (Invitrogen), purified using mini RNeasy columns (Qiagen), and the integrity and quantity of the RNA was assessed using an Agilent Bioanalyzer and Nanodrop RNA 6000, respectively. Total RNA was labeled using the Affymetrix Whole Transcript Sense Labeling kit and hybridized to the Affymetrix Mouse Exon 1.0 ST array following the manufacturer's protocol at the Microarray Shared Resource Facility, Ohio State University Comprehensive Cancer Center.

Affymetrix GeneChip Mouse Exon 1.0 ST Array with 23,332 probe-sets was used for gene expression profiling of 5 control (miR-122^{loxP/loxP}) and 5 LKO mice. Signal intensities were quantified by Affymetrix software. Background correction and normalization was performed and gene expression level was summarized over probes using the RMA method [149]. A filtering method based on the percentage of samples with expression values below the noise level was applied to filter out probe-sets with little or

no expression, resulting in 11,670 detectable probe-sets. Generalized linear models were used to detect differentially expressed genes between the control (floxed) and LKO mice. In order to improve the estimates of variability and statistical tests for differential expression, a variance smoothing method was employed [150]. The significance level was determined by controlling the average number of false positives [151]. A p-value of 0.0001 was used as the significance cutoff, allowing an average number of false positives of 1.2. The microarray data was deposited in the GEO database (accession number GSE20610).

2.3.15 Microarray analysis of the tumor RNA

The Agilent 4X44 platform was used to assess gene expression in liver tumors from 4 LKO and 4 KO mice and in normal liver from age-matched control mice using manufacturer's protocol. Briefly, highly purified total RNA from each group was hybridized to microarray slides overnight, washed, and then scanned with an Agilent G2505C Microarray Scanner. The raw signal intensity for each probe was extracted from the image data using Agilent Feature Extraction 10.5 (FE) and analyzed by the mathematical software package "R". The log₂ intensity ratio of red to green was normalized to the sum of log₂ intensities of red and green. This normalization adjusts the red and green intensities relative to one another so that the red/green ratios are an unbiased representation of true ratios. The microarray data has been deposited in the GEO database (accession number GSE31731).

2.3.16 Ingenuity Pathway Analysis

The IPA application (<http://www.ingenuity.com/products/IPA/Free-Trial-Software.html>) was used to identify gene networks that were overrepresented among the genes that exhibited ≥ 1.5 fold up- or down-regulation with a *P*-value ≤ 0.0001 in LKO livers. A significance score of ≥ 3 indicates that there is a less than 1 in 1000 chance that the highlighted genes were assembled into a network due to a random chance.

2.3.17 Plasmid construction

Coding regions and/or 3' UTRs were PCR amplified from 129/SvJ genomic DNA and subsequently cloned into the multiple cloning sites of psiCHECK2 (Promega), a reporter vector expressing both renilla and firefly luciferase.

2.3.18 Accession numbers

The microarray data on control and LKO livers and tumors was deposited in the GEO database (accession numbers GSE20610 and GSE31731, respectively).

2.4 Results

2.4.1 Liver specific (LKO) and germ-line (KO) miR-122 loss-of-function results in an altered serum lipid profile

The *mmu-miR-122* gene is located on chromosome 18 and is transcribed independently of any known gene. To determine its biological function, we generated a miR-122 conditional knockout allele (*miR-122^{loxP}*) in mice using homologous recombination. *miR-122^{loxP}* mice were crossed to *Albumin (Alb)-Cre* mice to produce LKO mice (**Figure 2.1A**). To generate KO mice, *miR-122^{loxP}* mice were initially crossed to *E2a-Cre* mice and then backcrossed to remove the Cre transgene. Both KO and LKO mice were born alive, fertile and were not notably different from control (floxed or wild-type) mice in terms of their body weight and growth (data not shown).

Northern and Southern blotting and real-time RT-PCR were used to confirm deletion of the *miR-122* gene and loss of miR-122 expression in LKO livers of 10 week-old mice, a time-point sufficient for complete Cre-mediated deletion in *Alb-Cre* hepatocytes [110] (**Figure 2.2A, 2.1B, 2.3A**). A significant increase in the expression of known targets such as *AldoA*, *Slc7a1*, *Cs*, and *Ccng1* [131, 152] confirmed functional depletion of miR-122 in LKO livers (**Figure 2.3B**). In KO mice, expression of miR-122 was abolished without influencing the levels of several other abundant liver-enriched miRNAs such as miR-148, miR-192 and miR-194 (**Figure 2.2B**). Real-time RT-PCR and western blot analysis demonstrated increased expression of known miR-122

targets including Adam-10 [80], Pparb/d, Smarcd1/Baf60a [153], and Iqgap1 [130] (**Figure 2.3C, D**).

We next examined liver function in 8-10 week-old LKO mice by measuring the serum profile of liver enzymes and metabolites after overnight fasting (**Table 2.1**). Among the lipids, total cholesterol was reduced in the serum of LKO mice by 30% ($P=1.8E-04$) without significantly altering triglyceride levels, corroborating previous observations in mice [130, 131] and primates [120, 133] depleted of miR-122 by administration of antisense oligonucleotides. These mice also exhibited a pronounced decrease in low-density lipoprotein (LDL)-cholesterol (~56.5%, $P=1.56E-06$) and a moderate decrease in high-density lipoprotein (HDL)-cholesterol (~25.1%, $P=0.01$). Finally, serum alkaline phosphatase (ALP) increased two-fold ($P=4.67E-11$) in LKO mice. The serum profile of 5 week old KO mice was very similar to that of the LKO mice (**Table 2.2**).

2.4.2 LKO mice develop hepatic microsteatosis due to triglyceride accumulation in early adult life

Histopathological analysis revealed distinctive features in livers of 8-10 week old LKO mice. Sinusoids in LKO mice were compressed by swollen hepatocytes containing multiple small clear vacuoles, likely representing lipid droplets (**Figure 2.4A**). Microsteatosis in LKO mice was confirmed by Oil-Red-O staining (**Figure 2.4B**) and transmission electron microscopy (TEM) (**Figure 2.5A**). Storage of liver glycogen was reduced in LKO mice after

overnight fasting, as demonstrated by PAS staining (**Figure 2.4B**). LKO livers also exhibited proliferation of bile duct and oval cells as shown by increased CK-19 and A6 positive cells, respectively (**Figure 2.5B**). Liver histology and serology were similar in male and female LKO mice (data not shown).

Quantification of hepatic lipids revealed a 2.5-fold increase in triglyceride levels without a change in cholesterol levels in LKO mice (**Figure 2.6A,B**). The accumulation of triglyceride could be the result of altered synthesis, secretion, and/or uptake. Measurement of $^3\text{H}_1$ -glycerol incorporation into hepatic triglycerides showed a small (25%) but significant ($P=0.02$) increase in *de novo* triglyceride synthesis in LKO mice (**Figure 2.6C**). Hepatic triglyceride secretion in LKO mice was measured by monitoring serum triglyceride levels after injecting Triton WR1339, an inhibitor of lipoprotein lipase. Triglyceride secretion was reduced to 43% and 46% of control levels after 1 and 3 hours, respectively, (**Figure 2.6D**). Thus, increased synthesis and reduced secretion contribute to triglyceride accumulation in the livers of LKO mice.

2.4.3 Genes involved in lipid metabolism and cellular proliferation and survival are abnormally expressed in livers of LKO mice

To investigate the mechanisms underlying the abnormalities observed in miR-122-deficient mice, hepatic gene expression was examined in 8-10 week old control and LKO mice (n=5 of each genotype) by microarray analysis. An examination of the potential enrichment of all possible

hexamers, heptamers, and octamers in the 3' UTRs of the transcripts upregulated in miR-122-deficient livers using the Sylamer algorithm [154] revealed that the only statistically-significantly enriched motifs of these lengths corresponded to sites that match the miR-122 seed sequence (**Figure 2.7**). These results indicate that the altered expression of a significant fraction of dysregulated transcripts in LKO livers is attributable to direct, canonical targeting by miR-122.

Ingenuity Pathway Analysis (IPA) of molecular and cellular functions of a stringent set (threshold $P \leq 0.0001$) of 194 upregulated and 121 downregulated genes in LKO livers identified 7 major networks of dysregulated genes (**Table 2.3**). Genes involved in lipid metabolism were highly represented within these networks. Notably, among the upregulated genes were two key enzymes, *Agpat1* and *Mogat1* that catalyze triglyceride biosynthesis [155]. Microarray analysis also showed increased expression of several additional genes in this pathway including *Agpat3*, *Agpat9*, *Ppap2a*, *Ppap2c*, and *Dgat1*, albeit at a lower significance threshold ($P \leq 0.05$) (**Table 2.4**). Real-time RT-PCR confirmed the significant upregulation of these transcripts (**Figure 2.8A**). Additionally, *Cidec* (*Fsp27*), a lipid droplet-binding protein that promotes triglyceride accumulation in hepatocytes *in vivo* [156], was elevated (**Figure 2.8A**). Western blot analysis confirmed increased protein levels of *Agpat1* and *Ppap2a* in microsomal extracts (**Figure 2.8B**) without significant alteration of *Cyp2e1*, a microsomal marker. *Agpat3*, *Agpat9*, *Cidec*, *Dgat1*, and *Mogat1* were elevated in whole liver extracts

(**Figure 2.8C**). Collectively, the altered expression of these genes would be expected to increase triglyceride biosynthesis and storage in the liver, as observed in KO/LKO mice.

To assess whether miR-122 can indeed regulate the expression of the aforementioned factors involved in triglyceride metabolism, we measured their mRNA levels in a mouse hepatoma cell line (Hepa) after transient overexpression (~40 fold increase) or depletion (~40% decrease) of miR-122 (**Figure 2.9A,B**). Ectopic miR-122 reduced *Agpat1*, *Agpat3*, *Agpat9*, *Dgat1*, *Cidec*, *Ppap2a* and *Ppap2c* expression, whereas depletion of miR-122 upregulated these transcripts (**Figure 2.9C**). *Mogat1* was not detectable in these cells (data not shown). Furthermore, reporter plasmids were constructed with a *renilla* luciferase open reading frame followed by the 3' UTRs of *Agpat1* or *Cidec* [harbouring 3 and 1 miR-122 binding sites, respectively, as predicted by TargetScan [157]]. miR-122 strongly repressed luciferase expression from the *Agpat1* reporter and, to a lesser extent, from the *Cidec* reporter (**Fig. 2.10**). Mutations in the putative miR-122 binding sites abrogated reporter repression consistent with the direct targeting of these transcripts by this miRNA. Finally, knockdown of *Agpat1* in hepatocytes isolated from LKO/KO mice reduced TG synthesis, suggesting that *Agpat1* plays a key role in TG accumulation in LKO/KO livers (**Figure 2.11A, B**).

In addition to genes that regulate lipid metabolism, IPA highlighted the abnormal expression of many genes involved in development, cellular proliferation and death, and cancer (**Table 2.3**). Many of these dysregulated

genes are known to exhibit altered expression in HCC and, in some cases, functionally contribute to hepatocarcinogenesis. Such genes include components of the insulin-like growth factor 2 (*Igf2*), Ras, and b-catenin (*Ctnnb1*) signaling pathways (**Figure 2.12**), as well as other genes known to play a role in HCC such as *Epcam* [158], *c-Myc* [159], *Mapre1* [160], and *Rhoa* [161]. Real-time RT-PCR validated the upregulation of several of these transcripts in LKO livers (**Figure 2.13A and Table 2.5**) and western blotting documented the increased expression of the majority of these proteins in KO livers (**Figure 2.13B**). In addition, miR-122 overexpression or inhibition in Hepa cells resulted in concordant expression changes of selected key genes including *H19*, *Igf2*, *Ctnnb1*, *Epcam*, *Mapre1*, *Mapkapk2*, and *c-Myc* (**Figure 2.9D**). Among these, *Mapre1* was validated as a target of miR-122 using reporter assays (**Figure 2.10**). In contrast, *Igf2* and *H19* do not appear to be directly regulated by miR-122 since comparable upregulation of both unspliced hnRNA and fully-spliced mRNA was observed for these transcripts (**Figure 2.14A**). Although *Igf2* and *H19* appear to be transcriptionally upregulated in LKO/KO livers, bisulfite sequencing did not reveal significant changes in the methylation status of DMR located between these two genes (**Figure 2.14B**). The observed upregulation of these genes in early adult life suggested that these mice might be predisposed to liver cancer as they age.

2.4.4 Recruitment of monocytes and neutrophils to livers of miR-122

LKO/KO mice leads to inflammation and production of pro-tumorigenic cytokines

Since many genes involved in cell proliferation and survival were significantly upregulated in LKO/KO livers, we aged these animals to determine whether they are tumor prone or exhibit any other adult-onset pathology. Importantly, aged miR-122 LKO mice did not exhibit significant repopulation of the liver with hepatocytes that escape Cre-mediated deletion, as has been observed in mice with liver-specific deletion of *Dicer* [138] (**Figure 2.15**). At 6 months of age, LKO/KO mice developed severe steatohepatitis (**Figures 2.16-18**) with visible foci of altered hepatocytes (inset of second panel of **Figure 2.16**). Trichrome staining revealed bridging fibrosis. Like younger LKO mice, 6 month old KO mice exhibited increased hepatic triglyceride levels without a significant change in hepatic cholesterol after overnight fasting (**Figure 2.17B**). A significant increase in serum ALP and GGT levels, consistent with hepatobiliary disease, was observed (**Table 2.7**).

Inflammation is a major contributing factor to malignant transformation in HCC and other tumor types [162]. In particular, the inflammatory cytokines IL-6 and TNF- α have been shown to promote HCC development [163]. We therefore characterized the inflammatory cells that infiltrate hepatic parenchyma in miR-122 LKO/KO mice and the cytokines they produce. Consistent with the histologic appearance of LKO/KO livers (**Figures 2.16-**

18), direct quantification of infiltrating inflammatory cells revealed a two-fold increase in the livers of KO mice (**Figure 2.19A**). Flow cytometry documented that the hepatic population of CD11b^{high}Gr1⁺ cells, previously classified as monocytes and neutrophils [164], was >3-fold higher in 10-month old non-tumor bearing KO mice than in controls (**Figure 2.19B, C**). Intracellular flow cytometry demonstrated that CD11b^{high}Gr1⁺ cells from KO livers produce a high level of IL-6 (**Figure 2.20A**) and TNF- α (**Figure 2.20B**).

In settings of chronic liver injury, the myeloid chemo-attractant *Ccl2* is induced in hepatocytes and other liver resident cells [165] and is an important driver of hepatic inflammation [166]. In miR-122 LKO/KO mice, intrahepatic CD11b^{high}Gr1⁺ cells expressed *Ccr2*, the *Ccl2* receptor, and displayed higher expression of *Ccr2* than those in the peripheral blood (**Figure 2.20C**). We therefore hypothesized that activation of the *Ccl2*-*Ccr2* axis in miR-122 LKO/KO mice leads to recruitment of CD11b^{high}Gr1⁺ cells, causing hepatic inflammation and injury. Indeed, microarray analysis of mRNA from 5 week old KO livers showed a >3 fold ($P=0.0003$) increase in expression of *Ccl2* (data not shown), which was confirmed by real-time RT-PCR in LKO/KO livers (**Figure 2.21A**) and cultured hepatocytes (**Figure 2.21B**). Ectopic miR-122 expression downregulated *Ccl2* in LKO/KO hepatocytes (**Figure 2.21C, D**) and in Hepa cells (**Figure 2.22A, B**) whereas depletion of miR-122 increased *Ccl2* levels (**Figure 2.22A, B**). Moreover, in KO livers, *Ccl2* mRNA levels were increased greater than unspliced hnRNA levels (**Figure 2.22C**), consistent with both transcriptional and post-transcriptional mechanisms

contributing to *Ccl2* upregulation. The RNA22 algorithm [167] identified a potential miR-122 binding site in the 3' UTR of *Ccl2* (**Figure 2.22D**). Upon inhibition of miR-122 in Hepa cells, a *Ccl2* 3' UTR reporter construct produced a moderate but significant increase in luciferase activity whereas a reporter with a mutation in the miR-122 binding site was not affected by miR-122 inhibition (**Figure 2.22E**). These data support a model whereby *Ccl2* is induced in miR-122 LKO/KO livers both directly through the targeting of this transcript by miR-122 and indirectly as a response to the underlying hepatocyte injury present in these animals. The resulting recruitment of CD11b^{high}Gr1⁺ cells leads to the production of pro-inflammatory and tumor-promoting cytokines including IL-6 and TNF- α , initiating a well-described pathogenic sequence which would be expected to predispose to HCC [163].

2.4.5 LKO and KO mice develop HCC with age

Consistent with the upregulation of oncogenic pathways and the infiltration of liver with inflammatory cells that produce pro-inflammatory cytokines (**Figure 2.19-22**), both LKO and KO mice developed moderately to poorly differentiated Afp-positive HCCs with age (**Figure 2.23A**). Thirteen out of 26 male LKO mice developed spontaneous liver tumors (1-12 macroscopic tumors observed per animal) whereas 2 out of 20 female LKO mice developed HCC in 12-17 months (**Table 2.8**). In contrast, both male (10/20) and female (9/19) KO mice developed HCCs with approximately equal penetrance after 11-15 months (**Figure 2.9**). However, the average tumor

weight and grade were significantly higher in male compared to female KO mice. One out of 20 heterozygous KO mice also developed HCC at 4.5 month of age (data not shown). Among the tumor-bearing mice, three were also found to have lung metastases (**Figure 2.23A**). Serum IL-6 was significantly increased in tumor-bearing male but not in female LKO/KO mice (**Figure 2.23B**), which correlated with greater tumor incidence in male LKO mice and higher tumor burden and tumor grade in the male KO mice. Western blot analysis of tumors from miR-122 LKO/KO mice demonstrated significant upregulation of several proteins that are known to be increased in human HCC e.g. Afp, Cxcr4 [168], Mapre1 [160] or play a causal role in tumorigenesis, e.g. c-Myc [169], b-catenin [170], Rhoa [171], RhoC [172] (**Figure 2.23C**). Similar upregulation of these proteins in a lung tumor is consistent with its identity as a metastatic HCC.

Gene expression profiles were assessed in LKO/KO tumors and compared to a previously reported analysis of gene expression in human HCCs with high and low miR-122 expression [173]. A moderated t-test was first used to obtain a list of genes that were dysregulated in LKO/KO tumors, which include 29 upregulated genes and 51 downregulated genes (**Figure 2.23D**). The expression levels of these genes were sufficient to stratify the human tumor samples into high and low miR-122 expressing clusters ($P=0.046$), indicating that loss of miR-122 expression results in similar effects on gene expression in human and mouse tumors.

2.5 Discussion

In this study, we investigated the biologic function of miR-122 through the generation and characterization of mice with liver-specific (LKO) and constitutional (KO) deletion of this miRNA locus. These experiments extend previous findings obtained through transient miR-122 inhibition in mice using antisense oligonucleotides, which reported that inhibition of this miRNA is well tolerated and results in reduced serum cholesterol. In contrast to these prior results, our study revealed that prolonged loss-of-function of miR-122 leads to accumulation of hepatic triglycerides and hepatic inflammation, which precedes the later onset of fibrosis and tumors resembling HCC. The upregulation of several gene products that catalyze triglyceride biosynthesis and storage in *miR-122* LKO/KO mice, including the newly identified direct miR-122 targets *Agpat1* and *Cidec*, provides a plausible explanation for the triglyceride accumulation and steatosis observed in the livers of these animals. Although a tumor suppressor role for miR-122 has previously been proposed based on *in vitro* studies and expression analyses of human HCC samples, our findings provide the first *in vivo* evidence that loss of this miRNA is sufficient to initiate highly-penetrant HCC development. Furthermore, the analysis of miR-122 LKO/KO animals has provided important novel mechanistic insights into the tumor suppressor activity of this miRNA.

It is well established that liver damage and inflammation potentially promote the development of HCC and, in humans, this tumor type nearly always arises in the setting of underlying liver injury [134]. Thus, chronic

steatohepatitis in miR-122 LKO/KO mice is an important component of the pathology, which leads to HCC in these animals. The earliest observable abnormality in miR-122 LKO/KO animals is steatosis which is a well-known cause of hepatic injury and inflammation [174]. In addition, upregulation of the chemokine *Ccl2*, both directly through loss of targeting by miR-122 and indirectly as a consequence of liver injury, results in the intrahepatic recruitment of CD11b^{high}Gr1⁺ inflammatory cells which locally produce pro-tumorigenic cytokines including IL-6 and TNF- α [163]. The importance of underlying inflammation in HCC development in these mice is further highlighted by the greater tumor incidence and higher tumor burden and grade in male LKO and KO mice, respectively. In humans, HCC exhibits a similar sex bias with 2-4 fold greater incidence in males [134, 175]. This bias is believed to be partially attributable to the greater susceptibility of males to injury-induced hepatic inflammation and hepatocyte proliferation mediated by IL-6, whose production is suppressed by estrogens in females [176]. Indeed, circulating IL-6 is increased in tumor-bearing male, but not female LKO/KO mice, likely contributing to the increased severity of hepatocarcinogenesis in male mice in this model.

The ability of miR-122 to suppress tumorigenesis when delivered to a non-inflammatory Myc-driven HCC model establishes that this miRNA performs a tumor suppressor function that is independent of its role in reducing inflammation and maintaining hepatocyte integrity. This activity is likely mediated by the ability of miR-122 to directly and indirectly control a

broad program of gene expression, which includes key factors that influence HCC pathogenesis such as *Igf2*, *b-catenin*, *Cyclin D1*, *c-Myc*, *Epcam*, *Mapre1*, *Iggap1*, and *Rhoa*. miR-122 also appears to be essential for maintenance of the mature hepatocyte gene expression program as manifested by the re-activation of fetal genes including *Afp*, *H19*, and *Igf2* in LKO/KO mice. In the setting of tonically increased signaling through canonical oncogenic pathways, the expansion of immature hepatocytes in an inflammatory microenvironment likely results in a state of highly increased Since miR-122 is downregulated in NASH [135], the efficacy of miR-122 delivery for reducing progression to cirrhosis and HCC in relevant animal models of this disease is worthy of investigation. However, given the essential role of miR-122 in HCV replication [177], the treatment of HCC or other liver diseases arising in the context of HCV infection would not be an appropriate setting for miR-122 delivery.

Lastly, miR-122 inhibition therapy using an LNA-modified antisense oligonucleotide, SPC3639, is currently in phase II clinical trials for the treatment of HCV infection [133]. Treatment of HCV-infected chimpanzees with SPC3639 reduced viremia and hepatitis without causing any adverse effects during the 12 week period of the study [133]. However, our examination of miR-122 LKO or KO mice has demonstrated that the chronic loss of miR-122 causes steatohepatitis and altered liver function that ultimately leads to liver cancer. Multiple explanations may account for the apparent discrepancy between the phenotypes observed after transient

inhibition *versus* genetic deletion of miR-122. First, the more severe phenotype in LKO and KO mice might arise due to a developmental defect resulting from the absence of miR-122 throughout gestation or it may result from the effects of complete deletion of the miRNA as opposed to partial loss-of-function achieved with chemical inhibitors. Alternatively, the development of liver damage and the resulting sequela might simply require a longer period of miR-122 depletion beyond that which has been examined using injected inhibitors. Distinguishing between these possibilities will be a priority for future research. Nevertheless, the insights gained through the study of mice lacking miR-122 should aid the design of safe therapeutic strategies based on miR-122 inhibition.

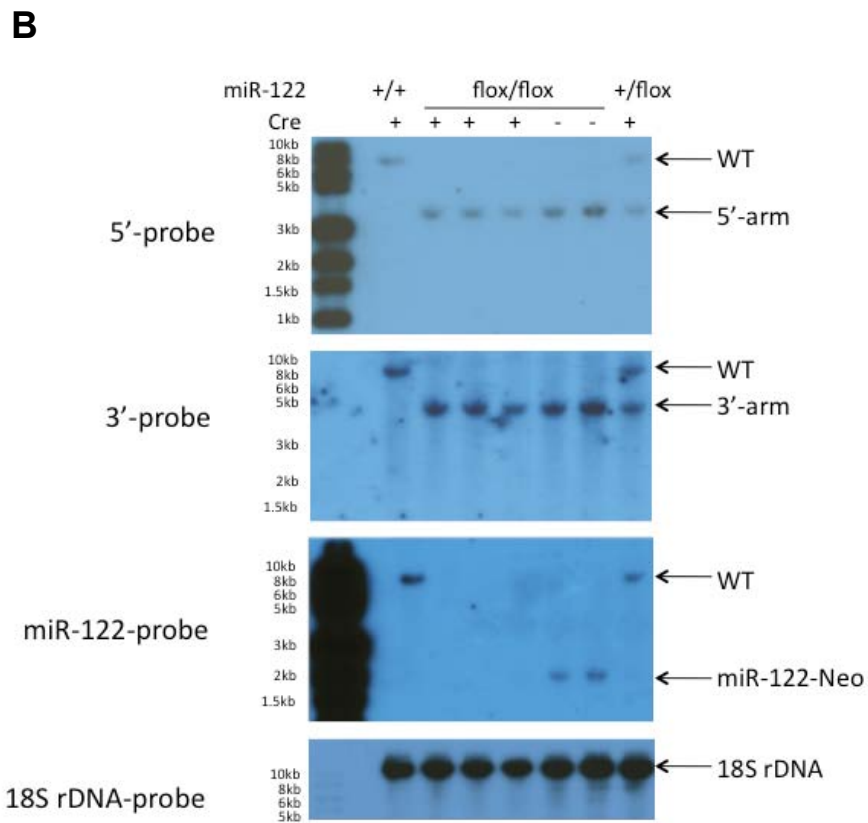
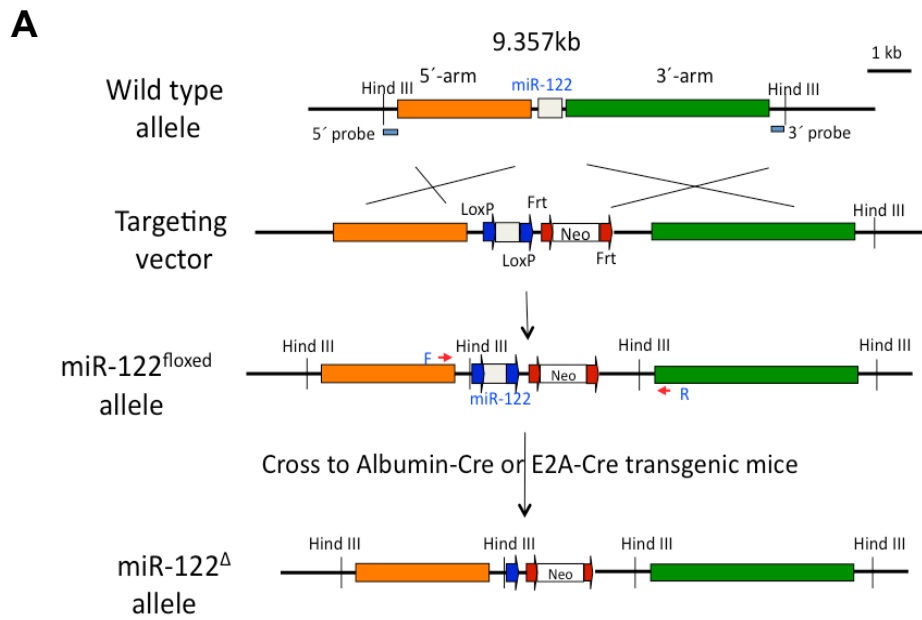
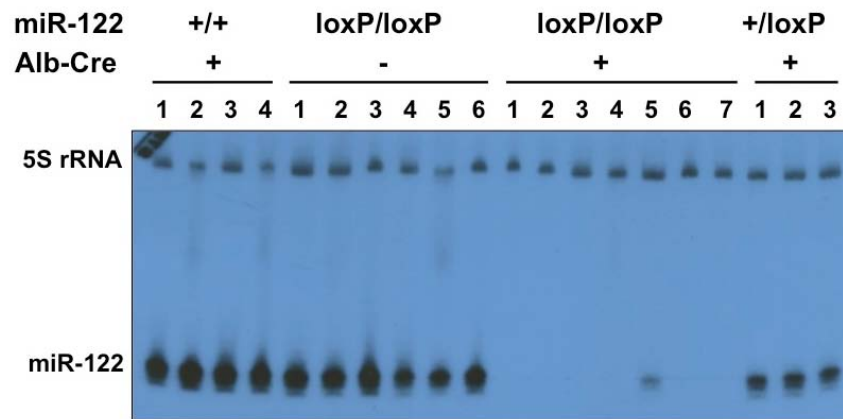


Figure 2.1 Generation of conditional and germ-line miR-122 knockout mice (A) Schematic representation of the generation of conditional and

germ-line miR-122 knockout mice. The targeting vector was generated by amplifying homology arms from 129SvJ genomic DNA, which were cloned into pBSK. Targeted mouse ES cell clones and chimeric mice were generated at the University of Michigan Knockout Mouse Core Facility. Two independent targeted clones were transmitted through the mouse germ line. **(B) Southern blot analysis of liver DNA from 10 week-old mice of the indicated genotypes.** Hind III-digested liver DNA was subjected to Southern blot analysis with probes specific for 5'- and 3'- arms as well as the *miR-122* locus to confirm correct targeting and Cre-mediated recombination. The 5' probe recognizes a ~9.5 kb fragment from the WT allele and a ~3.3 kb fragment from *miR-122*^{loxP} allele. The 3' probe recognizes a ~9.5 kb WT fragment and a ~4.6 kb *miR-122*^{loxP} fragment. Cre-mediated deletion of *miR-122* was confirmed by loss of a ~1.8 kb fragment detected with the *miR-122* probe.

A



B

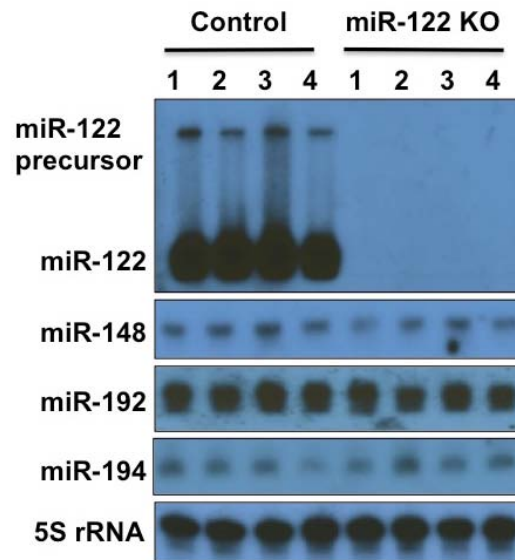


Figure 2.2 Northern blot analysis of miRNA levels in liver of LKO (A) and KO (B)

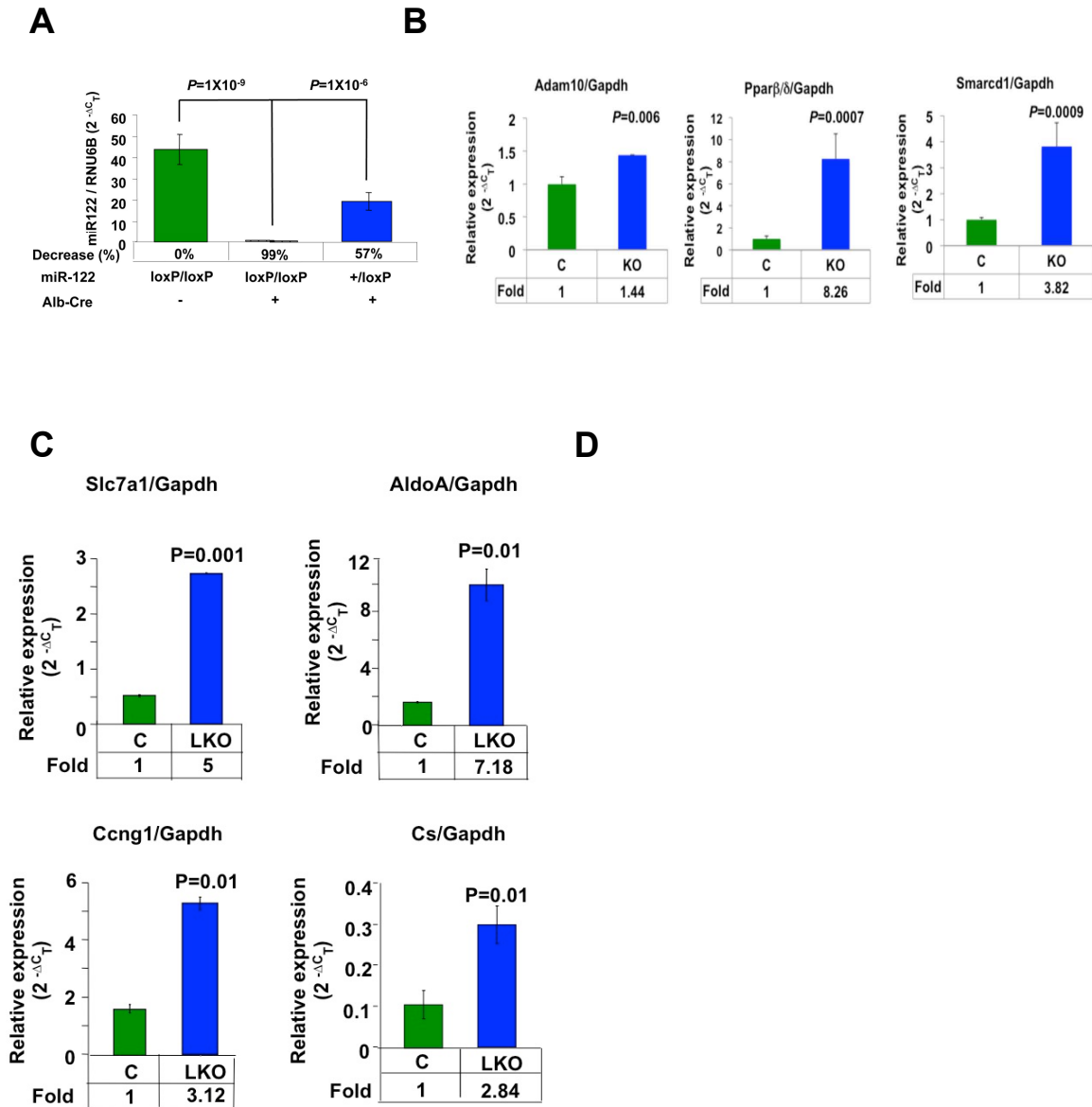


Figure 2.3 Expression of miR-122 target genes in LKO mice. (A) Quantitative PCR (qPCR) analysis of liver RNA from 10 week-old mice confirmed reduced miR-122 expression in heterozygous and homozygous LKO mice. miR-122 and RNU6B were measured in DNase-treated total RNA using respective Taqman assay kits (Invitrogen). Each sample was analyzed in triplicate (n=4). (B,C) qPCR analysis confirmed

upregulation of validated miR-122 targets in LKO (B) and KO livers (C).

DNase-treated total RNA was subjected to qPCR using the SYBR Green method (n=4 mice per condition). Data was normalized to Gapdh. C, LKO, and KO denote control (floxed), liver-specific (LKO), and germline (KO) miR-122 knockout mice, respectively. **(D) Protein levels of validated miR-122 targets are increased in livers of 5 week-old miR-122 KO mice.** Whole liver extracts prepared as described [178] were subjected to western blot analysis with specific antibodies.

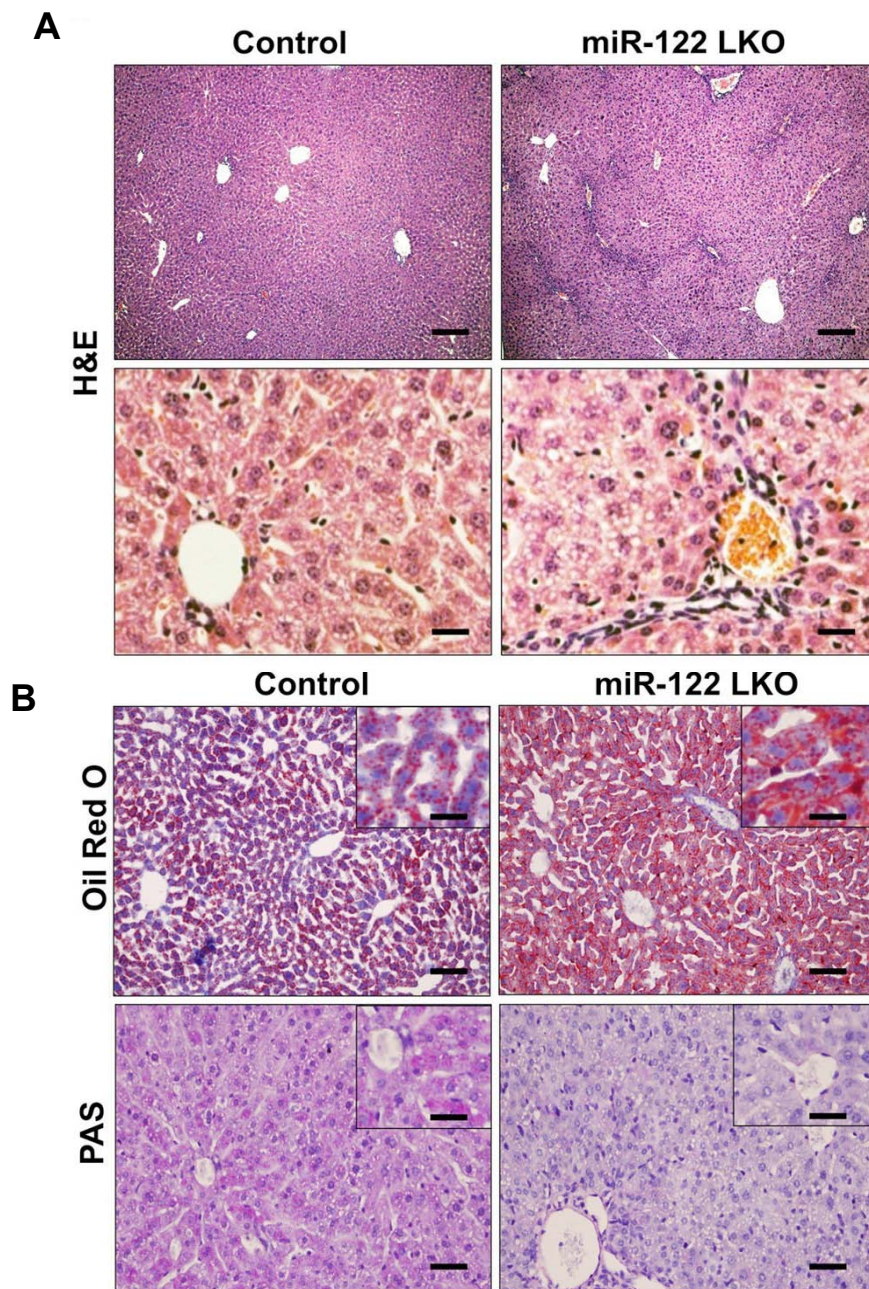


Figure 2.4 Liver morphology, lipid accumulation and glycogen depletion of LKO mice. (A) Representative liver sections of 8 week old control (floxed) and LKO mice after overnight fasting (n=8-10 mice per genotype). Scale bars: upper panel 200 μ m, lower panel, 25 μ m. **(B)** Oil-Red-O and PAS-stained liver sections from 8 week old LKO mice after overnight fasting (n=5 pe genotype). Scale bars: upper panel, 100 μ m; lower panel, 100 μ m; insets, 25 μ m.

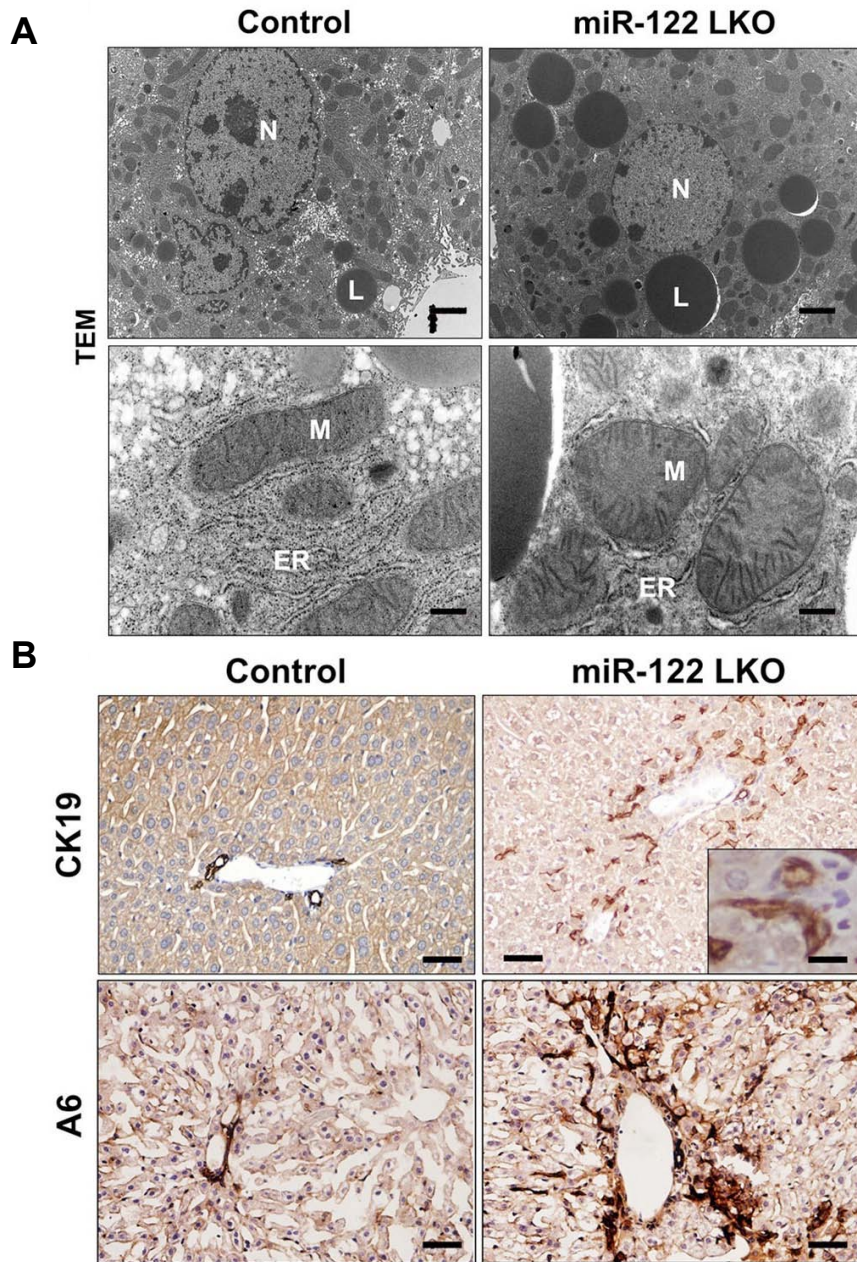


Figure 2.5 Electronic microscopy (EM) and immunohistochemical analysis of LKO mice. (A) EM of liver sections from 12 week old LKO mice. Lipid droplets (L), endoplasmic reticulum (ER), mitochondria (M), and nucleus (N) are labeled. Scale bars: upper panel: 2 μ m; lower panel: 450nm. **(B)** CK19 and A6 staining of bile duct and oval cells, respectively, in LKO livers (n=3 mice per genotype). Scale bars: upper panels: 100 μ m, inset, 5 μ m; lower panel: 25 μ m.

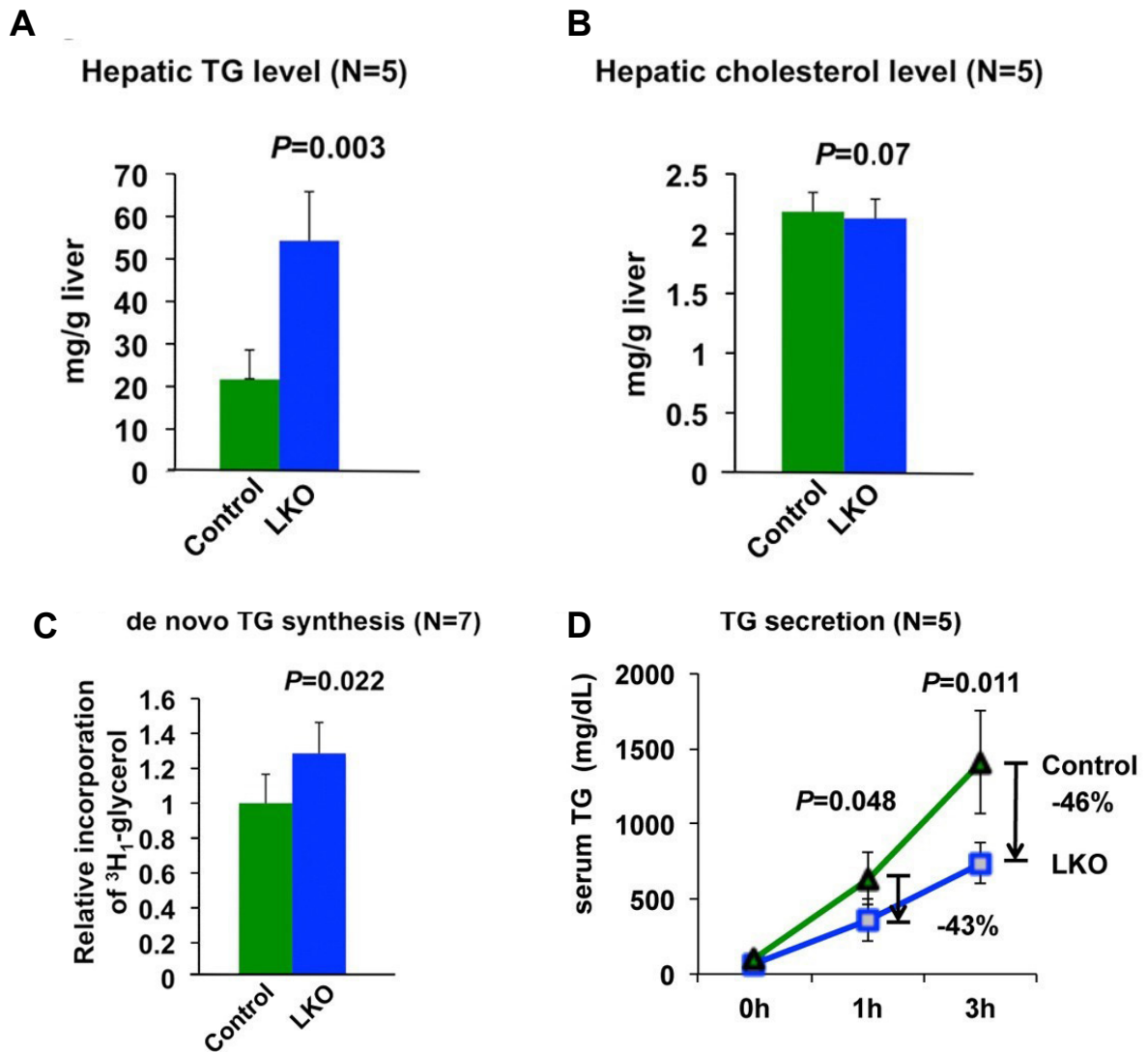


Figure 2.6 Dysregulated metabolism of triglyceride (TG) and cholesterol in LKO (A) Hepatic triglyceride (TG) and (B) cholesterol levels in 10 week old LKO mice. For this and subsequent panels, error bars represent standard deviations. (C) *De novo* TG synthesis in liver as measured by $^3\text{H}_1$ -glycerol incorporation. (D) TG secretion as measured by monitoring serum TG levels after administration of Triton WR1339.

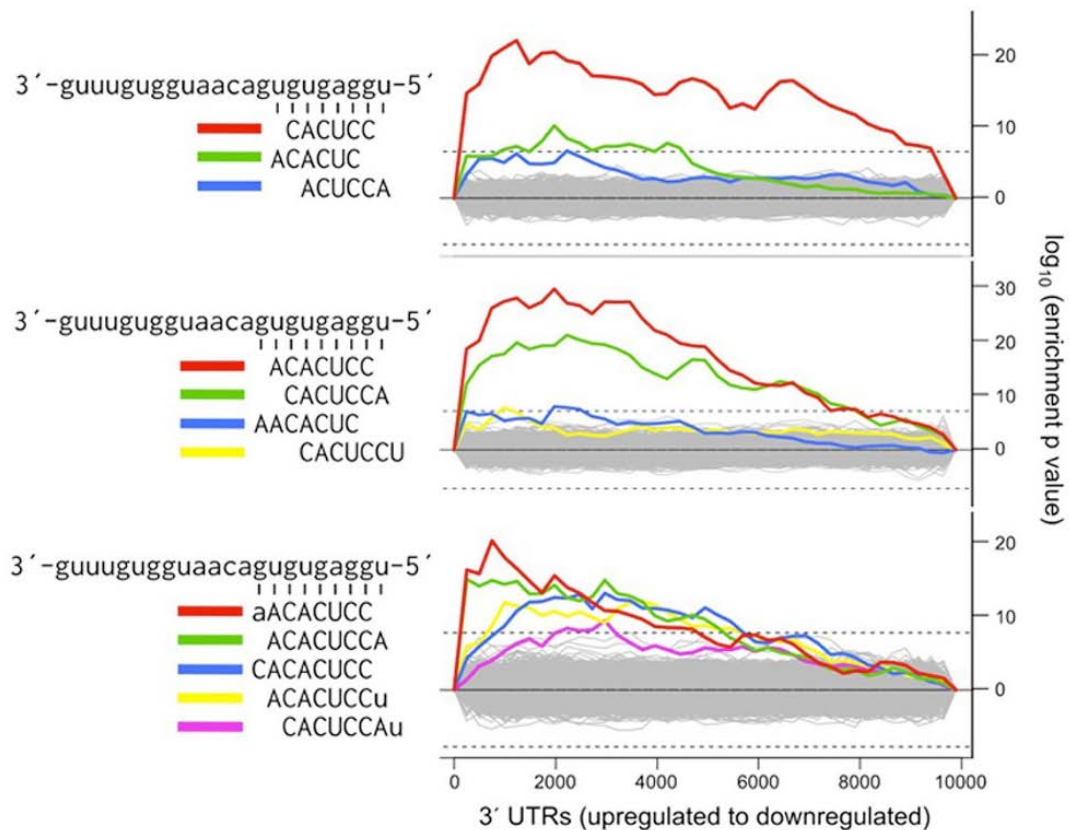


Figure 2.7 Sylamer analysis of mRNA expression from miR-122 LKO
 Sylamer plots [154] showing the enriched hexamers (upper), heptamers (middle), and octamers (lower) in transcripts that are upregulated in LKO livers. All motifs that reached statistical significance are highlighted in color on the plots and correspond to matches to the miR-122 seed sequence as shown on the left.

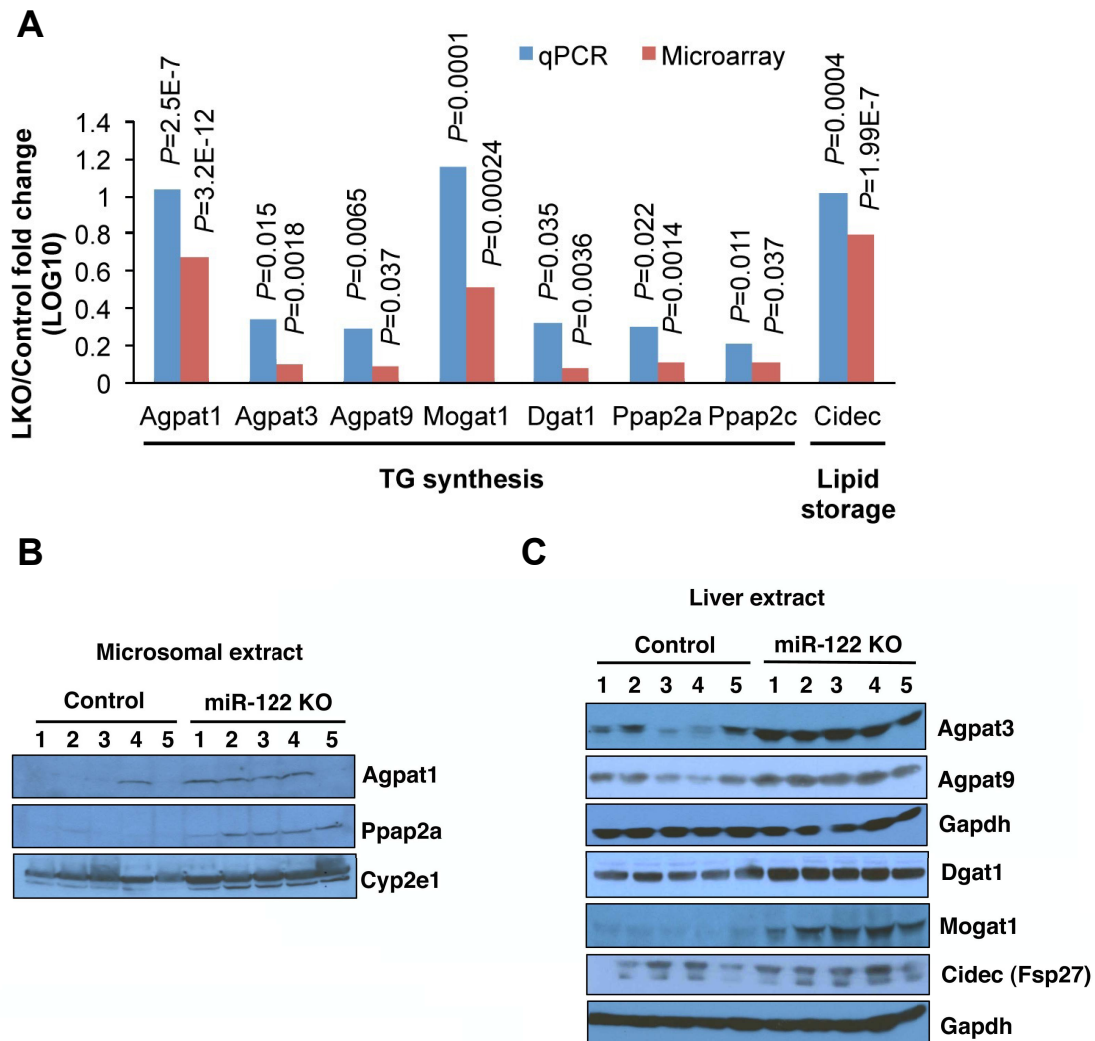


Figure 2.8 RNA and protein expression of genes involved in triglyceride synthesis and storage in LKO livers. (A) Expression of genes involved in triglyceride synthesis and storage in LKO livers. For this and subsequent panels, qPCR values represent means from triplicate measurements with multiple samples (n=4-5). Statistical significance was calculated using a 2-tailed t-test. (B,C) Protein was extracted from (B) microsomal or (C) whole liver extract. Cyp2e1 and Gapdh are the normalizers in each panel.

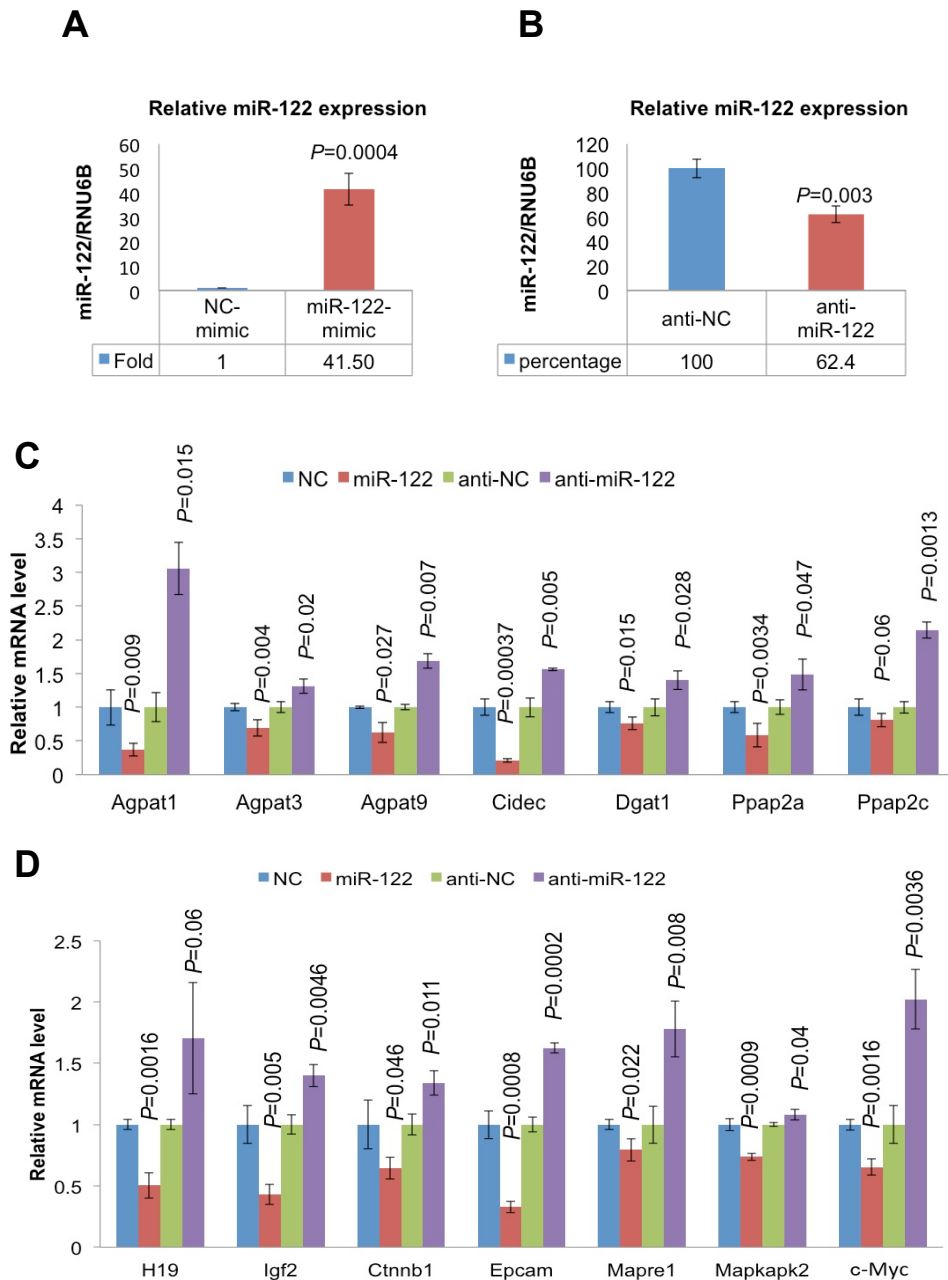


Figure 2.9 miR-122 negatively regulates the expression of genes involved in triglyceride biosynthesis and hepatocarcinogenesis. (A,B) miR-122 expression in mouse Hepa cells after transient transfection of miR-122 (A) mimic or (B) inhibitor. NC-mimic and anti-NC represent negative controls. **(C)** Relative expression of genes in the triglyceride biosynthesis pathway

normalized to Gapdh expression 40-48 hours after transfection with miR-122 mimic or inhibitor. Expression in negative control-transfected cells was assigned a value of 1. The data represent the mean of 2 independent experiments \pm standard deviations (each sample analyzed in triplicate). Statistical analyses were performed using the 2-tailed t test. mimic. . **(D)** miR-122 negatively regulates the expression of genes involved in hepatocarcinogenesis. The experiment was performed as described in Fig. S3B.

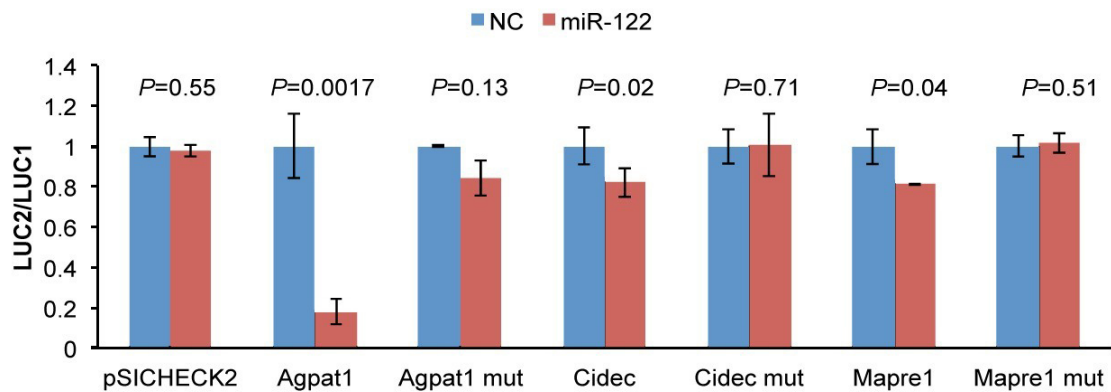


Figure 2.10 *Agpat1* and *Mapre1* are the direct targets of miR-122 *Renilla* luciferase activity (LUC2) produced from wild type or mutant *Agpat1*, *Cidec*, and *Mapre1* 3' UTR reporter plasmids or empty vector normalized to firefly luciferase activity (LUC1) produced from the same plasmid after transfection into Hepa cells together with negative control RNA (NC) or miR-122 Error bars represent standard deviations derived from 3 independent experiments.

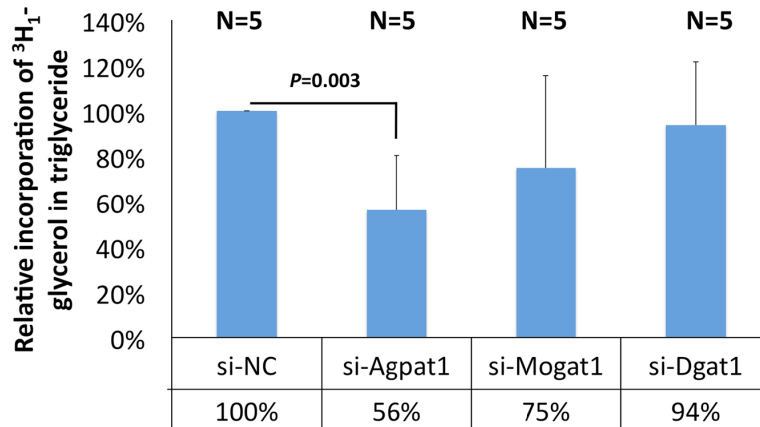
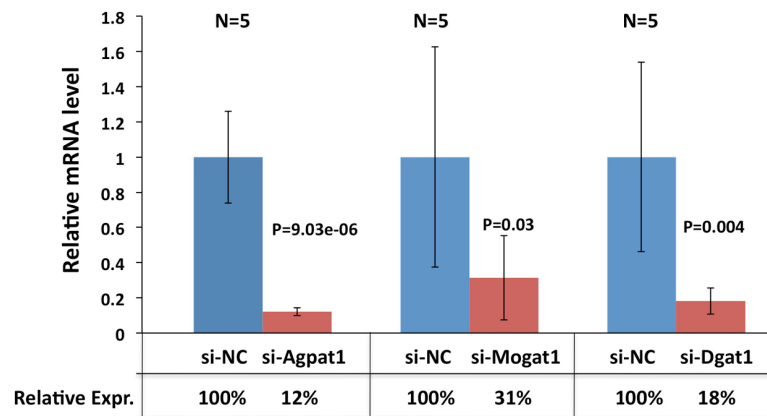
A**B**

Figure 2.11 TG synthesis was mainly affected by Agpat1 in hepatocytes

(A) Hepatocytes isolated from 3 LKO and 2 KO mice were transfected with 50nM gene-specific or scrambled siRNA for 6h and after 48h cells were incubated with ³H₁-glycerol for 15 minutes and ³H₁-incorporation in purified TG was measured in 5x10⁵ cells. **(B)** qRT-PCR analysis demonstrating depletion of specific RNAs in hepatocytes transfected with gene-specific siRNAs.

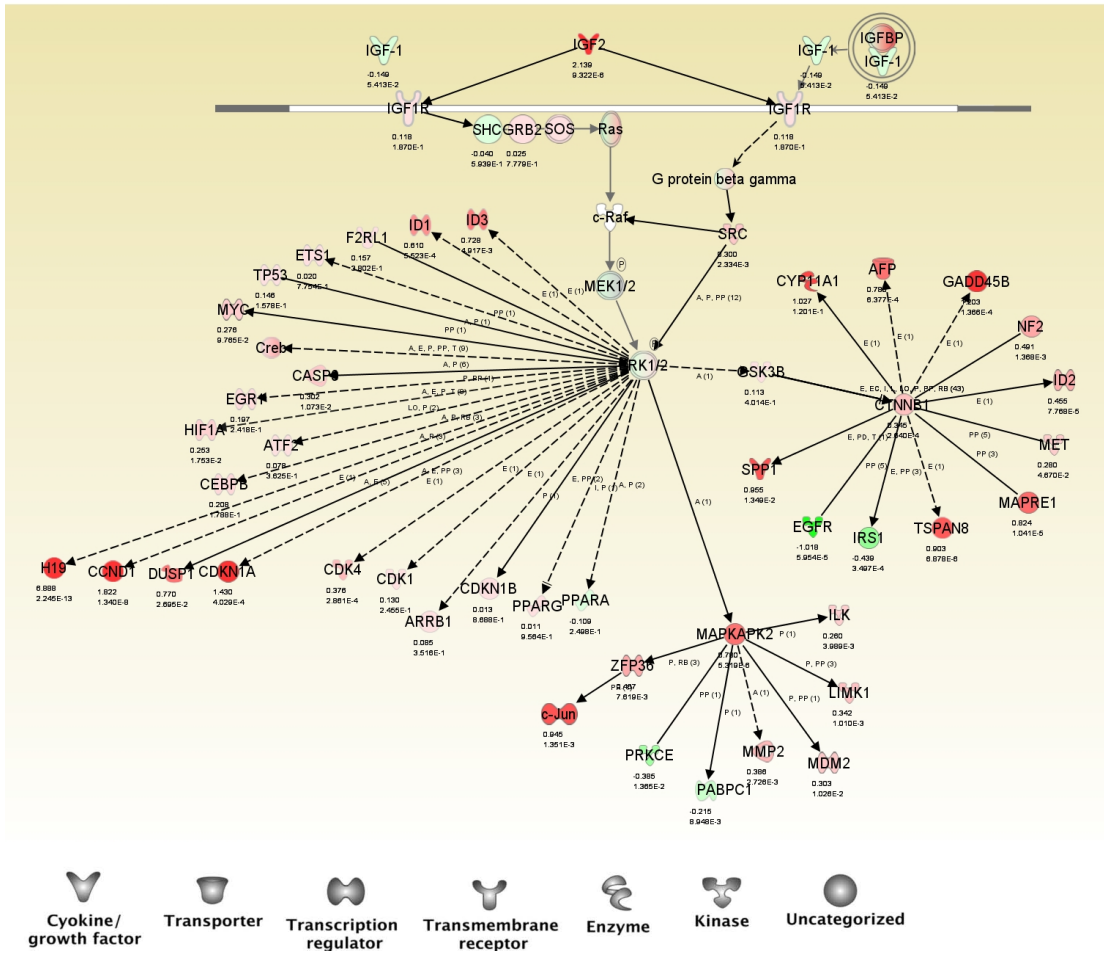


Figure 2.12 The IPA network of Igf2 signaling and downstream effectors including Ras and b-catenin (CTNNB1) is dysregulated in LKO livers. The first number below each gene represents the fold change in expression (\log_2) in LKO livers compared to controls while the second number represents the P value associated with the expression change. The shapes represent the functional class of each gene.

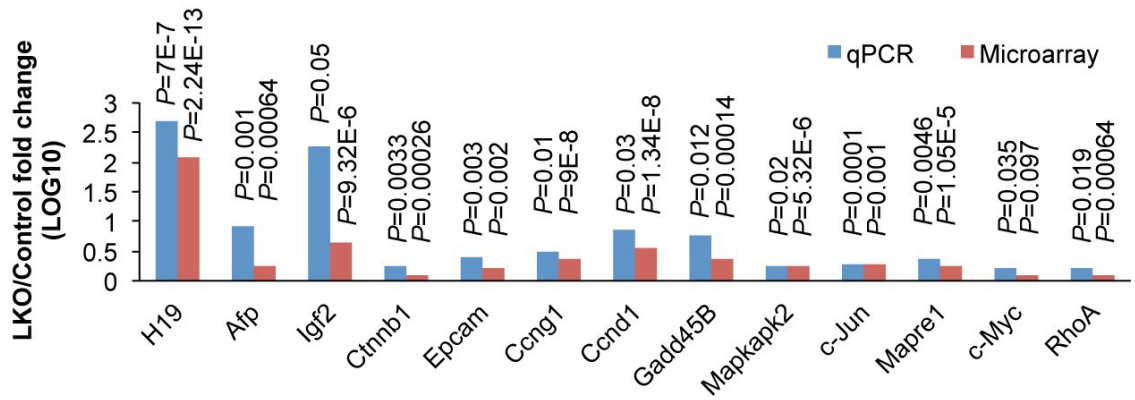
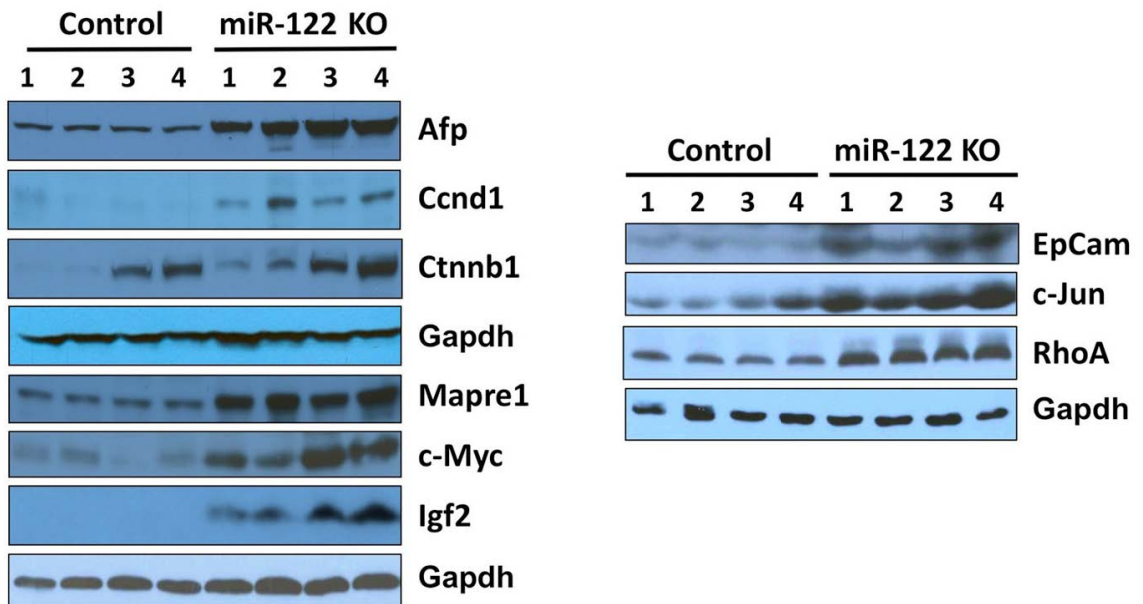
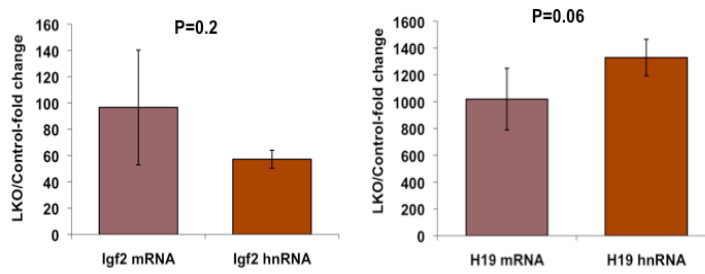
A**B**

Figure 2.13 Expression of genes involved in development, cellular proliferation and death, and cancer Expression of transcripts (A) and proteins (B) related to hepatocarcinogenesis in LKO/KO livers

A



B

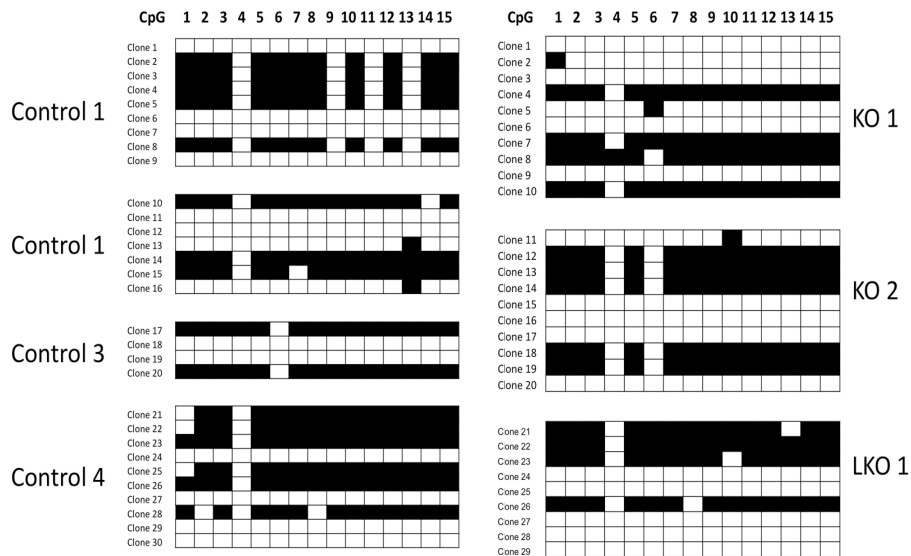


Figure 2.14 Igf2 and H19 are transcriptionally upregulated in miR-122 LKO livers. (A) qPCR analysis demonstrated comparable upregulation of Igf2 and H19 unspliced hnRNA and fully spliced mRNA in LKO livers. n=4. **(B)** Methylation profile of DMR (Differentially Methylated Region) upstream of H19 gene is not significantly altered. Genomic DNA from LKO/KO and control livers was subjected to bisulfite sequencing with DMR-specific primers [179]. Black and white boxes represent methylated and unmethylated CpG respectively.

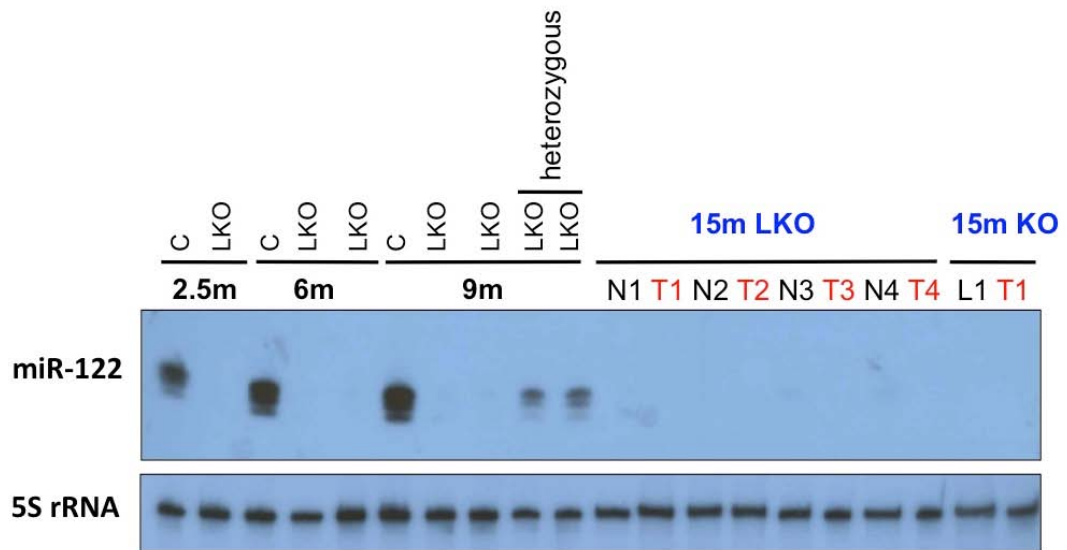


Figure 2.15 miR-122 LKO livers do not undergo repopulation with non-recombined miR-122-expressing hepatocytes. Northern blot analysis confirmed that expression of miR-122 is negligible in tumors (T) and matching benign liver tissues (N or L) in aged LKO mice. C, control mice.

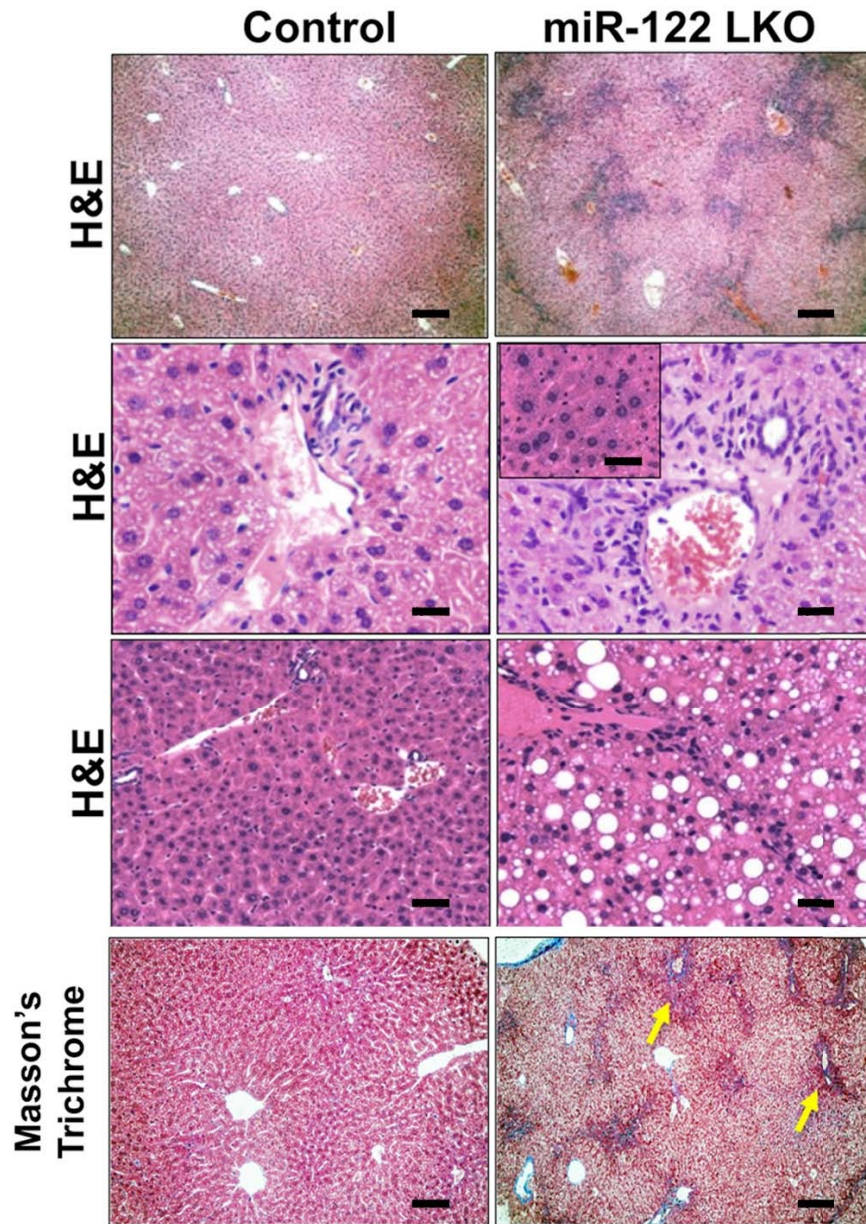


Figure 2.16 miR-122 LKO mice develop hepatitis and fibrosis with age. Portal inflammation, steatosis, and fibrosis in 6 month old LKO mice. The inset depicts foci of altered hepatocytes as observed in some livers. 8-10 mice of each genotype were analyzed after overnight fasting. Scale bars: top panel, 200 μ m; second and third panel and inset, 25 μ m; fourth panel; 200 μ m.

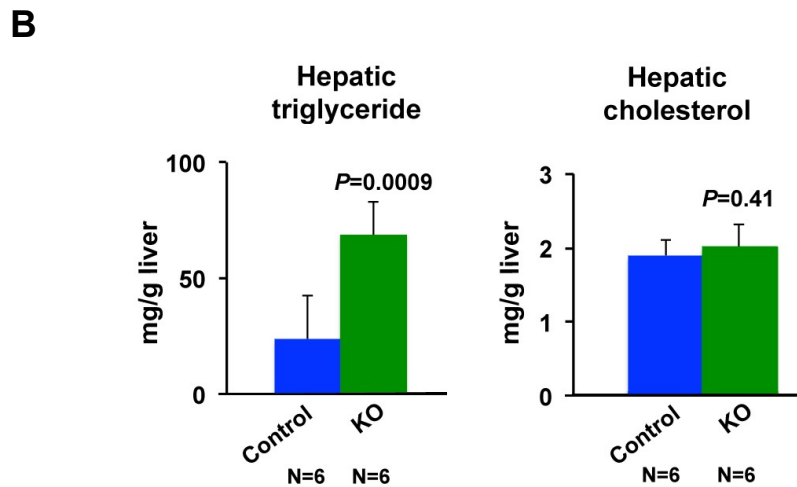
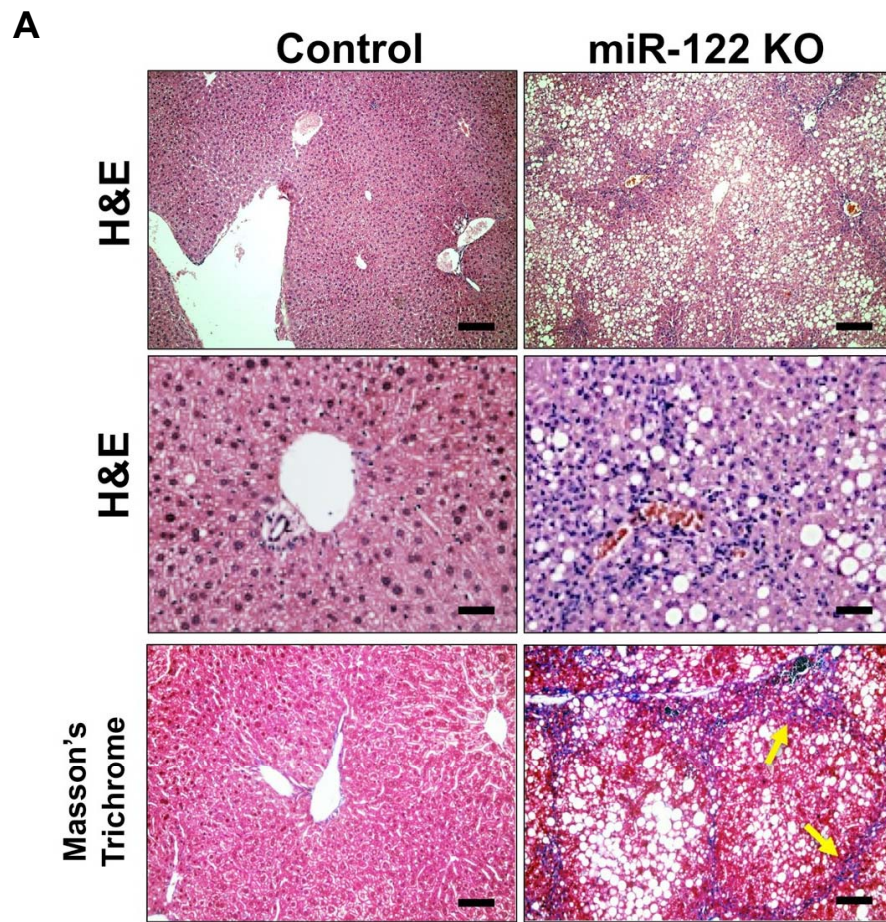


Figure 2.17 miR-122 KO mice develop hepatitis and fibrosis with age. (A) Portal inflammation, steatosis, and fibrosis in 6 month old KO mice. Scale bars: upper panel, 200 μ m; middle panel, 25 μ m and lower panel, 100 μ m. **(B)** Hepatic triglyceride and cholesterol levels in 6 month old mice.

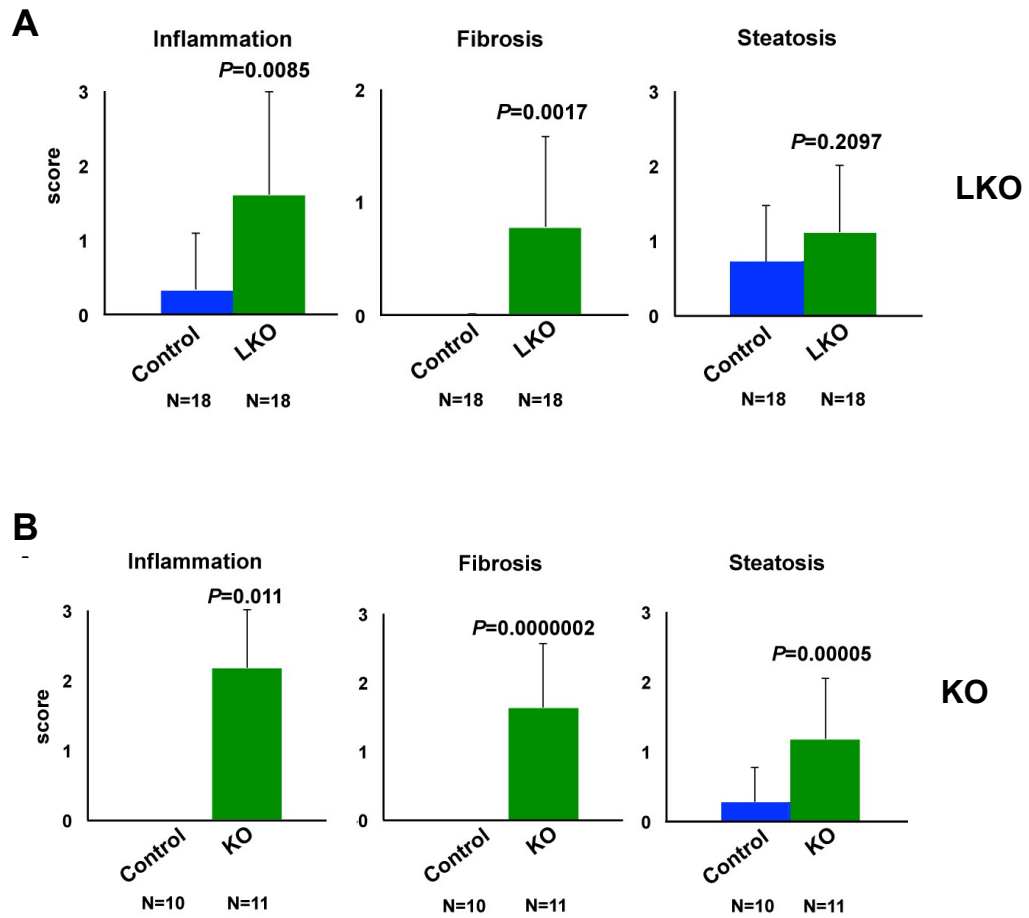


Figure 2.18 miR-122 LKO and KO mice develop hepatitis and fibrosis with age. (A,B) Portal inflammation, steatosis, and fibrosis in 6 month old (A) LKO and (B) KO mice. Scale bars: upper panel, 200 μ m; middle panel, 25 μ m and lower panel, 100 μ m.

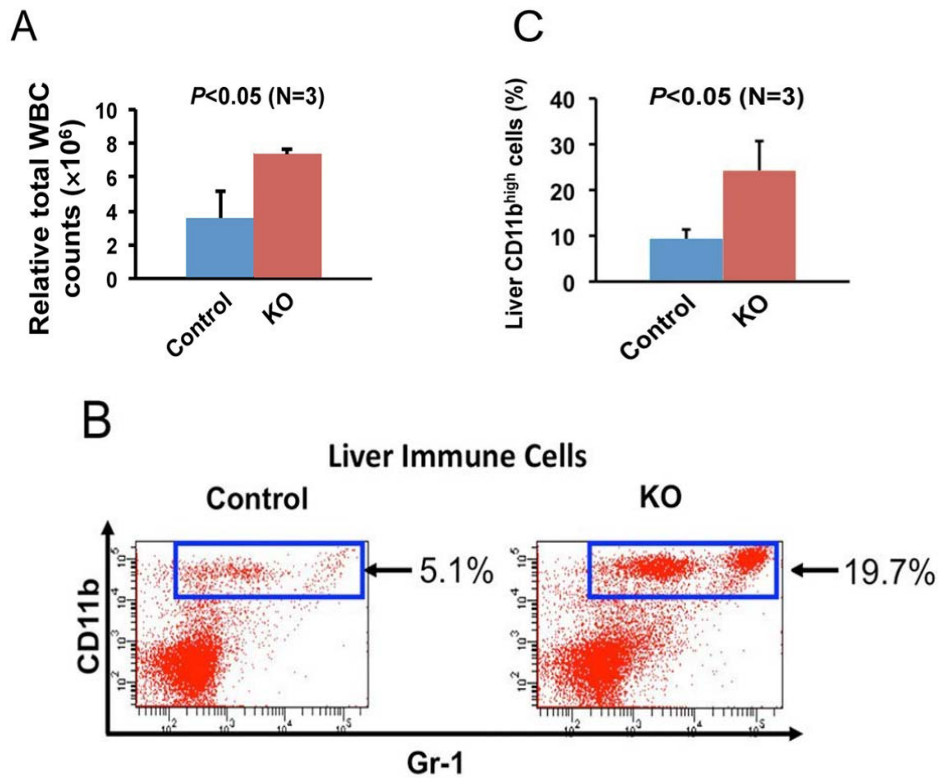


Figure 2.19. Infiltration of IL-6-producing CD11b^{high}Gr1⁺ cells in livers of LKO/KO mice. (A) Immune cells from the liver of 10-week old male KO and control mice were quantified by trypan blue exclusion. (B, C) The percentage of CD11b^{high}Gr1⁺ cells is significantly increased in 10-month old non-tumor bearing LKO/KO mice. Flow cytometric data for one representative pair of mice (B) and summary data for three mice (C) are shown.

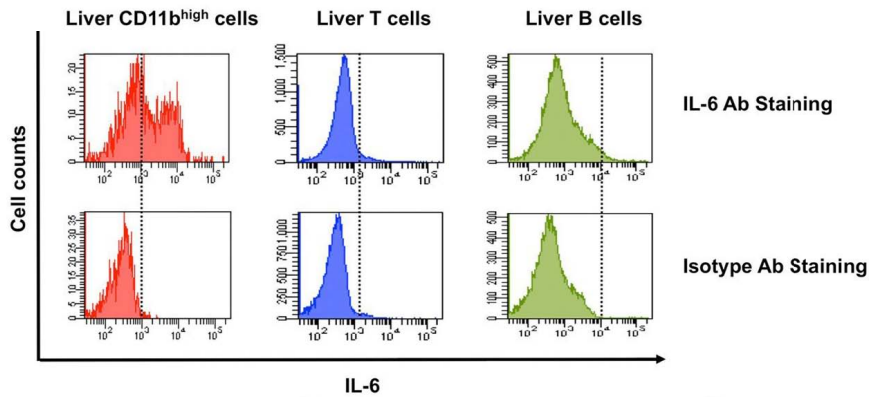
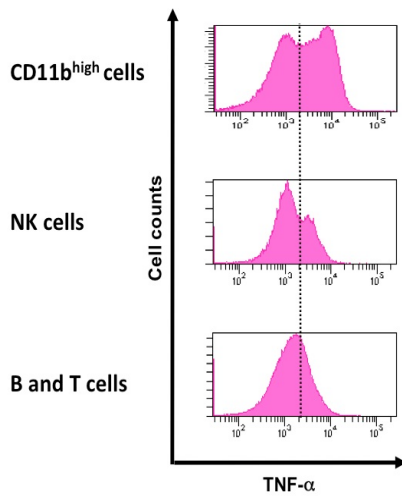
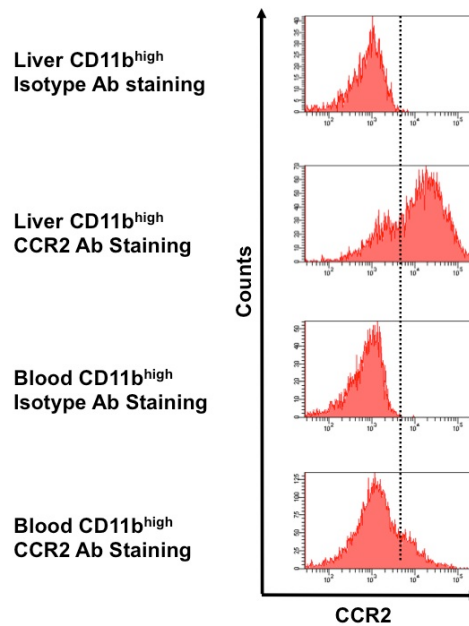
A**B****C**

Figure 2.20 Cytometric analysis of cell types expressing IL6, TNF- α , and

CCR2 (A) Intracellular flow cytometric analysis indicates that CD11b^{high}Gr1⁺ cells but not lymphocytes from the liver express IL-6. **(B)** Liver CD11b^{high}Gr1⁺ cells produce TNF- α . Liver immune cells were enriched by Percoll density gradient centrifugation and subjected to surface staining with Gr1, CD11b, CD3, CD19, and NK1.1 antibodies, followed by intracellular staining for TNF-

α . **(C)** Liver CD11b^{high} cells have higher surface expression of Ccr2 than peripheral blood CD11b^{high} cells. Liver immune cells were enriched by Percoll density gradient centrifugation and peripheral blood cells were collected after clearance by red blood cell lysis buffer. Both liver and blood immune cells were subjected to surface staining with Gr1, CD11b, CCR2, CD3, CD19, and NK1.1 antibodies.

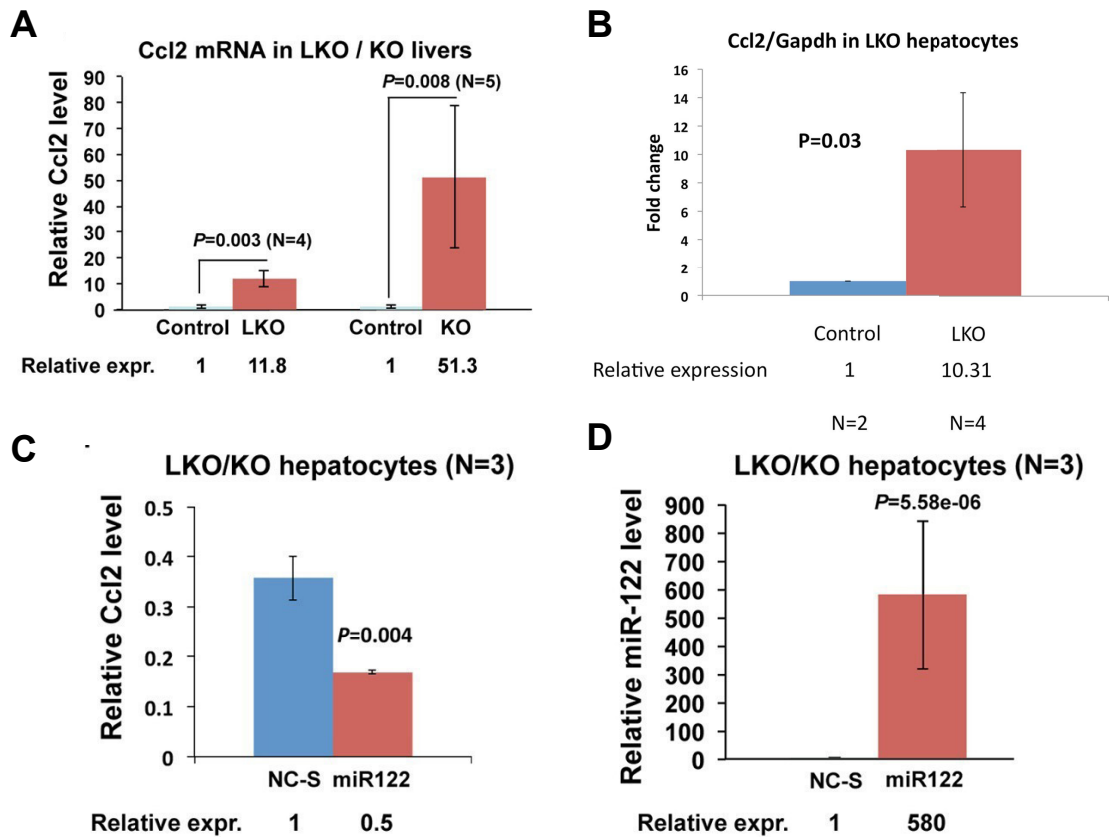


Figure 2.21 Loss of miR-122 correlated with *Ccl2* expression in primary hepatocytes (A) qPCR analysis of *Ccl2* expression in LKO (10 week old) and KO (5 week old) livers compared to age-matched controls. (B) *Ccl2* expression is increased in LKO hepatocytes. Hepatocytes isolated from KO and control (floxed) male mice were cultured overnight before RNA isolation. *Ccl2* mRNA abundance was measured by qPCR and the data was normalized to Gapdh. (C, D) *Ccl2* expression (C) is reduced in LKO/KO hepatocytes (isolated from 2 LKO and 1 KO mouse) upon overexpression of miR-122 (D). NC-S, scrambled negative control.

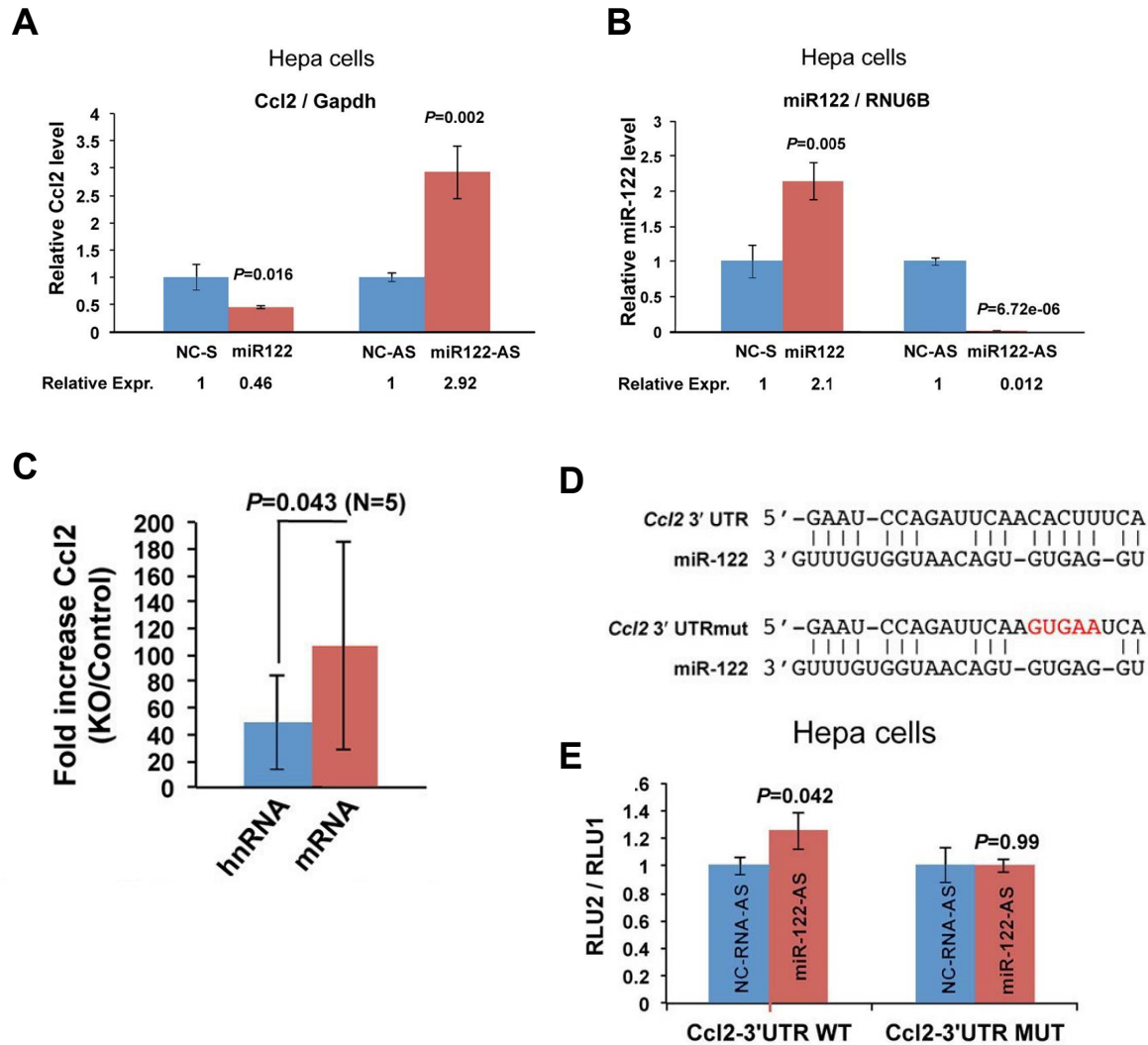


Figure 2.22 Ccl2 is a direct target gene of miR-122. (A, B) *Ccl2* (A) or miR-122 (B) expression in Hepa cells transfected with miR-122 mimic vs. control (NC-S) or anti-miR-122 (miR-122-AS) vs. control (NC-AS). **(C)** Induction of spliced *Ccl2* mRNA and unspliced *Ccl2* hnRNA in KO livers (paired t-test shown). **(D)** Predicted miR-122 binding site in the 3' UTR of *Ccl2* and corresponding mutant site. **(E)** Luciferase reporter assays as described in Fig. 2D.

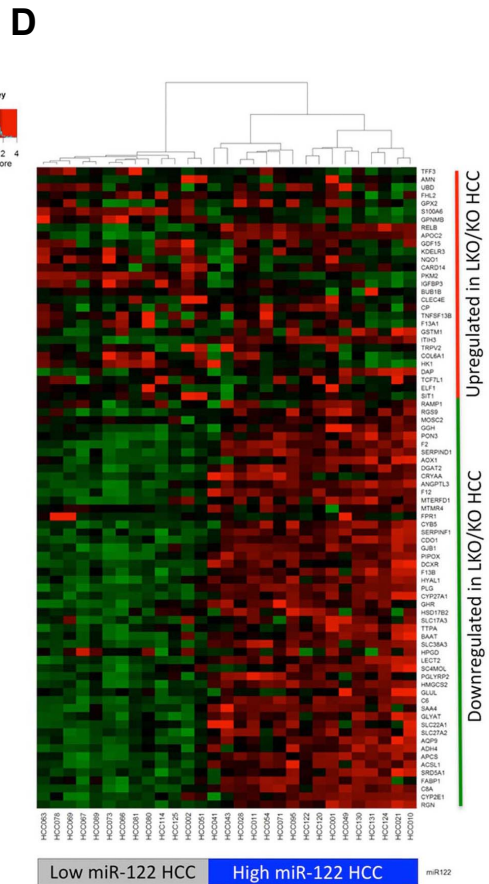
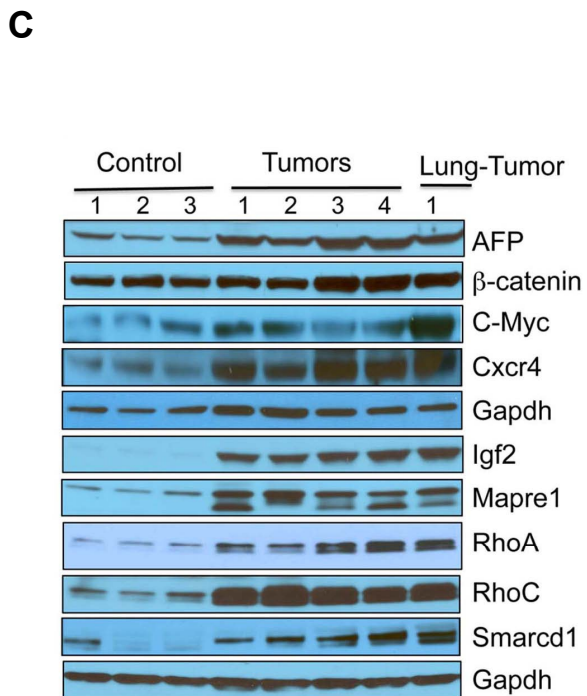
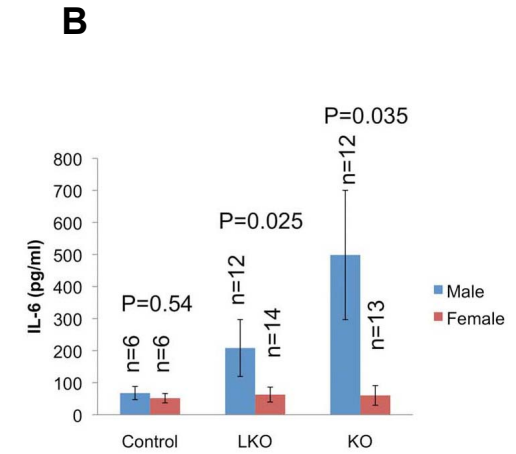
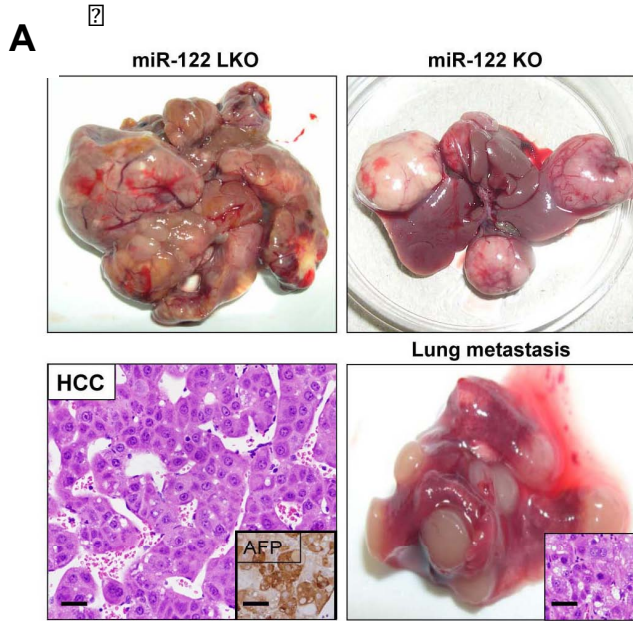


Figure 2.23 miR-122 LKO mice develop spontaneous HCC with age. (A) Representative photographs of liver and lung tumors that developed in LKO/KO mice. Left lower panel shows a representative H&E and Afp (inset)-stained section. Inset in right lower panel shows an H&E stain identifying the lung tumor as metastatic HCC. Scale bars: lower left panel: 25 μ m; left insets: 35 μ m; right insets: 25 μ m. **(B)** Analysis of serum markers of liver function in control and tumor-bearing LKO/KO mice represented as mean \pm SEM. P values were calculated using the Welch's test after log transformation. **(C)** Serum IL-6 levels in control and tumor-bearing LKO/KO mice represented as mean \pm SEM. P values were calculated using 2-tailed t-test. **(D)** Western blot analysis of whole tissue extracts demonstrated upregulation of HCC related proteins in liver and lung tumors. **(E)** Heat map and dendrogram showing that the expression levels of genes that are dysregulated in tumors from LKO/KO mice are sufficient to classify human HCCs into high and low miR-122-expressing subsets. Significance of this classification was assessed by using a bootstrap method. The heatmaps and dendrograms were generated after sampling of random gene lists of the same size from all mouse genes, then. P-value was obtained by calculating percentage of equal or better classification of HCC samples compared to the mouse gene list.

	ALP (U/L)	ALT (U/L)	Chl (mg/dL)	HDL-Chl (mg/dL)	LDL-Chl (mg/dL)	TG (mg/dL)
Control (n=16)	102.6 ± 33.2	71.3 ± 19.7	116.6 ± 28.3	63.3± 19.2	32.6 ± 9.8	103.9 ± 28.8
Median ± SE						
LKO (n=14)	225.6 ± 31.7	91.7 ± 96.5	79.7 ± 15.9	47.4 ± 11.5	14.2 ± 4.3	95.3 ± 13.1
Median ± SE						
P-value	4.67E-11*	0.41	1.8E-04*	0.01*	1.56E-06*	0.33

Table 2.1 Serum profiles of 8-10 week old control and miR-122 LKO mice.

Serum was collected from mice by cardiac puncture after overnight fasting. Biochemical analysis of serum enzymes, and lipids was performed at the OSU mouse phenotyping core facility using VetAce (Alfa Wassermann system). The control mice included 7 male and 9 female. The LKO mice included 6 male and 8 female. Bilirubin levels (total and direct) were not altered (data not shown). Abbreviations: ALP, alkaline phosphatase; ALT, alanine aminotransferase; Chl, cholesterol; HDL-Chl, high-density lipoprotein cholesterol; TG, triglyceride; LDL-Chl, low-density lipoprotein cholesterol. Statistical significance was determined by student's 2-tailed t test. *P*-value<0.05 indicated by asterisks.

	ALP (U/L)	ALT (U/L)	Chl (mg/dL)	HDL-Chl (mg/dL)	TG (mg/dL)
Control					
(n=7)	262.9 ± 51.5	42.5 ± 15.3	130.2 ± 70.7	47.4 ± 27.7	194 ± 101.5
Median ± SE					
KO					
(n=8)	615.1 ± 69.2	44.2 ± 13.7	61.8 ± 25.0	21.6 ± 10.0	156.2 ± 74.7
Median ± SE					
P-value	5.82E-07*	0.812	0.033*	0.039*	0.421

Table 2.2 Serum profiles of 5 week old control and miR-122 KO mice

Serum was collected from mice by cardiac puncture after overnight fasting. Control mice included 4 male and 3 female. KO mice included 4 male and 4 female. Statistical significance was determined by student's 2-tailed t test. *P*-value < 0.05 indicated by asterisks.

#	IPA Score	Network functions
1	33	Organismal Survival, Cellular Movement, Cellular Growth and Proliferation
2	18	Lipid Metabolism, Small Molecule Biochemistry, Nucleic Acid Metabolism
3	16	Lipid Metabolism, Small Molecule Biochemistry, Molecular Transport
4	15	Amino Acid Metabolism, Molecular Transport, Small Molecule Biochemistry
5	15	Organismal Development, Hematological Disease, Immunological Disease
6	13	Lipid Metabolism, Molecular Transport, Small Molecule Biochemistry
7	13	Cell Death, Gene Expression, Cancer

Table 2.3. Networks identified by Ingenuity Pathway Analysis among dysregulated genes in livers of miR-122 LKO mice. The IPA application (<http://www.ingenuity.com/products/IPA/Free-Trial-Software.html>) was used to identify gene networks that were overrepresented among the genes that exhibited ≥ 1.5 fold up- or down-regulation with a *P*-value ≤ 0.0001 in LKO livers. A significance score of ≥ 3 indicates that there is a less than 1 in 1000 chance that the highlighted genes were assembled into a network due to a random chance.

Pathway	Gene	qPCR (LKO/control)	P-value	Microarray (LKO/control)	P-value
Triglyceride synthesis	Agpat1	10.8	2.5E-07	4.72	3.15E-12
	Agpat3	2.2	0.015	1.25	0.002
	Agpat9	2.0	0.007	1.22	0.037
	Mogat1	14.5	0.000	3.23	0.000
	Dgat1	2.1	0.036	1.2	0.004
	Ppap2a	2.0	0.022	1.3	0.001
	Ppap2c	1.6	0.011	1.3	0.034
Fatty acid synthesis	Acly	0.62	0.031	0.65	1.93E-05
	Chrebp	0.59	0.000	0.58	2.86E-07
	Srebp1c	0.56	0.010	0.58	7.05E-05
	Scd1	0.18	0.050	0.28	0.0002
	Acs14	2.34	0.010	1.91	2.65E-05
Fatty acid oxidation	Ehhadh	2.10	0.002	2.32	1.38E-05
	Ucp2	4.92	0.000	4.39	1.00E-09
Cholesterol synthesis	Hmgcr	0.69	0.050	0.68	0.000
Lipid transport	Stard4	0.59	0.014	0.69	3.24E-06
	(Stard2)	3.38	0.05	1.78	6.00E-05
	Slc27a1 (FATP1)	3.52	0.008	2.19	0.000
Lipid storage	Cidec (Fsp27)	10.42	0.000	6.29	1.99E-07

Table 2.4. Genes involved in lipid metabolism that are dysregulated in the livers of miR-122 LKO mice. qPCR analyses were performed in triplicate. The primer sequences are provided in the supplemental methods. Relative expression was calculated using the $\Delta\Delta C_T$ method [178]. Statistical analysis of the qPCR data was performed using the student's t 2-tailed test.

Pathway	Gene	qPCR (LKO/control)	P-value	Microarray (LKO/control)	P-value
Cancer	H19	493	0.000	118.45	0.000
	Afp	8.33	0.001	1.72	0.001
	Igf2	185	0.050	4.41	0.000
	MapKapk2	1.73	0.020	1.72	0.000
	Ctnnb1	1.27	0.000	1.71	0.000
	c-Jun	1.9	0.000	1.93	0.001
	Epcam	2.58	0.003	1.59	0.002
	Ccng1	3.12	0.010	2.27	0.000
	Ccnd1	7.13	0.030	3.54	0.000
	Gadd45b	5.66	0.012	2.30	0.000
	c-Myc	1.60	0.035	1.21	0.097
	Rhoa	1.60	0.010	1.26	0.000

Table 2.5 Genes related to hepatocarcinogenesis are significantly upregulated in miR-122 LKO livers. qRT-PCR analyses were performed in triplicate. The primer sequences are provided in the supplemental methods. Relative expression was calculated using the $\Delta\Delta C_T$ method [178]. Statistical analysis of the qPCR data was performed using the student's t 2-tailed test.

Pathway	Gene	qPCR (LKO/control)	P-value	Microarray (LKO/control)	P-value
Cancer	H19	493	0.000	118.45	0.000
	Afp	8.33	0.001	1.72	0.001
	Igf2	185	0.050	4.41	0.000
	MapKapk2	1.73	0.020	1.72	0.000
	Ctnnb1	1.27	0.000	1.71	0.000
	c-Jun	1.9	0.000	1.93	0.001
	Epcam	2.58	0.003	1.59	0.002
	Ccng1	3.12	0.010	2.27	0.000
	Ccnd1	7.13	0.030	3.54	0.000
	Gadd45b	5.66	0.012	2.30	0.000
	c-Myc	1.60	0.035	1.21	0.097
	Rhoa	1.60	0.010	1.26	0.000

Table 2.6 Genes related to hepatocarcinogenesis are significantly upregulated in miR-122 LKO livers. qRT-PCR analyses were performed in triplicate. The primer sequences are provided in the supplemental methods. Relative expression was calculated using the $\Delta\Delta C_T$ method [178]. Statistical analysis of the qPCR data was performed using the student's t 2-tailed test.

	ALP (U/L)	ALT (U/L)	GGT (U/L)
Control			
(n=7)	81.0 ± 42.64	54.6 ± 18.2	0.67 ± 0.82
Median ± SE			
KO			
(n=5)	252.3 ± 63.0	54.6 ± 18.2	4.2 ± 2.4
Median ± SE			
P-value	0.0002*	0.10	0.007*

Table 2.7 Serum profiles of 6 month old control and miR-122 KO mice

Serum was collected from mice by cardiac puncture after overnight fasting. Control mice included 7 males and KO mice included 5 males. Statistical significance was determined by student's 2-tailed t test. *P*-value < 0.05 indicated by asterisks.

	Control	miR-122 LKO
mice examined	27 (M:F=15:12)	46 (M:F=26:20)
mice with HCC	0	15 (M:F=13:2)
HCC grade 1	0	2 (M:F=2:0)
HCC grade 2	0	7 (M:F=7:0)
HCC grade 3	0	6 (M:F=4:2)
tumor size (mm²)	0	219.9 ± 197.4
tumor numbers	0	2.69 ± 3.11
total tumor weight (g)	0	2.98 ± 3.43
largest tumor weight (g)	0	1.48 ± 1.23

Table 2.8 Summary of the incidence and characteristics of the tumors that developed in 12-17 month-old LKO mice Mice within the age group of 12-17 months were randomly selected to examine. HCC grading was based on Edmondson-Steiner's grading system [PMID: 13160935]. All measurements of tumor were presented as mean ± SD. Abbreviation: M, male; F, female.

	Control	miR-122 KO
mice examined	24 (M:F=12:12)	39 (M:F=20:19)
mice with tumor	0	19 (M:F=10:9)
tumor size (mm²)	0	146.2 ± 97.1
tumor numbers	0	2.55 ± 2.11
total tumor weight (g)	0	1.63 ± 1.12
largest tumor weight (g)	0	1.15 ± 0.78

Table 2.9 Summary of the incidence and characteristics of the tumors that developed in 10-15 month old KO mice Mice within the age group of 10-15 months were randomly selected to examine. All measurements of tumor were presented as mean ± SD. Abbreviation: M, male; F, female.

	miR-122 KO-male	miR-122 KO-female
HCC incidence	10/20	9/19
HCC grade 1	3	6
HCC grade 2	6	2
HCC grade 3	1	1
tumor size >50 mm²	8/10	5/9
tumor numbers	2.50 ± 1.38	2.89 ± 2.52
total tumor weight (g)	2.02 ± 1.03	1.20 ± 0.88
largest tumor weight (g)	1.37 ± 0.64	0.91 ± 0.78

Table 2.10 Summary of the incidence and characteristics of HCC developed in 10-15 month old KO male and female mice Mice within the age group of 10-15 months were randomly selected to examine. HCC grading was based on Edmondson-Steiner's grading system [PMID: 13160935]. HCC incidences were presented as the number of HCC bearing mice divided by the total examined mice number. Similar way was used for the number of mice bearing tumor size over 50 mm². All measurements of tumor were presented as mean ± SD.

Chapter 3. Liposomal delivery of miR-122 to HCC cell lines and DEN induced HCC animal model

3.1 Abstract

To restore dysregulated gene expression resulting from loss of microRNA, lipid nanoparticles (LNPs) were developed as vehicles for systemic delivery. The novel LNPs, termed LNP-DP1, consist of a conditionally ionizable cationic lipid, 2-dioleyloxy-N,N-dimethyl-3-aminopropane (DODMA), egg PC, cholesterol (Chol) and Chol-polyethylene glycol (Chol-PEG). miR-122 is the most abundant liver-specific tumor suppressor microRNA, which is downregulated in primary HCC. Transfection of miR-122 to HCC cell lines by LNP-DP1 diminished expression of miR-122 targets by >95%. LNP-DP1 was preferentially taken up by hepatocytes and tumor epithelial cells as demonstrated by systemic delivery of fluorescence labeled siRNA by LNP-DP1 in different mouse models of HCC. LNP-DP1 did not induce significant liver or kidney damage in mice. miR-122 was successfully delivered and found to be functional in hepatocytes and tumor

cells as demonstrated by downregulation of several target genes. To demonstrate therapeutic potential of miR-122, LNP-DP1 encapsulating miR-122 was intratumorally injected into HCC xenograft developed in *nude* mice. The tumor growth was significantly suppressed within 30 days after delivery of miR-122, which correlated well with reduced expression of its target genes and proliferation marker. These data demonstrate the potential of LNP mediated microRNA delivery as an alternate strategy for HCC therapy.

3.2 Introduction

Hepatocellular carcinoma (HCC) is the fifth most common cancer worldwide and the third leading cause of cancer-related deaths [134, 180, 181]. In United States, the incidence of HCC has almost tripled during the past two decades and has become one of the fastest growing cancers [182]. HCC often occurs in the liver predisposed to hepatic steatosis, chronic hepatitis, fibrosis, and cirrhosis [134]. The major factor contributing to the increase in HCC-related deaths is late diagnosis and the lack of effective drugs or therapeutic strategies. While surgical removal of tumor tissues is an effective approach to protect relatively healthy liver tissue [183], it is only applicable to a small subset of HCC patients who have with specific pathological conditions, such as confined tumor mass without portal

hypertension. Therefore, there is an urgent need to develop novel therapeutic strategy to treat this deadly disease.

A promising strategy is to deliver the tumors either microRNAs (miR mimics) that function as tumor suppressors or anti-oligos to miRs that exhibit oncogenic characteristics. MicroRNAs regulate many biological processes including development, metabolism and aging [184, 185]. MicroRNAs are essential for liver homeostasis since loss of Dicer1, a central enzyme in microRNA processing, compromises liver functions and promotes hepatocarcinogenesis in mice [138, 186, 187]. Recent findings have suggested therapeutic potential of microRNAs against liver cancer [86, 90, 188]. We have demonstrated that the level of miR-122, the most abundant and developmentally regulated liver-specific microRNA [129, 152], is drastically reduced in human and rodent HCCs and that its overexpression inhibits the growth of HCC cell lines [80, 81]. More importantly, miR-122 is a biomarker for HCCs with poor prognosis and metastasis [189-191]. Other microRNAs, including miR-199a and miR-26a, also inhibit hepatocarcinogenesis and, therefore, exhibit therapeutic potential against this cancer [85].

Several approaches, such as hydrodynamic injection [192, 193], viral infection [194, 195] and nanoparticles [124, 196], were developed to deliver siRNA/microRNAs to cells to modulate gene expression. Cationic lipids, or lipid-like materials based nanoparticles, are the most well studied vesicles for delivery of siRNA *in vivo* [197, 198]. After endocytosis, the cationic lipids form

ion pairs with anionic phospholipids of the endosomal membrane. Subsequently, this newly formed cone shape ion pairs may disrupt the endosomal membrane and promote the release of encapsulated siRNA from the endosome to exert its biological function within cells [199, 200]. For example, stable nucleic acid lipid particle (SNALP), a new formulation of cationic LNPs, has been successfully used to deliver siRNA for silencing target genes in non-human primates and is currently being tested in clinical trials [124, 201, 202].

In this study, we developed a new LNP-DP1 formulation to systemically deliver liver-specific miR-122 to HCC and thus provide proof-of-concept for the potential of exogenous miR-122 mimic in HCC therapy. Because synthetic miRNA and siRNA molecules share similar properties, we used the fluorescence labeled siRNA to demonstrate the preferential uptake of LNP-DP1 by the liver and HCC. A miR-122 knockout mouse model generated in our laboratory was used to evaluate the altered expression of cancer-related genes by systemic administration of miR-122 using novel LNP-DP1 for delivery. Here, we report significant inhibition of HCC growth in xenograft mice model following intratumoral delivery of miR-122 by LNP-DP1.

3.3 Materials and Methods

3.3.1 Materials

2-Dioleyloxy-N,N-dimethyl-3-aminopropane (DODMA) was purchased from Genzyme Pharmaceuticals (Cambridge, MA). Egg phosphatidylcholine (egg PC) was purchased from Lipoid (Newark, NJ). Cholesterol (Chol) was purchased from Sigma-Aldrich (St. Louis, MO). 1,2-Dimyristoyl-sn-glycerol [methoxy(polyethylene glycol)-2000] (DMG-PEG), 1,2-Distearoyl-sn-glycerol [methoxy(polyethyleneglycol)- 2000] (DSG-PEG), α -(3 β)-Cholest-5-en-3-yl-W-hydroxy [methoxy (polyethylene glycol)] (Chol-PEG) were from NOF America Corporation (White Plains, NY). N-palmitoyl-sphingosine-1 -succinyl [methoxy(polyethylene glycol) 2000] (Ceramide- PEG), 1,2-Dimyristoyl-sn-glycero-3-phosphoethanolamine-N-[methoxy(polyethylene glycol)-2000] (C14-PE-PEG), 1,2-Distearoyl-*sn*-glycero-3-phospho- ethanolamine-N-[methoxy(polyethylene glycol)-2000] (DSPE-PEG), 1,2-Dipalmitoyl-*sn*-glycero- 3-phosphoethanolamine-N-[methoxy(polyethylene glycol)-2000] (C16-PE-PEG) were obtained from Avanti Polar Lipids (Alabaster, AL). Other chemicals and reagents were obtained from Sigma-Aldrich (St. Louis, MO) and were of analytical grade. All tissue culture media and supplies were obtained from Invitrogen (Carlsbad, CA). Luciferase (GL2 + GL3) siRNA (AM 4629), negative control siRNA (AM 4611), cy3 labeled control siRNA (AM 4621) and FAM labeled control siRNA (AM 4620) were obtained from Applied Biosystems (Austin, TX). miRNA-122 mimic and non-targeted control mimic were purchased from Dharmacon (Pittsburgh, PA).

3.3.2 Preparation of miRNA encapsulated LNPs

The cationic liposomes were prepared as described previously with minor modification[203]. Briefly, an ethanolic lipid solution composed of DODMA/EggPC/Chol/PEG-lipid at 45:15:35:5 (molar ratio) was mixed with 20 mM HEPES (pH7.4) solution at room temperature. Ethanol was removed by dialysis using a MWCO 10,000 Dalton Float-A-Lyzer (Spectrum Laboratories Inc., Rancho Dominguez, CA) against 20 mM HEPES (pH=7.4) buffer for 2 hours at room temperature. The resulting liposomes were filtered and sterilized. miRNA encapsulated LNPs were prepared by mixing cationic liposomes with an equal volume of miRNA in 20 mM HEPES buffer at room temperature for 15 min. The weight ratio of lipids to miRNA was 10:1. For intravenous injection to mice, the miRNA-LNPs were centrifuged and concentrated to 200 ml using the Amicon® Ultra-4 Ultracel-50k Da centrifugal device (Millipore, Billerica, MA). The encapsulation efficiency of miRNA in LNPs was determined by RiboGreen assay (Invitrogen, Carlsbad, CA). The siRNA encapsulated LNPs were prepared by following the same method. The particle size of LNPs was determined by dynamic light scattering using a particle sizer BI-200SM (Brookhaven Instruments Corp., Holtsville, NY) in an intensity-weighted mode. Following dilution in water, the zeta potentials (ζ) of LNPs were measured using a ZetaPALS zeta potential analyzer (Brookhaven Instrument Corp., Holtsville, NY). The Smoluchowski model was used to calculate the zeta potential and the mean \pm SD was reported.

3.3.3 Liver tumor models

The animal studies were carried out in accordance with the internal Institutional Animal Care and Use Committee guidelines at The Ohio State University. All athymic nude mice were obtained from Harlan Laboratory (Indianapolis, IN). *Nude* mice were inoculated subcutaneously with SK Hep-1 cells (5×10^6) to produce HCC xenograft model. Biodistribution study was performed when the tumors reached $\sim 200 \text{ mm}^3$. DEN induced tumor model was developed as described[176]. Briefly, on postnatal day 14, miR-122 knockout mice received IP injections of DEN (25 μg of DEN/g body weight; Sigma-Aldrich, (St. Louis, MO), which induced hepatocyte DNA damage through DNA adduct formation and subsequently led to liver tumor after 6-8 months. For orthotopic tumor model, SK Hep-1 cells (5×10^6) were mixed with 50ml Matrigel (1 $\mu\text{g}/\mu\text{L}$; BD Biosciences, San Diego, CA) and were intrahepatically implanted into *nude* mice under sterile conditions.

3.3.4 Antitumor activity of miR-122 encapsulated LNP-DP1 in xenograft model

Female athymic nude mice (16~18 g) (Harlan Laboratory, Indianapolis, IN) were used for investigating the antitumor efficacy *in vivo*. Briefly, approximately 5×10^6 SK Hep-1 cells were injected subcutaneously into the flanks of the *nude* mice. When tumors reached 150~180 mm^3 in volume, mice

were randomly divided into three treatment groups (eight for each). Mice were injected intratumorally twice a week for 4 weeks with 10 mg of miR-122 mimic or scrambled siRNA (Dharmacon, Pittsburgh, PA) encapsulated in LNP-DP1. Anti-tumor activity was evaluated in terms of tumor size (V), which was estimated by the equation $V = a \times b^2 / 2$, where a and b are the major and minor axes of the tumor, respectively, as measured by a caliper.

3.3.5 Cell culture and transfection study

SK Hep-1 cells, stably expressing the firefly luciferase gene, were plated at a concentration of 2×10^4 cells/well in 48-well plates and grown to 60-70% confluency prior to transfection. Luciferase specific siRNA (Luci-siRNA) and negative control siRNA (NC siRNA) (Dharmacon, Pittsburgh, PA) were formulated into LNPs. Cells were treated with various siRNA-LNPs at indicated concentrations and incubated for 24 hours at 37°C and 5% CO₂. The downregulation of luciferase activity was determined using Luciferase Reagent (Promega, Madison, WI), using a Berthold MicroLumatPlus LB96V plate luminometer and normalized to the total protein of each well. Lipofectamine 2000 (Invitrogen, Carlsbad, CA) transfected and nontransfected cells were used as control. SMMC-7221 cell line was transfected with Bcl-2 siRNA using LNP-DP1. Hiperfect (Qiagen, Valencia, CA) transfected and non-transfected cells were used as control. The downregulation of Bcl-2 was measured by quantitative real time PCR (qRT-PCR). Similarly, Hep3B cells were transfected with miR-122 mimic and negative control miR using LNP-

DP1. The miR-122 level and downregulation of several miR-122 targets were measured by qRT-PCR.

3.3.6 *In vivo* biodistribution study of LNP-DP1

All animal studies were conducted with approval from Institutional Animal Care and Use Committee at The Ohio State University. To study the *in vivo* biodistribution of LNP-DP1, cy3-labeled siRNA was formulated into LNP-DP1 as a probe. LNP-DP1 containing 50 µg of cy3-labeled siRNA in a total volume of 0.2 ml was delivered into normal ICR mice (Harlan Laboratory, Indianapolis, IN) or mice bearing various tumors by i.v. injection. Mice were sacrificed after 4 hours, tissue samples from lung, kidney, spleen, heart and tumor were harvested and fixed in 4% paraformaldehyde in PBS (pH=7.4) for 6 hours followed by overnight incubation in a 30% sucrose/PBS solution at 4°C. Fixed tissue samples were then placed into block holders containing O.C.T. freezing medium (Fisher Scientific, Pittsburgh, PA) and snap-frozen on dry ice. The frozen blocks were sectioned using cryostat at 4mm. Cellular membranes and nuclei were stained with Alexa-488 Phalloidin (Invitrogen, Carlsbad, CA) and DAPI (Vector, Burlingame, CA), respectively for 5 min at room temperature. Green fluorescence of actin filament, red fluorescence of cy3-siRNA and blue fluorescence of DAPI were observed by an Olympus FV1000 Filter Confocal Microscope (Olympus Optical Co., Tokyo, Japan). The liver and tumor tissues were also observed under Olympus FV1000MPE two-photon microscopy (Olympus Optical Co., Tokyo, Japan) to check the

collagen distribution. For IVIS imaging, ICR mice were given i.v. injections of cy5-labeled siRNA encapsulated LNP-DP1. After 4 hours, mice were euthanized and tissues were collected and fixed in 4% paraformaldehyde for 12 hours. The tissues were then soaked in 30% sucrose for another 12 hours. The fluorescence signals of cy5 emitted by the whole tissues were measured using a Xenogen IVIS-200 Optical *In Vivo* Imaging System (Caliper Life Sciences, Hopkinton, MA).

3.3.7 Biological evaluation of LNP-DP1 mediated delivery of miR-122 in miR-122KO model

Eight- to twelve-week-old miR-122 knockout mice were treated with either negative control or miR-122 mimic (Dharmacon, Pittsburgh, PA) conjugated LNPs via tail vein injection at a dose of 2.5 mg/kg for three times within 9 days. The Livers were harvested and analyzed by qRT-PCR and Western blot to determine the expression level of miR-122 and its targets, respectively. Total RNA was extracted using Trizol reagent (Invitrogen, Carlsbad, CA). To measure mature miR-122 expression, total RNA was first reverse transcribed into cDNA using the TaqMan MicroRNA reverse transcription kit (Applied Biosystems, Carlsbad, CA). The qRT-PCR amplification of cDNA was then performed using TaqMan MicroRNA assay (Applied Biosystems, Carlsbad, CA). To measure the expression of miR-122 target genes at the mRNA level, the total RNA was transcribed into cDNA using the first-strand cDNA synthesis kit (Invitrogen, Carlsbad, CA). The

resulting cDNA was amplified by qRT-PCR. To analyze the expression of miR-122 target genes at the protein level, protein extracts from liver tissues were separated by SDS-PAGE and subjected to Western blot analysis with specific antibodies.

3.3.8 Statistical analysis The data is presented as the mean \pm SD of triplicate unless otherwise indicated. Statistical significance is calculated by student t-test and a p-value <0.05 is considered as significant.

3.4 Results

3.4.1 Optimization of PEG-lipids for LNPs mediated delivery of miR-122 to HCC cell lines

LNPs are comprised of an ionizable cationic lipid DODMA, EggPC, cholesterol (Chol) and PEG-lipid (**Figure 3.1A,B**). Owing to the steric shielding of hydrophilic PEG materials, PEG-lipids are widely used to increase the *in vivo* stability and enhance circulation half-life of LNPs compared to their non-PEGylated counterparts. Since very strong shielding would influence the transfection ability of LNPs, we sought to identify the optimal amount of PEG-lipid for miRNA delivery *in vivo*. LNPs consisting of seven different PEG-lipids with average diameter of ~ 100 nm and neutral surface charge were prepared. The mean diameter and zeta potential of LNP-

DP1 containing Chol-PEG were 102.2 ± 15.2 nm and -3.94 ± 0.75 mV, respectively (**Figure 3.1C**).

To test the transfection efficiency of different LNPs, we first examined the efficacy of luciferase specific siRNA in silencing luciferase expression in a HCC cell line (Sk Hep-1) stably expressing firefly luciferase (**Figure 3.1C**). The data suggested that LNP-DP1 formulation, in which PEG was conjugated to cholesterol, was the best modification of PEG particles in terms of luciferase silencing among all LNPs examined. Its transfection efficiency was better than that of lipofectamine® 2000, a well-known commercial transfection agent.

To evaluate the efficiency LNP-DP1 in targeting mRNA, LNP-DP1 containing Bcl-2 specific siRNA (LNP-DP1-Bcl-2-siRNA) was used to transfect SMMC7721 cells. qRT-PCR analysis showed that the Bcl-2 level was significantly reduced in cells transfected with LNP-DP1-Bcl-2-siRNA compared to cells transfected with scrambled siRNA and nontransfected cells (**Figure 3.1D**). Notably, the knockdown efficiency of LNP-DP1-Bcl-2-siRNA was comparable to Hiperfect®, a commercially available lipid based transfection agent. We then studied the delivery of miR-122 in Sk Hep-1 cells that do not express this liver specific microRNA and performed qRT-PCR to quantify the level of miR-122 and its target genes. As expected, the miR-122 level significantly increased (over 500-fold) in cells transfected with LNP-DP1-miR-122 compared to the negative control (**Figure 3.2A**). Consistent with the elevated levels of this miRNA, its target genes such as Srf, Igf1r and Adam10

were significantly downregulated by 99.2%, 99.6% and 97.6%, respectively (**Figure 3.2B**). These results confirm that Chol-PEG based LNP is an excellent delivery system for si/miRNAs in HCC cells *in vitro*.

3.4.2 *In vivo* liver targeting delivery mediated by LNP-DP1

Due to their vital role in liver related diseases such as hepatocellular carcinoma, hepatocytes are the major cells for liver-targeted delivery. Because the properties of miRNA mimics are similar to those of synthetic siRNAs, a cy3 labeled siRNA encapsulated into LNP-DP1 was used to evaluate the efficacy of LNP-DP1 mediated systemic delivery of miRNA to the liver. The *in vivo* distributions of LNP-DP1 in mice were examined by confocal and IVIS imaging. Confocal images of sections of the liver and other organs showed that the labeled particles predominantly accumulated in the liver (**Figure 3.3A**) and to a lesser extent in the spleen (**Figure 3.3B**). In the liver, the particles were not just trapped in the sinusoid space but were efficiently taken up by the hepatocytes as shown under a higher magnification. The fluorescent signal of delivered particles was not detectable in other organs, such as heart, kidney and lung and was barely detectable in the spleen (**Figure 3.3B**).

We also evaluated the distribution of LNP-DP1 mediated siRNA delivery using the IVIS imaging system. LNP-DP1 facilitated predominant accumulation of cy5 labeled siRNA in the liver and to a much lower level in

the spleen and kidney (**Figure 3.3C**). These results corroborated very well with the confocal data (**Figs. 3.3A, B**). Notably, LNP-DP1 was more efficient than commercially available InvivoFectamine in delivering the siRNA to the liver tumor.

Serum analysis showed insignificant toxicity in mice treated with the LNP-DP1 formulation (**Figure 3.4**). Comparable serum alanine aminotransferase (ALT) and aspartate aminotransferase (AST) levels between LNP-DP1 and saline-injected animals indicated that there was no significant liver damage caused by the particles. The normal serum level of blood urea nitrogen (BUN) and creatine kinase (CK) suggested that the kidney function was normal in these mice. Taken together, these data suggested that LNP-DP1 formulation could be used to deliver siRNA and miRNA specifically to the liver without causing systemic toxicity.

3.4.3 Efficacy evaluation of LNP-DP1 mediated delivery to liver tumors

To examine the efficiency of LNP-DP1 delivery to tumor tissues, we used diethylnitrosamine (DEN)-induced HCC model. DEN, a liver carcinogen, is frequently used as an animal model for HCC because its tumor structure and vessel formation resemble those of human HCC [204]. Therefore, we used this model to test whether LNP-DP1 can be systemically delivered to tumors localized in the liver. Four hours after injecting intravenously LNP-DP1 particles encapsulated with cy3-siRNA, both tumors (section I) and

peritumoral liver lobes (section II) from mice were processed for sectioning and staining. Confocal microscopy showed significant levels of cy3-siRNA particles (red) in hepatocytes in the liver and in tumors (**Figure 3.5A**), indicating significant uptake of LNP-DP1 particles to HCCs. The higher collagen density in tumor is known to impede deeper penetration of nanoparticles [205]. Two-photon confocal microscopic analysis in the present study, however, showed low collagen density (shown in yellow color in images) in both HCC (section I) and benign liver (section II), which explains efficient localization of LNP-DP1 in the DEN-induced HCC (**Figure 3.5B**).

We next investigated the delivery of LNP-DP1 in two additional liver cancer models, namely SK Hep-1 xenograft and Hep-3B orthotopic models. After 4 hours of intravenous administration of cy3-siRNA encapsulated in LNP-DP1, the mice were sacrificed. Confocal microscopy of liver and tumor sections showed much higher accumulation of cy3-siRNA in livers relative to tumors in both models (**Figs. 3.6A, B**). Very high collagen content surrounding the tumor cells was detected by two-photon confocal imaging in both xenograft and orthotopic models (**Figure 3.6C**), indicating poor blood supply and strong delivery barriers for LNPs in the tumors.

3.4.4 LNP-DP1 mediated delivery of miR-122 specifically downregulates miR-122 target genes in liver and tumor tissues

To evaluate the efficiency of LNP-DP1 mediated delivery of microRNA and the resultant downregulation of specific target genes, we took advantage

of miR-122 knockout (miR-122KO) mice that do not express miR-122 in the liver. LNP-DP1-miR-122 and LNP-DP1-negative control was injected intravenously (2.5 mg/kg) to the miR-122KO. Following LNP-mediated delivery of miR-122, the expression level of its target genes was measured by qRT-PCR and Western blot analyses. qRT-PCR analysis of the livers from these animals after one week of treatment showed significant increase (2.79 fold, $P=0.002$) in the miR-122 level with concomitant decrease in two target mRNAs of miR-122 namely, Adam10 and Mapre1 (**Figures 3.7A, B**).

To determine if miR-122 can also be delivered to the tumors, LNP-DP1-miR-122 was injected intravenously to the animals bearing the DEN-induced liver tumors. Five miR-122KO mice injected twice a week with LNP-DP1-miR-122 (2.5 mg/kg) showed a significantly higher miR-122 level in the liver after one week (**Figure 3.7C**), and the protein levels of Adam10, Srf, Mapk inversely correlated with the delivered miR-122 level in the tumors that originally lacked miRNA (**Figure 3.7D**). Adam10 and Srf were identified earlier as direct targets of miR-122 [80]. Notably, suppression of target genes and Mapk was significantly higher in the tumor than in the liver, which was consistent with higher uptake of miR-122 in the tumor (14 fold vs 4 fold). These results suggested that microRNAs could be delivered to both normal liver and tumor tissues. Furthermore, the downregulation of several target genes of miR-122 suggested that the LNP-DP1 carrying miR-122 could be released from the nanoparticles to exert its function *in vivo*.

3.4.5 Intratumoral delivery of miR-122 containing LNP-DP1 suppresses the growth of HCC xenografts in nude mice

To assess the therapeutic potential of the miR-122 mimic, we chose to use a HCC xenograft mouse model bearing the SK Hep-1 tumor for effective monitoring of the temporal changes in tumor growth. Due to poor blood supply and high collagen distribution (**Figure 3.6C**) in subcutaneous xenograft tumors, the systemic delivery efficiency of the LNP-DP1 carrying microRNA to these tumors was lower than that in spontaneous tumor (**Figures 3.5A, 3.6A**). To increase the delivery efficiency, we injected LNP-DP1-miR-122 or LNP-DP1-negative control RNA intratumorally to xenograft tumors and monitored the tumor growth. As expected, the tumor size and weight of the group following miR-122 uptake were significantly smaller than that of the negative control group, which could be detected as early as 7 days after the first injection (**Figures 3.8A-C**). Notably, the tumor size of the group that received miR-122 mimic in LNP-DP1 increased nearly 2.5 fold (tumor size at 26th days: $380.1 \pm 69.1 \text{ mm}^3$) after 26 days of treatment whereas it increased about 6-fold (tumor size at 26th days: $995.5 \pm 259.1 \text{ mm}^3$) in the negative control group that did not receive exogenous miR-122. qRT-PCR analysis also showed significantly higher levels of miR-122 in the tumors supplemented with miR-122 (**Figure 3.9A**). Among the target genes of miR-122, Adam10 was significantly reduced in the xenograft tumor tissue (**Figure 3.9B**). Further, the proliferation of LNP-DP1-miR-122 injected tumors was significantly lower than the untreated controls, as demonstrated by the

reduced number of Ki-67 positive cells (**Figure 3.9C**). The body weight of both mouse groups was comparable (data not shown). Overall, this experiment showed that, miR-122 can be efficiently delivered to the xenograft tumor by intratumoral injection that leads to suppression of tumor growth probably due to inhibition of expression of its target genes.

3.5 Discussion

Gene therapy has been proposed and implemented in some cases to reverse the abnormal gene expression resulting from genetic or epigenetic alterations, without surgical removal of the tumors[206-208]. While siRNA-mediated silencing of the expression of a specific disease-causing target gene holds great promise for cancer therapy, it is likely that redundant genes with complementary functions could compensate for the function of the depleted genes. As an alternative, microRNA-based therapy is being intensely pursued because miRNAs can target multiple genes. Because of their low serum stability, the development of safe and effective *in vivo* delivery systems is of central importance to realize the effectiveness of DNA or RNA based therapeutic applications. Numerous strategies including viral [86, 195, 209] and non-viral systems [120, 192, 210, 211] have been applied in animal models of HCC or in patients for targeting RNAi to liver tumors. Although viral delivery of RNAi produces significant ectopic expression of target genes, non-viral systems are still considered a safer choice due to its lower

immunogenicity. Among the non-viral delivery approaches, LNPs have shown significantly higher potential for the delivery of DNA or RNA *in vitro* and *in vivo* [212, 213].

The LNP formulation developed in the present study is based on a commercially available cationic lipid, DODMA. DODMA has a protonatable tertiary amine head group and it is an ionizable cationic lipid [203, 214]. The charge of the head group of DODMA is pH dependent. The nanoparticle-mediated delivery of miRNAs has several advantages. First, when the particles are taken up by cells and encapsulated by endosomes, the more acidic environment in the endosomes will promote the release of miRNA from LNP by the fusion between the cationic DODMA and anionic lipids of endosomal bilayers. Second, incorporation of PEG prevents aggregation and aids in the formation of uniform and small nanoparticles, which can be accomplished with the use of PEG-lipid conjugates to synthesize LNP. Seven PEG-lipids were examined by evaluating siRNA mediated luciferase silencing in SK Hep-1 cells. The LNP-DP1 formulation containing Chol-PEG lipid showed the best delivery efficiency of siRNA against the promoter sequence of luciferase among all examined PEG-lipids examined to date (**Figure 3.1C**).

The nano-sized particles may be accessible to hepatocytes by passive targeting delivery. Upon reaching the liver, the nanoparticles could exit the intravascular space to directly access hepatocytes as long as the particle size is smaller than the pore size of fenestrated vasculature (100~150 nm in diameter)[215, 216]. More recent research suggested that ApoE could act as

an endogenous targeting ligand to facilitate uptake of ionizable LNPs to hepatocytes *in vivo*[217]. LNPs can be more selectively accumulated in liver tumors by passive targeting via the enhanced permeability and retention (EPR) effect. It is noteworthy that three different HCC models exhibited dramatically different responses to LNP-DP1 mediated delivery of fluorescence labeled siRNA. Transport barriers to drug delivery arise from abnormal characteristics of the tumor microenvironment. The dense interstitial structure, such as high levels of collagen, is one of the major abnormal physical and physiological properties that contribute to the transport barriers for nanoparticles. Generally, the diffusion rate is inversely correlated with the collagen level. In the present study, the primary tumors developed in the DEN model exhibit minimal collagen distribution, thereby achieving the best uptake of LNP-DP1 compared to the subcutaneous and orthotopic HCC models.

We performed three different experiments to demonstrate the potential of the LNP-DP1-miR-122 complex. First, we used fluorescence microscopy to show that significant amount of siRNA/LNP-DP1 complex was taken up by HCC cells using fluorescence microscopy. Second, a significant increase in the miR-122 level detected by qRT-PCR with concomitant decrease in several miR-122 targets after delivery (**Figure 3.7D**) was indicative of the successful release of miR-122 from LNP-DP1. Third, we used an established xenograft animal model, instead of a long-term monitoring of liver tumor growth in animals, to precisely monitor the tumor progression after the delivery of the LNP-DP1-miR-122 complex. It is noteworthy that the tumor

growth was significantly suppressed after one month of treatment. The immunohistochemistry with the Ki67 antibody indicated reduced proliferation of the xenograft tumor after treatment. Admittedly, a large cohort of animal study in a DEN-induced HCC model will be necessary to determine the proper dosage and duration of LNP-DP1-miR-122 delivery. Nevertheless, the present study has provided important data that supports the potential application of the LNP-DP1-miR-122 complex in HCC therapy. In the absence of adequate success in the treatment of HCC and in light of dramatic increase in the incidence of HCC in the western world, this novel strategy to deliver an important liver-specific tumor suppressor miRNA directly to the tumor is a significant advance.

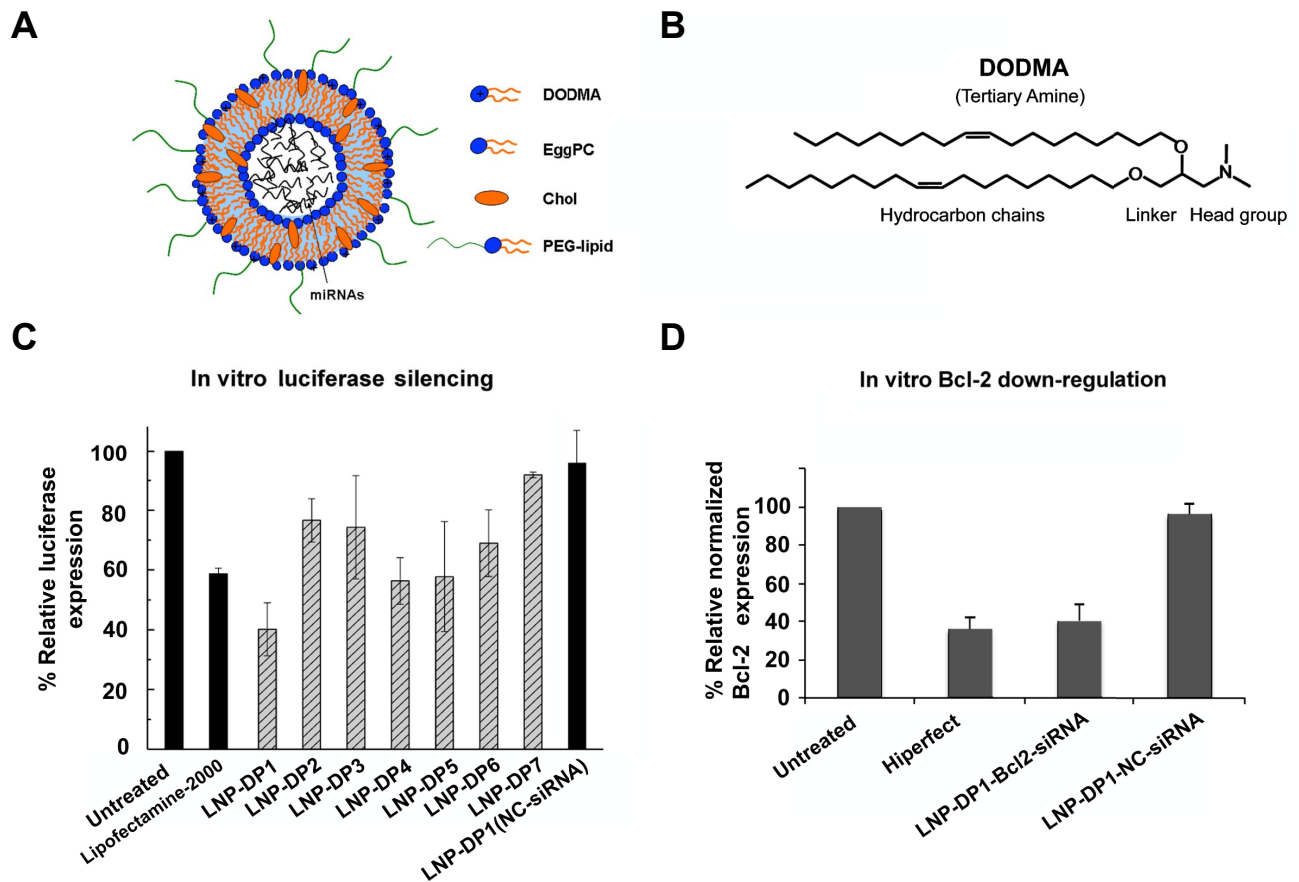
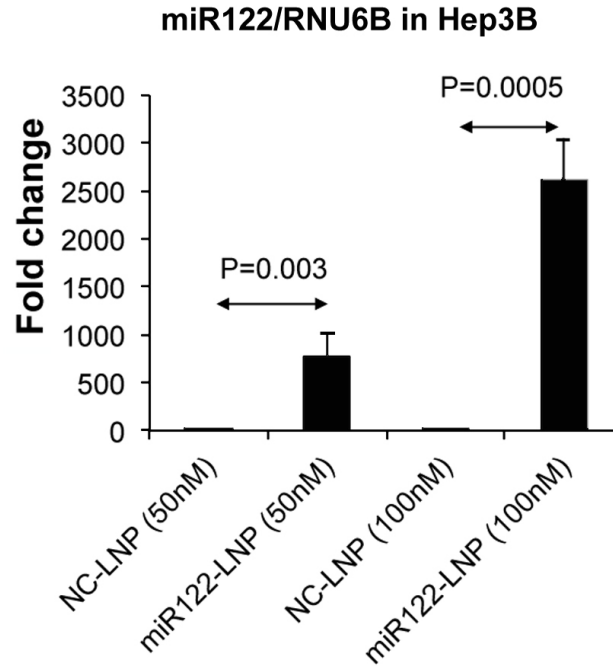


Figure 3.1 LNPs mediated delivery of miRNA122 to HCC cell lines *in vitro*.

(A) Schematic of miRNA encapsulated by PEG (green) modified LNPs and **(B)** the structure of cationic lipid DODMA. **(C)** Reduced luciferase expression in SK Hep1 cell lines transfected with siRNA. Using different types of LNPs, SK Hep-1 cell lines were transfected with 100 nM siRNA against the promoter sequence of luciferase. The reduction in luciferin luminescence intensity, detected at 24 hours post-transfection, was determined as the measure of luciferase knockdown. The signal intensity was normalized to that of control untreated cells. LNPs used and their components of PEG-lipids were: LNP-

DP1: Chol-PEG; LNP-DP2: Ceramide-PEG; LNP-DP3: DSPE-PEG; LNP-DP4: DMG-PEG; LNP-DP5: C14-PE-PEG; LNP-DP6: C16-PE-PEG; LNP-DP7: DSG-PEG. **(D)** SMMC7721 cell lines were transfected with Bcl-2 siRNA, using lipofectamine and LNP-DP1 for 48 hours. Reduction of Bcl-2 expression was determined by qRT-PCR. Bcl-2 level of each group was normalized to untreated cells.

A



B

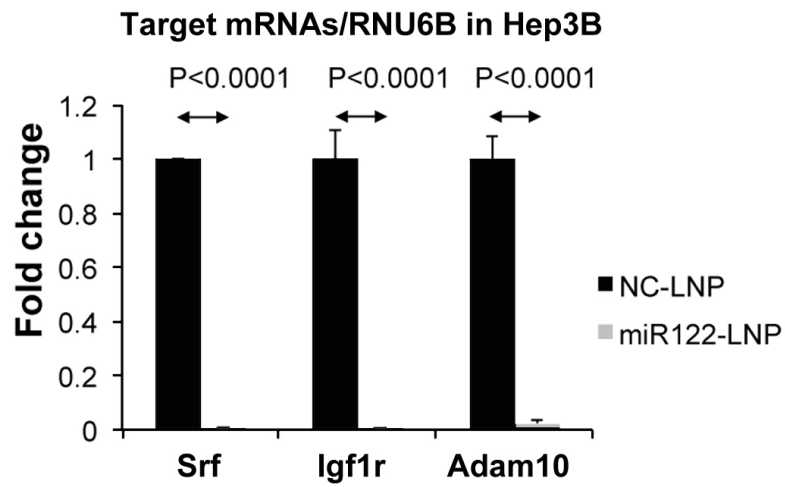
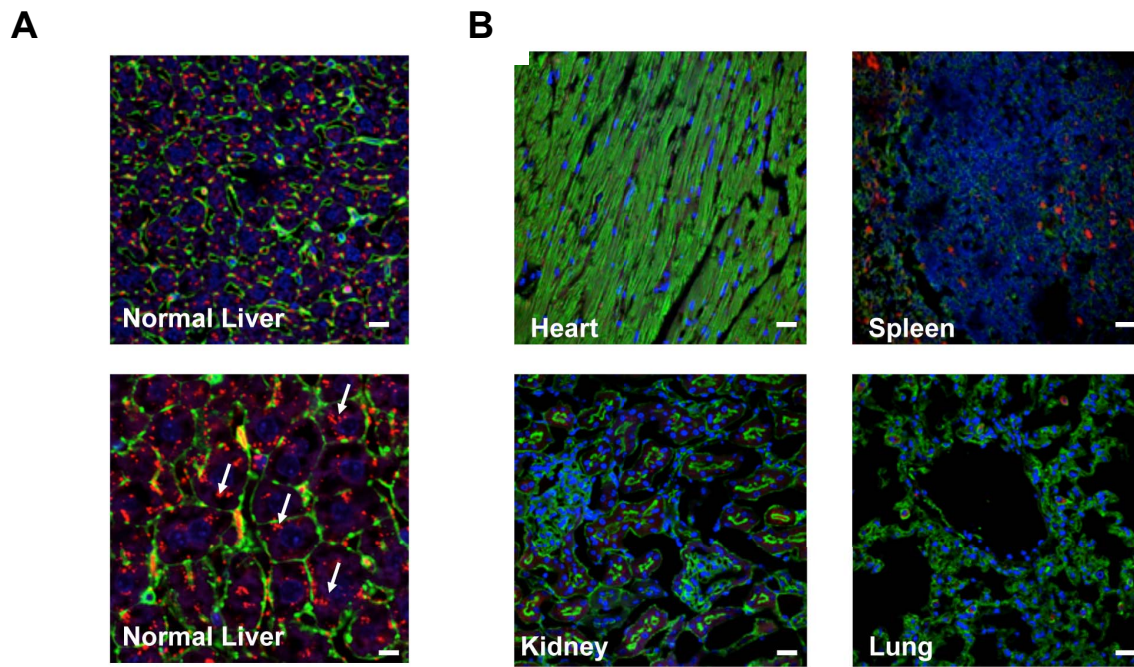


Figure 3.2 LNP-DP1 mediated delivery of miR-122 to HCC cell line *in vitro* (A) LNP-DP1 mediated delivery of miR-122 in Hep3B cell line and (B) the target gene downregulations were evaluated by qRT-PCR.



DODMA based formulation

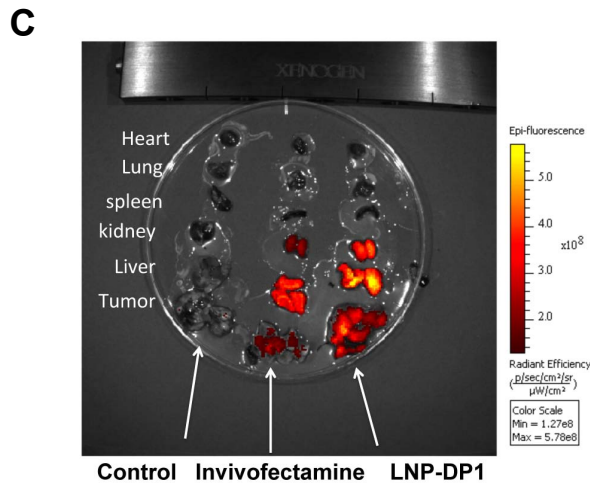


Figure 3.3 *In vivo* liver targeting delivery mediated by LNP-DP1 (A, B) Confocal microscopic imaging of liver sections (A) and other organs (B). Mice were injected with LNP-DP1 carrying cy3-siRNA via tail vein. After 4 hours the liver was harvested and sections were counterstained as described in methods and materials. Scale bar=20 μm . (C) Tissue distribution of LNP carrying cy5-siRNA. Four hours after intravenous administration, tissues were harvested and cy5 fluorescence signals were measured by IVIS imaging.

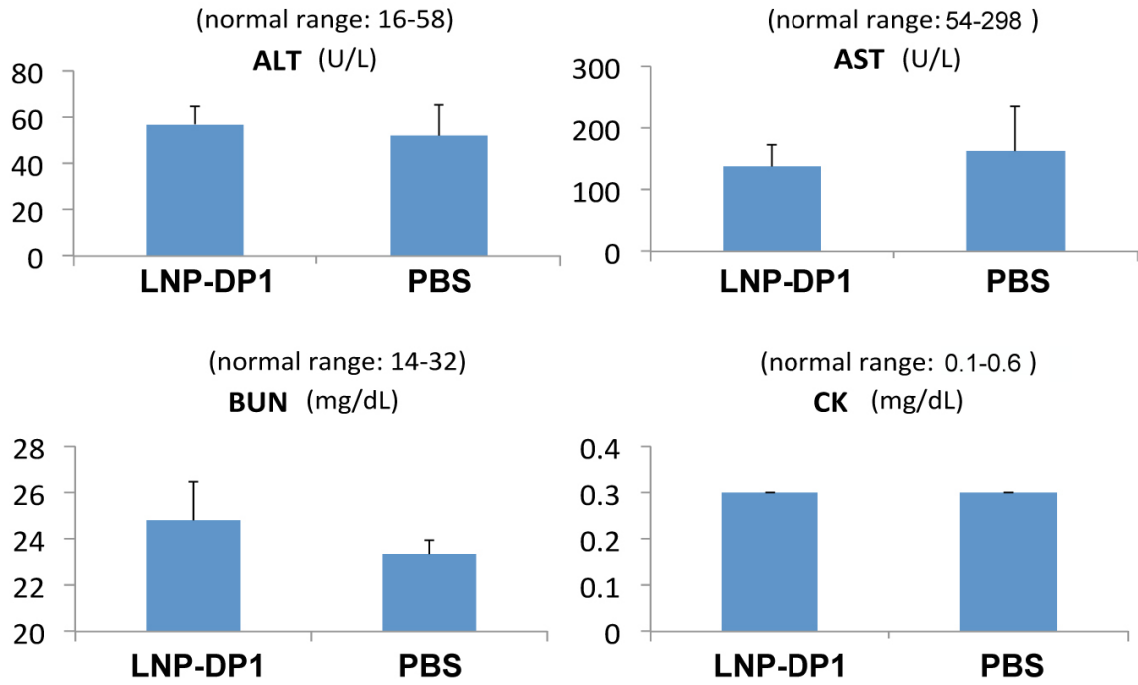


Figure 3.4 *In vivo* toxicity analysis of the systemic delivery of LNP-DP1 carrying miR-122.

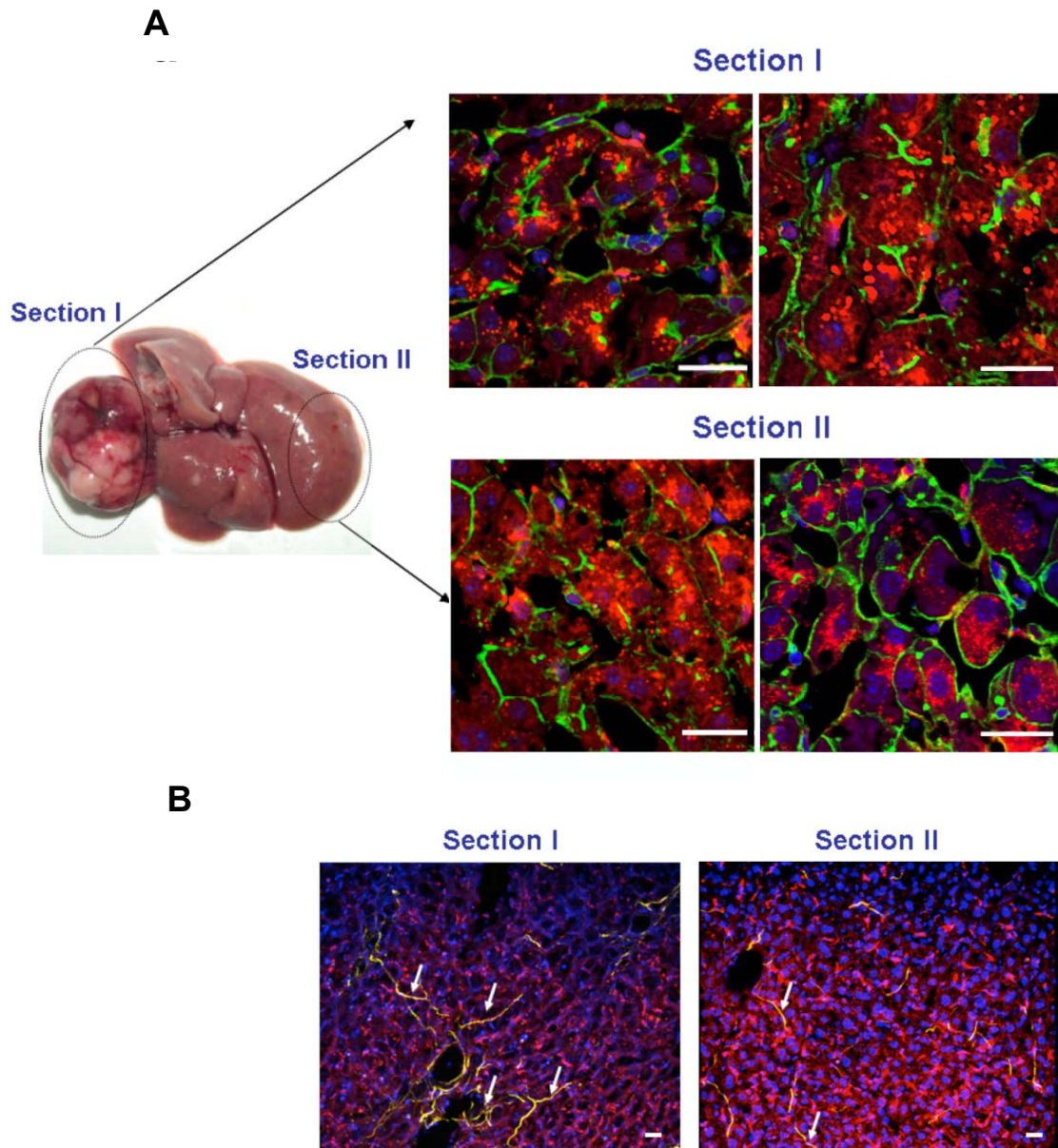
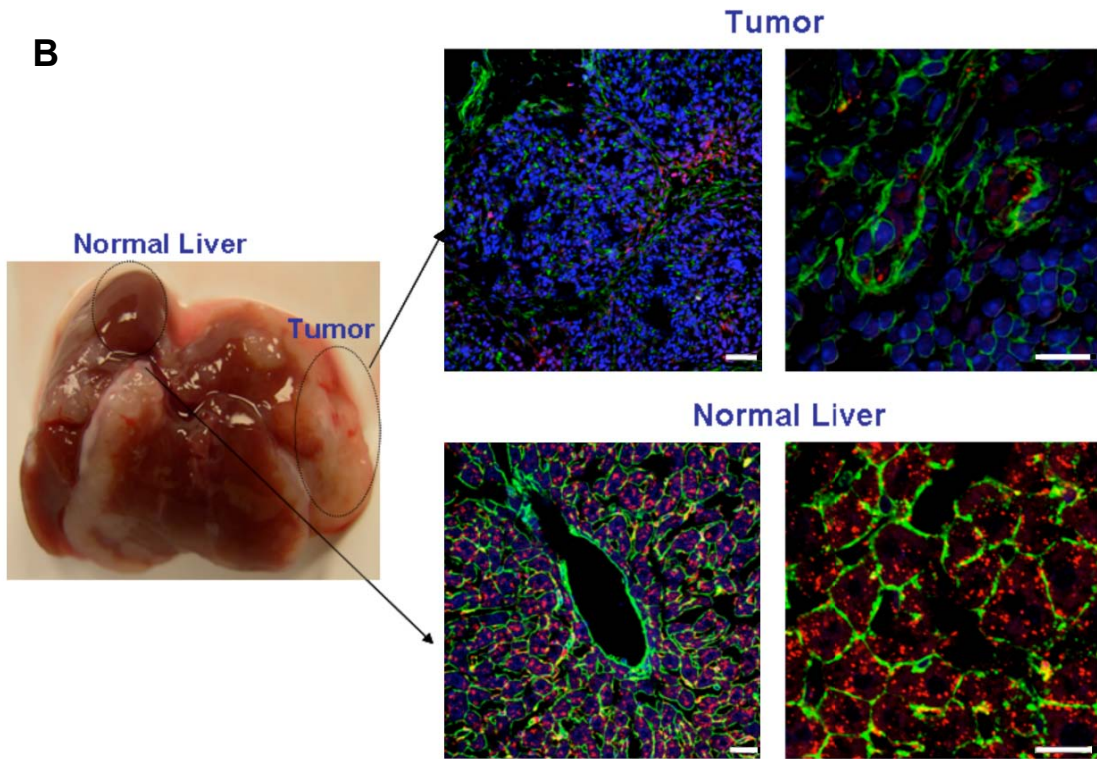
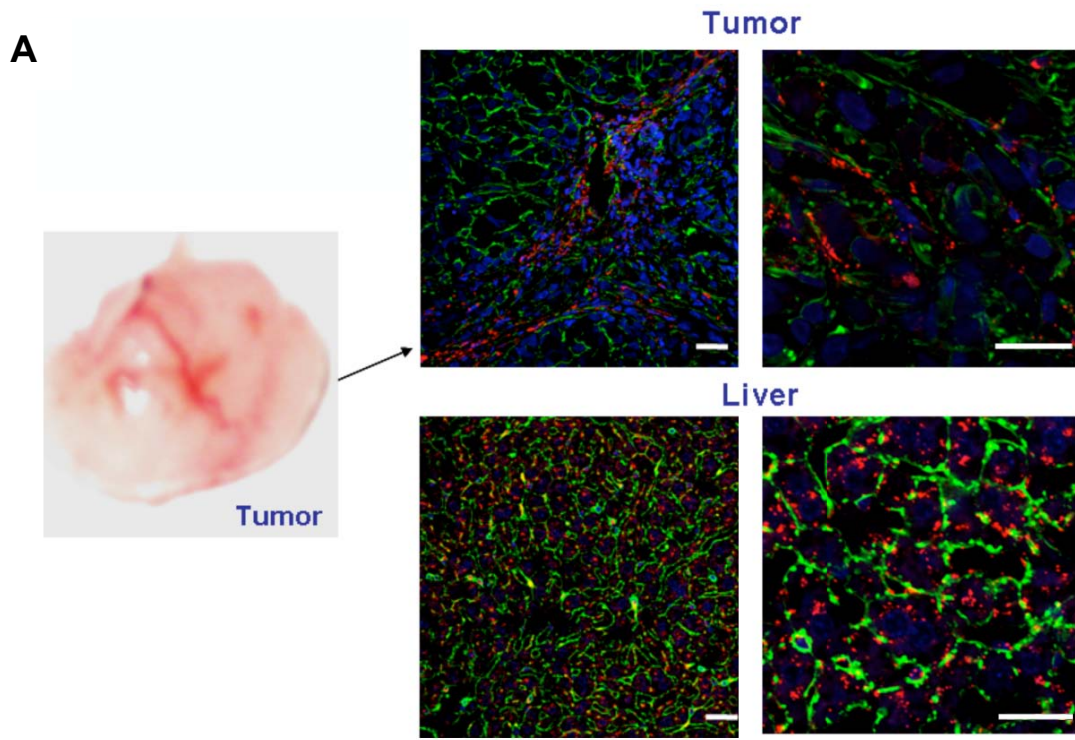


Figure 3.5 *In vivo* biodistribution of LNP-DP1 mediated delivery in three liver tumor models. (A) Confocal microscopic imaging analysis of liver (section II) and tumor (section I) for LNP-DP1. **(B)** Two-photon confocal imaging of collagen distribution in DEN induced mice model. All mice were treated by cy3 -siRNA (2.5 mg/kg) in LNP-DP1 by i.v. injection for 4 hours. Scale bar=20 μ m.



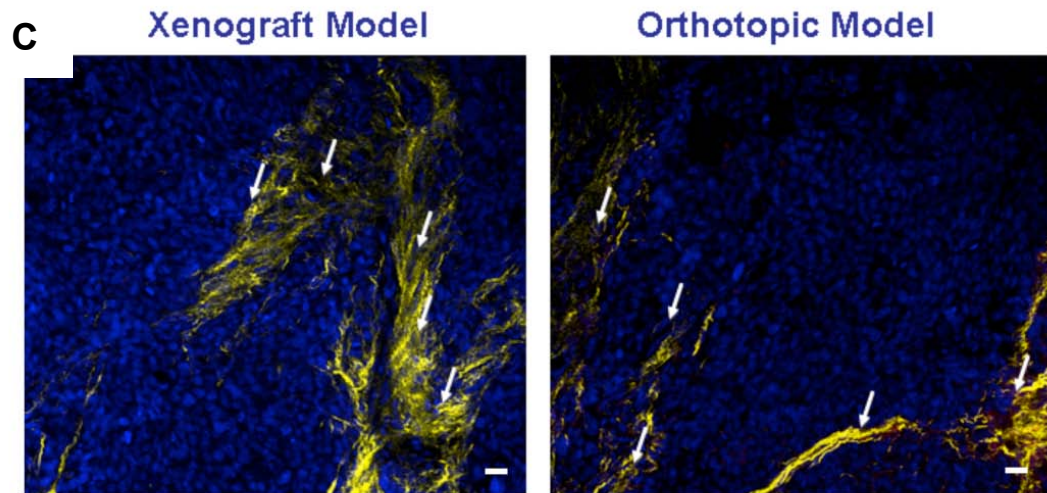


Figure 3.6 *In vivo* biodistribution of LNP-DP1 mediated delivery in xenograft and Hep3B orthotopic liver tumor models. **(A)** Confocal microscopic imaging of liver and tumor sections for LNP-DP1 in SK Hep-1 xenograft mice model. **(B)** Confocal microscopic imaging of liver and tumor sections for LNP-DP1 in Hep-3B orthotopic mice model. **(C)** Comparative studies of collagen distribution of xenograft and orthotopic models by two-photon confocal imaging. All mice were treated by cy3 -siRNA (2.5 mg/kg) in LNP-DP1 by i.v. injection for 4 hours. Scale bar=20 μ m.

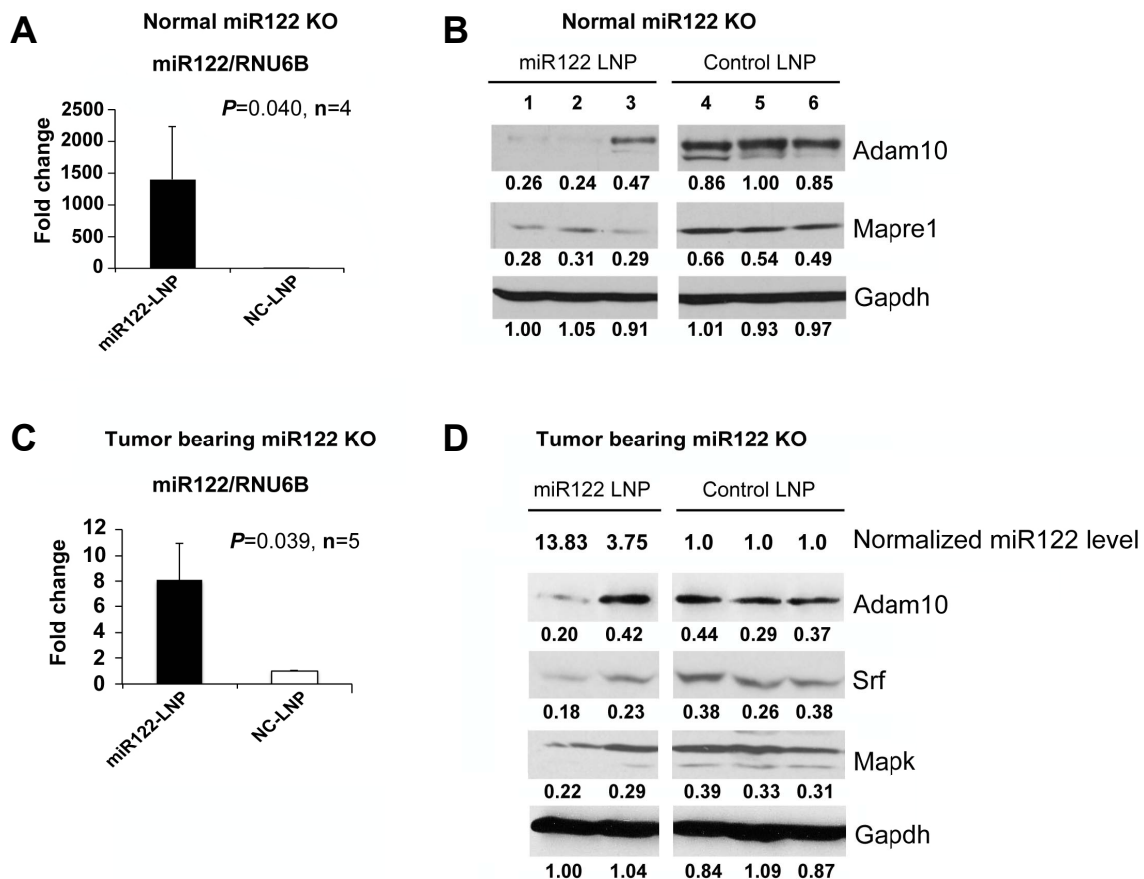


Figure 3.7 LNP-DP1 mediated delivery of miR-122 specifically downregulates target genes in liver and tumor tissues. LNP-DP1 encapsulated miR-122 was delivered twice a week to normal (n=4) or tumor-bearing (n=5) miR-122 knockout mice at a concentration of 2.5 mg/kg by i.v. injection. After one week, mice were sacrificed and processed. **(A, C)** Total liver RNAs from (A) normal and (C) tumor-bearing mice were extracted and analyzed by qRT-PCR to determine the level of miR-122 normalized to RNU6B. **(B, D)** Total liver proteins from (B) normal and (D) tumor-bearing mice were extracted and analyzed by Western blot with designated antibodies. The miR-122 level in miR-122KO injected with miR-122 mimic or scrambled (NC RNA). miR-122 level in mice injected with NC RNA was assigned as value of 1.

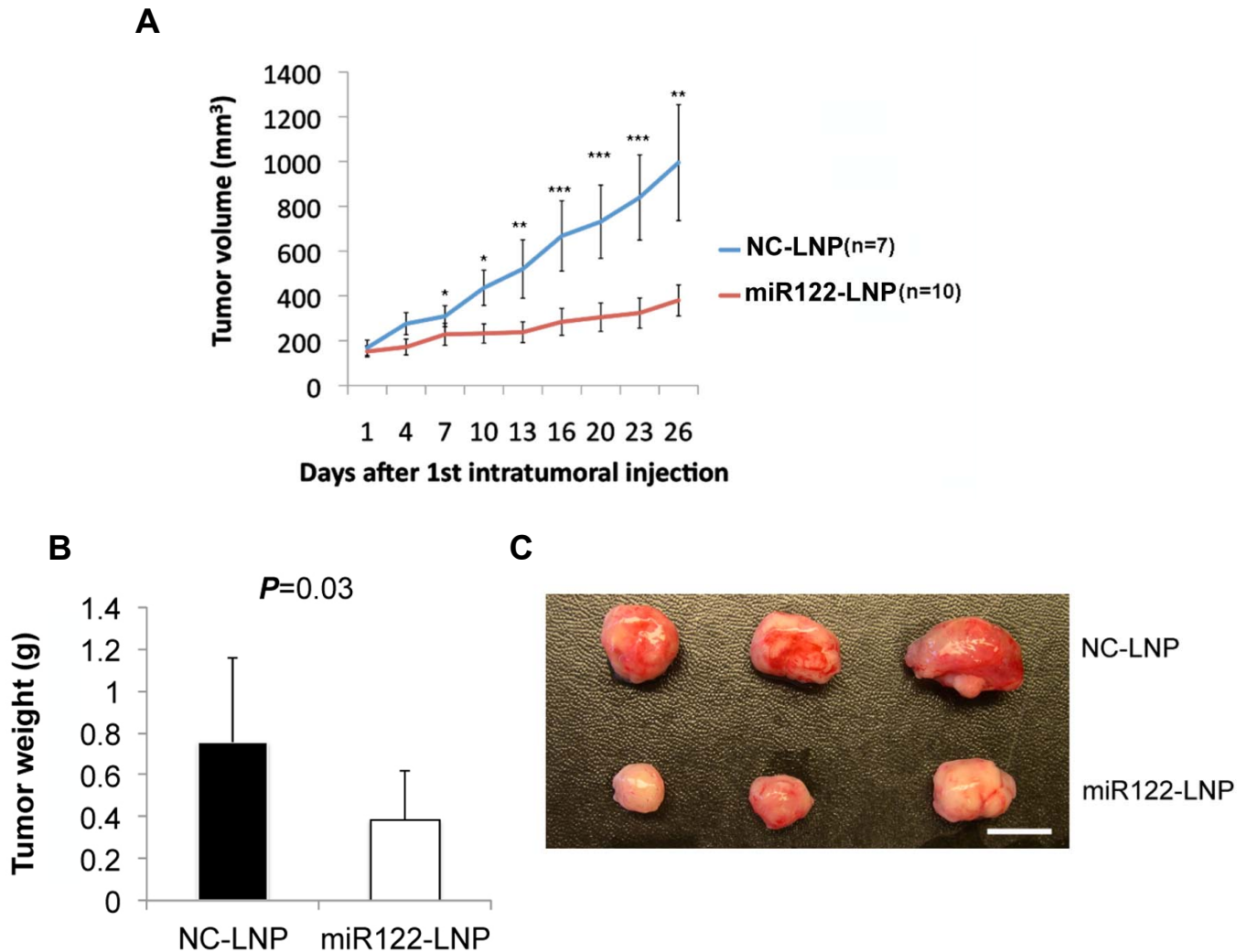


Figure 3.8 Intratumoral delivery of miR-122 in LNP-DP1 suppresses the growth of liver tumor xenografts in nude mice. (A) The tumor growth curves of xenograft tumors in *nude* mice intratumorally injected with negative control LNP-DP1-siRNA and LNP-DP1-miR-122. P-value: *, $P < 0.05$; **, $P < 0.01$; ***, $P < 0.001$. (B) The average weight of xenograft tumors harvested at the end of treatment. (C) Pictures of representative xenograft tumors harvested at the end of treatment. Scale bar=1 cm.

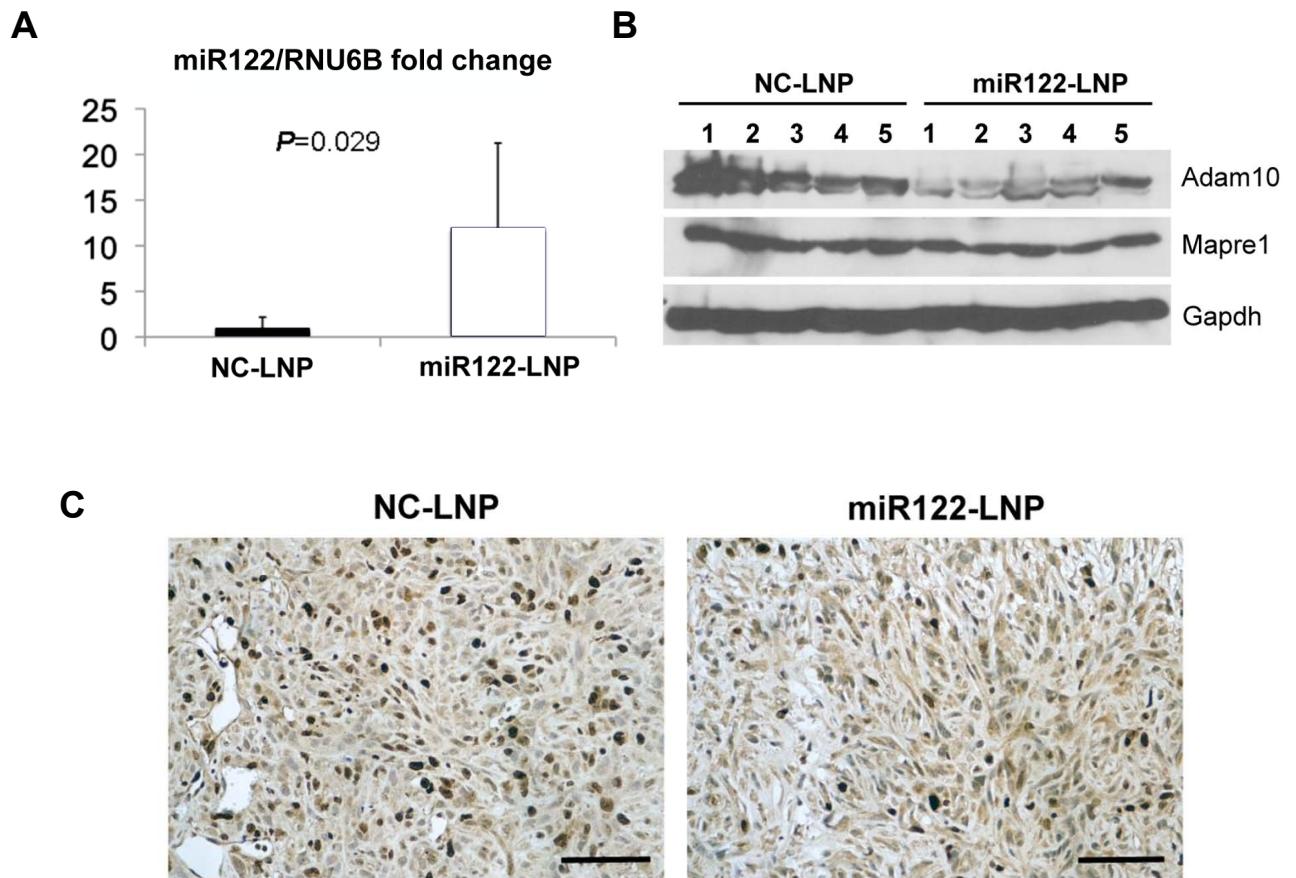


Figure 3.9 Intratumoral delivery of miR-122 in LNP-DP1 suppresses the growth of liver tumor xenograft in nude mice. **(A, B)** Expression of (A) miR-122 and (B) its targets. **(C)** Immunohistochemistry with Ki67 antibody. The dark brown stained cells are Ki67-positive. Scale bar=20 μ m.

Chapter 4. Conclusion and future development

MiRNA-122 is one of the very intensively studied miRNAs in the field and its multiple biological function determined by previous literature suggests its critical roles in metabolism, cell proliferation, and hepatocarcinogenesis. Our finding is the first report showing *in vivo* function of miR-122 using miR-122 knockout mouse model. Most importantly, the phenotypes of germ-line and liver-specific knockout mice strongly suggest that miR-122 functions as a tumor suppressor in the liver by maintaining differentiation state, normal lipid metabolism and orchestrating the infiltration of inflammatory cells in the liver. Our study has demonstrated that the loss of miR-122 alone is a critical causal factor to induce cholesterol downregulation, TG accumulation, hepatic inflammation, that eventually trigger HCC development in mouse liver. Microarray demonstrated that numerous important genes involved in lipid metabolism and cell proliferation are deregulated by the loss of miR-122. Furthermore, the delivery of the miR-122 using the novel cationic lipid based nanoparticles successfully knocked down its target genes in HCC cell lines, miR-122 KO liver, DEN induced tumor model, and, most importantly, suppressed the tumor growth in xenograft HCC model. Taken together, these evidences not only support the main impression about the role of miR-122 in

cholesterol reduction, but also suggest the therapeutic potential of miR-122 in HCC.

The establishment of the miR-122 KO mice provides a good animal model to study miR-122 related subjects and HCC development resulting from the loss of miR-122. First, miR-122 was discovered to promote hepatitis C viral (HCV) replication and translation by binding to 5'UTR of viral transcripts, which is responsible for tropism of HCV in hepatocytes [218, 219]. Therefore, our animal model provides a good platform to study the *in vivo* effect of the complete loss of miR-122 on HCV replication in liver. More importantly, it will be a good model to study the potential mutated clones of HCV may be developed after long term infection in miR-122 KO mice. To do this, it will be necessary to generate miR-122 KO overexpressing CD81 and occluding in livers in order to be infected by HCV[220]. In Chimpanzee, there is no mutation was detected in the genome of the HCV that escaped anti-miR-122 treatment for 12 weeks [133]. However, mutational status of the virus after prolonged treatment is lacking. Multiple treatment options can be tested on these mutated clones survived from anti-miR-122 treatment.

Second, our data pointed out an interesting observation that, at latter adult stage, miR-122 germ-line knockout (KO) exhibited a more advance phenotype than the miR-122 liver specific knockout (LKO). This is true for the phenotype of steatosis, hepatic inflammation, and the onset time and incidences of HCC. Therefore, it is highly possible that miR-122 deleted in non-hepatocytes cell types may have additive effect on the existing

phenotype originally caused by liver specific deletion of miR-122. For example, in mouse embryonic fibroblasts, miR-122 was found to repress cytoplasmic polyadenylation element binding protein (CPEB) and subsequently suppressed P53 expression. This effect can be reversed by GLD-2 depletion followed by miR-122 reduction [221]. Also, it cannot be ruled out the significant increased population of CD11b^{high}Gr-1⁺ may be due to the miR-122 deletion in immune cells since we did observe a severer hepatic inflammation in KO liver at six months. These observations suggested the possibilities that miR122 also play a role in non-hepatocyte cells.

Third, Gatfield et al. have found a miR-122-dependent circadian regulation of several important circadian genes, including Peroxisome proliferator-activated receptor α (*Ppar α*) [153]. The circadian regulated level of pri-miR-122, but not constant level of mature miR-122, is responsible for this circadian regulation. It will be interesting to study the alteration of circadian rhythm under the context of miR-122 knockout mice. The comparison of gene expression profile between miR-122 KO and anti-miR-122 treated mice may shed some light on the role of pri-miR-122. It is likely the deregulated lipid metabolism may be affected by the deregulated circadian rhythm.

In summary, miR-122 is now one of the most potential miRNA for therapeutic application in HCV infection and hypercholesterolemia. Our miR-122 knockout model extends the knowledge about the effect of long-term loss of miR-122 and coins new thoughts for the strategies of anti-miR-122 based

HCV treatment. Furthermore, in the near future, miR-122 deficient mice can be widely utilized to study its role in different liver disease including alcohol and NASH induced hepatocarcinogenesis.

Bibliography

1. Ferlay J, Shin HR, Bray F, Forman D, Mathers C, Parkin DM: **Estimates of worldwide burden of cancer in 2008: GLOBOCAN 2008.** *Int J Cancer* 2010, **127**(12):2893-2917.
2. Stravitz RT, Heuman DM, Chand N, Sterling RK, Shiffman ML, Luketic VA, Sanyal AJ, Habib A, Mihas AA, Giles HC *et al*: **Surveillance for hepatocellular carcinoma in patients with cirrhosis improves outcome.** *Am J Med* 2008, **121**(2):119-126.
3. Llovet JM, Burroughs A, Bruix J: **Hepatocellular carcinoma.** *Lancet* 2003, **362**(9399):1907-1917.
4. Beasley RP: **Hepatitis B virus. The major etiology of hepatocellular carcinoma.** *Cancer* 1988, **61**(10):1942-1956.
5. Stevens CE, Beasley RP, Tsui J, Lee WC: **Vertical transmission of hepatitis B antigen in Taiwan.** *The New England journal of medicine* 1975, **292**(15):771-774.
6. McMahan BJ, Bulkow LR, Singleton RJ, Williams J, Snowball M, Homan C, Parkinson AJ: **Elimination of hepatocellular carcinoma and acute hepatitis B in children 25 years after a hepatitis B newborn and catch-up immunization program.** *Hepatology* 2011, **54**(3):801-807.
7. Beasley RP, Hwang LY, Lee GC, Lan CC, Roan CH, Huang FY, Chen CL: **Prevention of perinatally transmitted hepatitis B virus infections with hepatitis B virus infections with hepatitis B immune globulin and hepatitis B vaccine.** *Lancet* 1983, **2**(8359):1099-1102.
8. Fortuin M, Chotard J, Jack AD, Maine NP, Mendy M, Hall AJ, Inskip HM, George MO, Whittle HC: **Efficacy of hepatitis B vaccine in the Gambian expanded programme on immunisation.** *Lancet* 1993, **341**(8853):1129-1131.
9. Garcia M, de The H, Tiollais P, Samarut J, Dejean A: **A hepatitis B virus pre-S-retinoic acid receptor beta chimera transforms erythrocytic progenitor cells in vitro.** *Proc Natl Acad Sci U S A* 1993, **90**(1):89-93.
10. Berasain C, Patil D, Perara E, Huang SM, Mouly H, Brechot C: **Oncogenic activation of a human cyclin A2 targeted to the endoplasmic reticulum upon hepatitis B virus genome insertion.** *Oncogene* 1998, **16**(10):1277-1288.
11. Gozuacik D, Murakami Y, Saigo K, Chami M, Mugnier C, Lagorce D, Okanoué T, Urashima T, Brechot C, Paterlini-Brechot P: **Identification of human cancer-related genes by naturally occurring Hepatitis B Virus DNA tagging.** *Oncogene* 2001, **20**(43):6233-6240.
12. Feitelson MA, Lee J: **Hepatitis B virus integration, fragile sites, and hepatocarcinogenesis.** *Cancer Lett* 2007, **252**(2):157-170.

13. Su Q, Schroder CH, Hofmann WJ, Otto G, Pichlmayr R, Bannasch P: **Expression of hepatitis B virus X protein in HBV-infected human livers and hepatocellular carcinomas.** *Hepatology* 1998, **27**(4):1109-1120.
14. Peng Z, Zhang Y, Gu W, Wang Z, Li D, Zhang F, Qiu G, Xie K: **Integration of the hepatitis B virus X fragment in hepatocellular carcinoma and its effects on the expression of multiple molecules: a key to the cell cycle and apoptosis.** *International journal of oncology* 2005, **26**(2):467-473.
15. Terradillos O, Billet O, Renard CA, Levy R, Molina T, Briand P, Buendia MA: **The hepatitis B virus X gene potentiates c-myc-induced liver oncogenesis in transgenic mice.** *Oncogene* 1997, **14**(4):395-404.
16. Kim SY, Lee PY, Shin HJ, Kim do H, Kang S, Moon HB, Kang SW, Kim JM, Park SG, Park BC *et al*: **Proteomic analysis of liver tissue from HBx-transgenic mice at early stages of hepatocarcinogenesis.** *Proteomics* 2009, **9**(22):5056-5066.
17. Ng SA, Lee C: **Hepatitis B virus X gene and hepatocarcinogenesis.** *Journal of gastroenterology* 2011, **46**(8):974-990.
18. Forner A, Llovet JM, Bruix J: **Hepatocellular carcinoma.** *Lancet* 2012, **379**(9822):1245-1255.
19. Forns X, Bukh J, Purcell RH: **The challenge of developing a vaccine against hepatitis C virus.** *J Hepatol* 2002, **37**(5):684-695.
20. Groopman JD, Kensler TW, Wild CP: **Protective interventions to prevent aflatoxin-induced carcinogenesis in developing countries.** *Annual review of public health* 2008, **29**:187-203.
21. Seitz HK, Poschl G, Simanowski UA: **Alcohol and cancer.** *Recent developments in alcoholism : an official publication of the American Medical Society on Alcoholism, the Research Society on Alcoholism, and the National Council on Alcoholism* 1998, **14**:67-95.
22. Farber E: **Alcohol and other chemicals in the development of hepatocellular carcinoma.** *Clinics in laboratory medicine* 1996, **16**(2):377-394.
23. Rabe C, Pilz T, Klostermann C, Berna M, Schild HH, Sauerbruch T, Caselmann WH: **Clinical characteristics and outcome of a cohort of 101 patients with hepatocellular carcinoma.** *World J Gastroenterol* 2001, **7**(2):208-215.
24. Kaczynski J, Hansson G, Hermodsson S, Olsson R, Wallerstedt S: **Minor role of hepatitis B and C virus infection in the etiology of hepatocellular carcinoma in a low-endemic area.** *Scand J Gastroenterol* 1996, **31**(8):809-813.
25. Laurent-Puig P, Legoix P, Bluteau O, Belghiti J, Franco D, Binot F, Monges G, Thomas G, Bioulac-Sage P, Zucman-Rossi J: **Genetic alterations associated with hepatocellular carcinomas define**

- distinct pathways of hepatocarcinogenesis.** *Gastroenterology* 2001, **120**(7):1763-1773.
26. Kato S, Tajiri T, Matsukura N, Matsuda N, Taniai N, Mamada H, Yoshida H, Kiyam T, Naito Z: **Genetic polymorphisms of aldehyde dehydrogenase 2, cytochrome p450 2E1 for liver cancer risk in HCV antibody-positive japanese patients and the variations of CYP2E1 mRNA expression levels in the liver due to its polymorphism.** *Scand J Gastroenterol* 2003, **38**(8):886-893.
 27. Nair J, Sone H, Nagao M, Barbin A, Bartsch H: **Copper-dependent formation of miscoding etheno-DNA adducts in the liver of Long Evans cinnamon (LEC) rats developing hereditary hepatitis and hepatocellular carcinoma.** *Cancer Res* 1996, **56**(6):1267-1271.
 28. Pogribny IP, Basnakian AG, Miller BJ, Lopatina NG, Poirier LA, James SJ: **Breaks in genomic DNA and within the p53 gene are associated with hypomethylation in livers of folate/methyl-deficient rats.** *Cancer Res* 1995, **55**(9):1894-1901.
 29. Lu SC, Alvarez L, Huang ZZ, Chen L, An W, Corrales FJ, Avila MA, Kanel G, Mato JM: **Methionine adenosyltransferase 1A knockout mice are predisposed to liver injury and exhibit increased expression of genes involved in proliferation.** *Proc Natl Acad Sci U S A* 2001, **98**(10):5560-5565.
 30. Bruix J, Sherman M, Llovet JM, Beaugrand M, Lencioni R, Burroughs AK, Christensen E, Pagliaro L, Colombo M, Rodes J: **Clinical management of hepatocellular carcinoma. Conclusions of the Barcelona-2000 EASL conference. European Association for the Study of the Liver.** *J Hepatol* 2001, **35**(3):421-430.
 31. Edmondson HA, Steiner PE: **Primary carcinoma of the liver: a study of 100 cases among 48,900 necropsies.** *Cancer* 1954, **7**(3):462-503.
 32. Livraghi T, Giorgio A, Marin G, Salmi A, de Sio I, Bolondi L, Pompili M, Brunello F, Lazzaroni S, Torzilli G *et al*: **Hepatocellular carcinoma and cirrhosis in 746 patients: long-term results of percutaneous ethanol injection.** *Radiology* 1995, **197**(1):101-108.
 33. Poon RT, Fan ST, Lo CM, Liu CL, Wong J: **Long-term survival and pattern of recurrence after resection of small hepatocellular carcinoma in patients with preserved liver function: implications for a strategy of salvage transplantation.** *Annals of surgery* 2002, **235**(3):373-382.
 34. Llovet JM, Fuster J, Bruix J: **Intention-to-treat analysis of surgical treatment for early hepatocellular carcinoma: resection versus transplantation.** *Hepatology* 1999, **30**(6):1434-1440.
 35. Maeda T, Shimada M, Harimoto N, Tsujita E, Aishima S, Tanaka S, Shirabe K, Maehara Y: **Prognosis of early hepatocellular carcinoma after hepatic resection.** *Hepato-gastroenterology* 2008, **55**(85):1428-1432.

36. Jonas S, Bechstein WO, Steinmuller T, Herrmann M, Radke C, Berg T, Settmacher U, Neuhaus P: **Vascular invasion and histopathologic grading determine outcome after liver transplantation for hepatocellular carcinoma in cirrhosis.** *Hepatology* 2001, **33**(5):1080-1086.
37. Adam R, Azoulay D, Castaing D, Eshkenazy R, Pascal G, Hashizume K, Samuel D, Bismuth H: **Liver resection as a bridge to transplantation for hepatocellular carcinoma on cirrhosis: a reasonable strategy?** *Annals of surgery* 2003, **238**(4):508-518; discussion 518-509.
38. Llovet JM, Fuster J, Bruix J: **The Barcelona approach: diagnosis, staging, and treatment of hepatocellular carcinoma.** *Liver Transpl* 2004, **10**(2 Suppl 1):S115-120.
39. Wang W, Shi J, Xie WF: **Transarterial chemoembolization in combination with percutaneous ablation therapy in unresectable hepatocellular carcinoma: a meta-analysis.** *Liver Int* 2010, **30**(5):741-749.
40. Marelli L, Stigliano R, Triantos C, Senzolo M, Cholongitas E, Davies N, Yu D, Meyer T, Patch DW, Burroughs AK: **Treatment outcomes for hepatocellular carcinoma using chemoembolization in combination with other therapies.** *Cancer treatment reviews* 2006, **32**(8):594-606.
41. Williams KJ, Parker CA, Stratford IJ: **Exogenous and endogenous markers of tumour oxygenation status: definitive markers of tumour hypoxia?** *Adv Exp Med Biol* 2005, **566**:285-294.
42. Lee Y, Kim M, Han J, Yeom KH, Lee S, Baek SH, Kim VN: **MicroRNA genes are transcribed by RNA polymerase II.** *Embo J* 2004, **23**(20):4051-4060.
43. Cai X, Hagedorn CH, Cullen BR: **Human microRNAs are processed from capped, polyadenylated transcripts that can also function as mRNAs.** *Rna* 2004, **10**(12):1957-1966.
44. Bracht J, Hunter S, Eachus R, Weeks P, Pasquinelli AE: **Trans-splicing and polyadenylation of let-7 microRNA primary transcripts.** *Rna* 2004, **10**(10):1586-1594.
45. Rodriguez A, Griffiths-Jones S, Ashurst JL, Bradley A: **Identification of mammalian microRNA host genes and transcription units.** *Genome research* 2004, **14**(10A):1902-1910.
46. Han J, Lee Y, Yeom KH, Kim YK, Jin H, Kim VN: **The Drosha-DGCR8 complex in primary microRNA processing.** *Genes & development* 2004, **18**(24):3016-3027.
47. Lee Y, Ahn C, Han J, Choi H, Kim J, Yim J, Lee J, Provost P, Radmark O, Kim S *et al*: **The nuclear RNase III Drosha initiates microRNA processing.** *Nature* 2003, **425**(6956):415-419.
48. Lund E, Guttlinger S, Calado A, Dahlberg JE, Kutay U: **Nuclear export of microRNA precursors.** *Science* 2004, **303**(5654):95-98.

49. Haase AD, Jaskiewicz L, Zhang H, Laine S, Sack R, Gatignol A, Filipowicz W: **TRBP, a regulator of cellular PKR and HIV-1 virus expression, interacts with Dicer and functions in RNA silencing.** *EMBO reports* 2005, **6**(10):961-967.
50. Zhang H, Kolb FA, Jaskiewicz L, Westhof E, Filipowicz W: **Single processing center models for human Dicer and bacterial RNase III.** *Cell* 2004, **118**(1):57-68.
51. Lingel A, Sattler M: **Novel modes of protein-RNA recognition in the RNAi pathway.** *Current opinion in structural biology* 2005, **15**(1):107-115.
52. Lee RC, Feinbaum RL, Ambros V: **The C. elegans heterochronic gene lin-4 encodes small RNAs with antisense complementarity to lin-14.** *Cell* 1993, **75**(5):843-854.
53. Wightman B, Ha I, Ruvkun G: **Posttranscriptional regulation of the heterochronic gene lin-14 by lin-4 mediates temporal pattern formation in C. elegans.** *Cell* 1993, **75**(5):855-862.
54. Liu J, Rivas FV, Wohlschlegel J, Yates JR, 3rd, Parker R, Hannon GJ: **A role for the P-body component GW182 in microRNA function.** *Nat Cell Biol* 2005, **7**(12):1261-1266.
55. Pillai RS, Bhattacharyya SN, Artus CG, Zoller T, Cougot N, Basyuk E, Bertrand E, Filipowicz W: **Inhibition of translational initiation by Let-7 MicroRNA in human cells.** *Science* 2005, **309**(5740):1573-1576.
56. Sheth U, Parker R: **Decapping and decay of messenger RNA occur in cytoplasmic processing bodies.** *Science* 2003, **300**(5620):805-808.
57. Cougot N, Babajko S, Seraphin B: **Cytoplasmic foci are sites of mRNA decay in human cells.** *J Cell Biol* 2004, **165**(1):31-40.
58. Liu J, Valencia-Sanchez MA, Hannon GJ, Parker R: **MicroRNA-dependent localization of targeted mRNAs to mammalian P-bodies.** *Nat Cell Biol* 2005, **7**(7):719-723.
59. Bhattacharyya SN, Habermacher R, Martine U, Closs EI, Filipowicz W: **Relief of microRNA-mediated translational repression in human cells subjected to stress.** *Cell* 2006, **125**(6):1111-1124.
60. Hendrickson DG, Hogan DJ, McCullough HL, Myers JW, Herschlag D, Ferrell JE, Brown PO: **Concordant regulation of translation and mRNA abundance for hundreds of targets of a human microRNA.** *PLoS Biol* 2009, **7**(11):e1000238.
61. Lim LP, Lau NC, Garrett-Engle P, Grimson A, Schelter JM, Castle J, Bartel DP, Linsley PS, Johnson JM: **Microarray analysis shows that some microRNAs downregulate large numbers of target mRNAs.** *Nature* 2005, **433**(7027):769-773.
62. Schmitter D, Filkowski J, Sewer A, Pillai RS, Oakeley EJ, Zavolan M, Svoboda P, Filipowicz W: **Effects of Dicer and Argonaute down-regulation on mRNA levels in human HEK293 cells.** *Nucleic Acids Res* 2006, **34**(17):4801-4815.

63. Yekta S, Shih IH, Bartel DP: **MicroRNA-directed cleavage of HOXB8 mRNA.** *Science* 2004, **304**(5670):594-596.
64. Behm-Ansmant I, Rehwinkel J, Doerks T, Stark A, Bork P, Izaurralde E: **mRNA degradation by miRNAs and GW182 requires both CCR4:NOT deadenylase and DCP1:DCP2 decapping complexes.** *Genes & development* 2006, **20**(14):1885-1898.
65. Eulalio A, Huntzinger E, Nishihara T, Rehwinkel J, Fauser M, Izaurralde E: **Deadenylation is a widespread effect of miRNA regulation.** *Rna* 2009, **15**(1):21-32.
66. Calin GA, Dumitru CD, Shimizu M, Bichi R, Zupo S, Noch E, Aldler H, Rattan S, Keating M, Rai K *et al*: **Frequent deletions and down-regulation of micro- RNA genes miR15 and miR16 at 13q14 in chronic lymphocytic leukemia.** *Proc Natl Acad Sci U S A* 2002, **99**(24):15524-15529.
67. Calin GA, Sevignani C, Dumitru CD, Hyslop T, Noch E, Yendamuri S, Shimizu M, Rattan S, Bullrich F, Negrini M *et al*: **Human microRNA genes are frequently located at fragile sites and genomic regions involved in cancers.** *Proc Natl Acad Sci U S A* 2004, **101**(9):2999-3004.
68. He L, Thomson JM, Hemann MT, Hernando-Monge E, Mu D, Goodson S, Powers S, Cordon-Cardo C, Lowe SW, Hannon GJ *et al*: **A microRNA polycistron as a potential human oncogene.** *Nature* 2005, **435**(7043):828-833.
69. Hayashita Y, Osada H, Tatematsu Y, Yamada H, Yanagisawa K, Tomida S, Yatabe Y, Kawahara K, Sekido Y, Takahashi T: **A polycistronic microRNA cluster, miR-17-92, is overexpressed in human lung cancers and enhances cell proliferation.** *Cancer Res* 2005, **65**(21):9628-9632.
70. Ota A, Tagawa H, Karnan S, Tsuzuki S, Karpas A, Kira S, Yoshida Y, Seto M: **Identification and characterization of a novel gene, C13orf25, as a target for 13q31-q32 amplification in malignant lymphoma.** *Cancer Res* 2004, **64**(9):3087-3095.
71. Rinaldi A, Poretti G, Kwee I, Zucca E, Catapano CV, Tibiletti MG, Bertoni F: **Concomitant MYC and microRNA cluster miR-17-92 (C13orf25) amplification in human mantle cell lymphoma.** *Leuk Lymphoma* 2007, **48**(2):410-412.
72. Diosdado B, van de Wiel MA, Terhaar Sive Droste JS, Mongera S, Postma C, Meijerink WJ, Carvalho B, Meijer GA: **MiR-17-92 cluster is associated with 13q gain and c-myc expression during colorectal adenoma to adenocarcinoma progression.** *Br J Cancer* 2009, **101**(4):707-714.
73. Costinean S, Zanesi N, Pekarsky Y, Tili E, Volinia S, Heerema N, Croce CM: **Pre-B cell proliferation and lymphoblastic leukemia/high-grade lymphoma in E(mu)-miR155 transgenic mice.** *Proc Natl Acad Sci U S A* 2006, **103**(18):7024-7029.

74. Chan JA, Krichevsky AM, Kosik KS: **MicroRNA-21 is an antiapoptotic factor in human glioblastoma cells.** *Cancer Res* 2005, **65**(14):6029-6033.
75. Landgraf P, Rusu M, Sheridan R, Sewer A, Iovino N, Aravin A, Pfeffer S, Rice A, Kamphorst AO, Landthaler M *et al*: **A mammalian microRNA expression atlas based on small RNA library sequencing.** *Cell* 2007, **129**(7):1401-1414.
76. Johnson SM, Grosshans H, Shingara J, Byrom M, Jarvis R, Cheng A, Labourier E, Reinert KL, Brown D, Slack FJ: **RAS is regulated by the let-7 microRNA family.** *Cell* 2005, **120**(5):635-647.
77. Burner GC, Loeb LA: **Mutations in the KRAS2 oncogene during progressive stages of human colon carcinoma.** *Proc Natl Acad Sci U S A* 1989, **86**(7):2403-2407.
78. Almoguera C, Shibata D, Forrester K, Martin J, Arnheim N, Perucho M: **Most human carcinomas of the exocrine pancreas contain mutant c-K-ras genes.** *Cell* 1988, **53**(4):549-554.
79. Tam IY, Chung LP, Suen WS, Wang E, Wong MC, Ho KK, Lam WK, Chiu SW, Girard L, Minna JD *et al*: **Distinct epidermal growth factor receptor and KRAS mutation patterns in non-small cell lung cancer patients with different tobacco exposure and clinicopathologic features.** *Clin Cancer Res* 2006, **12**(5):1647-1653.
80. Bai S, Nasser MW, Wang B, Hsu SH, Datta J, Kutay H, Yadav A, Nuovo G, Kumar P, Ghoshal K: **MicroRNA-122 inhibits tumorigenic properties of hepatocellular carcinoma cells and sensitizes these cells to sorafenib.** *J Biol Chem* 2009, **284**(46):32015-32027.
81. Kutay H, Bai S, Datta J, Motiwala T, Pogribny I, Frankel W, Jacob ST, Ghoshal K: **Downregulation of miR-122 in the rodent and human hepatocellular carcinomas.** *J Cell Biochem* 2006, **99**(3):671-678.
82. Fornari F, Gramantieri L, Giovannini C, Veronese A, Ferracin M, Sabbioni S, Calin GA, Grazi GL, Croce CM, Tavolari S *et al*: **MiR-122/cyclin G1 interaction modulates p53 activity and affects doxorubicin sensitivity of human hepatocarcinoma cells.** *Cancer Res* 2009, **69**(14):5761-5767.
83. Ladeiro Y, Couchy G, Balabaud C, Bioulac-Sage P, Pelletier L, Rebouissou S, Zucman-Rossi J: **MicroRNA profiling in hepatocellular tumors is associated with clinical features and oncogene/tumor suppressor gene mutations.** *Hepatology* 2008, **47**(6):1955-1963.
84. Callegari E, Elamin BK, Giannone F, Milazzo M, Altavilla G, Fornari F, Giacomelli L, D'Abundo L, Ferracin M, Bassi C *et al*: **Liver tumorigenicity promoted by microRNA-221 in a mouse transgenic model.** *Hepatology* 2012.
85. Hou J, Lin L, Zhou W, Wang Z, Ding G, Dong Q, Qin L, Wu X, Zheng Y, Yang Y *et al*: **Identification of miRNomes in human liver and hepatocellular carcinoma reveals miR-199a/b-3p as therapeutic**

- target for hepatocellular carcinoma.** *Cancer Cell* 2011, **19**(2):232-243.
86. Kota J, Chivukula RR, O'Donnell KA, Wentzel EA, Montgomery CL, Hwang HW, Chang TC, Vivekanandan P, Torbenson M, Clark KR *et al*: **Therapeutic microRNA delivery suppresses tumorigenesis in a murine liver cancer model.** *Cell* 2009, **137**(6):1005-1017.
87. Pineau P, Volinia S, McJunkin K, Marchio A, Battiston C, Terris B, Mazzaferro V, Lowe SW, Croce CM, Dejean A: **miR-221 overexpression contributes to liver tumorigenesis.** *Proc Natl Acad Sci U S A*, **107**(1):264-269.
88. Ng R, Song G, Roll GR, Frandsen NM, Willenbring H: **A microRNA-21 surge facilitates rapid cyclin D1 translation and cell cycle progression in mouse liver regeneration.** *J Clin Invest* 2012, **122**(3):1097-1108.
89. Furuta M, Kozaki KI, Tanaka S, Aii S, Imoto I, Inazawa J: **miR-124 and miR-203 are epigenetically silenced tumor-suppressive microRNAs in hepatocellular carcinoma.** *Carcinogenesis* 2010, **31**(5):766-776.
90. Hatzia Apostolou M, Polytaichou C, Aggelidou E, Drakaki A, Poultsides GA, Jaeger SA, Ogata H, Karin M, Struhl K, Hadzopoulou-Cladaras M *et al*: **An HNF4alpha-miRNA inflammatory feedback circuit regulates hepatocellular oncogenesis.** *Cell* 2011, **147**(6):1233-1247.
91. Lin CJ, Gong HY, Tseng HC, Wang WL, Wu JL: **miR-122 targets an anti-apoptotic gene, Bcl-w, in human hepatocellular carcinoma cell lines.** *Biochem Biophys Res Commun* 2008, **375**(3):315-320.
92. Gramantieri L, Fornari F, Ferracin M, Veronese A, Sabbioni S, Calin GA, Grazi GL, Croce CM, Bolondi L, Negrini M: **MicroRNA-221 targets Bmf in hepatocellular carcinoma and correlates with tumor multifocality.** *Clin Cancer Res* 2009, **15**(16):5073-5081.
93. Li Y, Tan W, Neo TW, Aung MO, Wasser S, Lim SG, Tan TM: **Role of the miR-106b-25 microRNA cluster in hepatocellular carcinoma.** *Cancer Sci* 2009, **100**(7):1234-1242.
94. Asangani IA, Rasheed SA, Nikolova DA, Leupold JH, Colburn NH, Post S, Allgayer H: **MicroRNA-21 (miR-21) post-transcriptionally downregulates tumor suppressor Pcd4 and stimulates invasion, intravasation and metastasis in colorectal cancer.** *Oncogene* 2008, **27**(15):2128-2136.
95. Frankel LB, Christoffersen NR, Jacobsen A, Lindow M, Krogh A, Lund AH: **Programmed cell death 4 (PDCD4) is an important functional target of the microRNA miR-21 in breast cancer cells.** *J Biol Chem* 2008, **283**(2):1026-1033.
96. Li T, Li D, Sha J, Sun P, Huang Y: **MicroRNA-21 directly targets MARCKS and promotes apoptosis resistance and invasion in prostate cancer cells.** *Biochem Biophys Res Commun* 2009, **383**(3):280-285.

97. Meng F, Henson R, Wehbe-Janek H, Ghoshal K, Jacob ST, Patel T: **MicroRNA-21 regulates expression of the PTEN tumor suppressor gene in human hepatocellular cancer.** *Gastroenterology* 2007, **133**(2):647-658.
98. Garofalo M, Di Leva G, Romano G, Nuovo G, Suh SS, Ngankeu A, Taccioli C, Pichiorri F, Alder H, Secchiero P *et al*: **miR-221&222 regulate TRAIL resistance and enhance tumorigenicity through PTEN and TIMP3 downregulation.** *Cancer Cell* 2009, **16**(6):498-509.
99. Li N, Fu H, Tie Y, Hu Z, Kong W, Wu Y, Zheng X: **miR-34a inhibits migration and invasion by down-regulation of c-Met expression in human hepatocellular carcinoma cells.** *Cancer Lett* 2009, **275**(1):44-53.
100. Salvi A, Sabelli C, Moncini S, Venturin M, Arici B, Riva P, Portolani N, Giulini SM, De Petro G, Barlati S: **MicroRNA-23b mediates urokinase and c-met downmodulation and a decreased migration of human hepatocellular carcinoma cells.** *FEBS J* 2009, **276**(11):2966-2982.
101. Leelawat K, Leelawat S, Tepaksorn P, Rattanasinganchan P, Leungchaweng A, Tohtong R, Sobhon P: **Involvement of c-Met/hepatocyte growth factor pathway in cholangiocarcinoma cell invasion and its therapeutic inhibition with small interfering RNA specific for c-Met.** *J Surg Res* 2006, **136**(1):78-84.
102. Ma PC, Tretiakova MS, Nallasura V, Jagadeeswaran R, Husain AN, Salgia R: **Downstream signalling and specific inhibition of c-MET/HGF pathway in small cell lung cancer: implications for tumour invasion.** *Br J Cancer* 2007, **97**(3):368-377.
103. Sipeki S, Bander E, Buday L, Farkas G, Bacsy E, Ways DK, Farago A: **Phosphatidylinositol 3-kinase contributes to Erk1/Erk2 MAP kinase activation associated with hepatocyte growth factor-induced cell scattering.** *Cell Signal* 1999, **11**(12):885-890.
104. Frese KK, Tuveson DA: **Maximizing mouse cancer models.** *Nature reviews Cancer* 2007, **7**(9):645-658.
105. Rygaard J, Povlsen CO: **Heterotransplantation of a human malignant tumour to "Nude" mice.** *Acta pathologica et microbiologica Scandinavica* 1969, **77**(4):758-760.
106. Hoffman RM: **Orthotopic metastatic (MetaMouse) models for discovery and development of novel chemotherapy.** *Methods Mol Med* 2005, **111**:297-322.
107. Newell P, Villanueva A, Friedman SL, Koike K, Llovet JM: **Experimental models of hepatocellular carcinoma.** *J Hepatol* 2008, **48**(5):858-879.
108. Jaenisch R: **Transgenic animals.** *Science* 1988, **240**(4858):1468-1474.

109. Lois C, Hong EJ, Pease S, Brown EJ, Baltimore D: **Germline transmission and tissue-specific expression of transgenes delivered by lentiviral vectors.** *Science* 2002, **295**(5556):868-872.
110. Postic C, Magnuson MA: **DNA excision in liver by an albumin-Cre transgene occurs progressively with age.** *Genesis* 2000, **26**(2):149-150.
111. Jonkers J, Berns A: **Conditional mouse models of sporadic cancer.** *Nature reviews Cancer* 2002, **2**(4):251-265.
112. Maeda S, Kamata H, Luo JL, Leffert H, Karin M: **IKKbeta couples hepatocyte death to cytokine-driven compensatory proliferation that promotes chemical hepatocarcinogenesis.** *Cell* 2005, **121**(7):977-990.
113. Verna L, Whysner J, Williams GM: **N-nitrosodiethylamine mechanistic data and risk assessment: bioactivation, DNA-adduct formation, mutagenicity, and tumor initiation.** *Pharmacology & therapeutics* 1996, **71**(1-2):57-81.
114. Vesselinovitch SD, Koka M, Mihailovich N, Rao KV: **Carcinogenicity of diethylnitrosamine in newborn, infant, and adult mice.** *Journal of cancer research and clinical oncology* 1984, **108**(1):60-65.
115. Solt DB, Medline A, Farber E: **Rapid emergence of carcinogen-induced hyperplastic lesions in a new model for the sequential analysis of liver carcinogenesis.** *The American journal of pathology* 1977, **88**(3):595-618.
116. Tamano S, Merlino GT, Ward JM: **Rapid development of hepatic tumors in transforming growth factor alpha transgenic mice associated with increased cell proliferation in precancerous hepatocellular lesions initiated by N-nitrosodiethylamine and promoted by phenobarbital.** *Carcinogenesis* 1994, **15**(9):1791-1798.
117. Davis ME, Chen ZG, Shin DM: **Nanoparticle therapeutics: an emerging treatment modality for cancer.** *Nat Rev Drug Discov* 2008, **7**(9):771-782.
118. Trang P, Medina PP, Wiggins JF, Ruffino L, Kelnar K, Omotola M, Homer R, Brown D, Bader AG, Weidhaas JB *et al*: **Regression of murine lung tumors by the let-7 microRNA.** *Oncogene* 2010, **29**(11):1580-1587.
119. Esquela-Kerscher A, Trang P, Wiggins JF, Patrawala L, Cheng A, Ford L, Weidhaas JB, Brown D, Bader AG, Slack FJ: **The let-7 microRNA reduces tumor growth in mouse models of lung cancer.** *Cell Cycle* 2008, **7**(6):759-764.
120. Elmen J, Lindow M, Schutz S, Lawrence M, Petri A, Obad S, Lindholm M, Hedtjarn M, Hansen HF, Berger U *et al*: **LNA-mediated microRNA silencing in non-human primates.** *Nature* 2008, **452**(7189):896-899.
121. Sato A, Takagi M, Shimamoto A, Kawakami S, Hashida M: **Small interfering RNA delivery to the liver by intravenous administration**

- of galactosylated cationic liposomes in mice.** *Biomaterials* 2007, **28**(7):1434-1442.
122. Rozema DB, Lewis DL, Wakefield DH, Wong SC, Klein JJ, Roesch PL, Bertin SL, Reppen TW, Chu Q, Blokhin AV *et al*: **Dynamic PolyConjugates for targeted in vivo delivery of siRNA to hepatocytes.** *Proc Natl Acad Sci U S A* 2007, **104**(32):12982-12987.
 123. Soutschek J, Akinc A, Bramlage B, Charisse K, Constien R, Donoghue M, Elbashir S, Geick A, Hadwiger P, Harborth J *et al*: **Therapeutic silencing of an endogenous gene by systemic administration of modified siRNAs.** *Nature* 2004, **432**(7014):173-178.
 124. Zimmermann TS, Lee AC, Akinc A, Bramlage B, Bumcrot D, Fedoruk MN, Harborth J, Heyes JA, Jeffs LB, John M *et al*: **RNAi-mediated gene silencing in non-human primates.** *Nature* 2006, **441**(7089):111-114.
 125. Burnett JC, Rossi JJ, Tiemann K: **Current progress of siRNA/shRNA therapeutics in clinical trials.** *Biotechnology journal* 2011, **6**(9):1130-1146.
 126. Winter J, Jung S, Keller S, Gregory RI, Diederichs S: **Many roads to maturity: microRNA biogenesis pathways and their regulation.** *Nat Cell Biol* 2009, **11**(3):228-234.
 127. Rossi JJ: **RNAi and the P-body connection.** *Nat Cell Biol* 2005, **7**(7):643-644.
 128. Gramantieri L, Fornari F, Callegari E, Sabbioni S, Lanza G, Croce CM, Bolondi L, Negrini M: **MicroRNA involvement in hepatocellular carcinoma.** *J Cell Mol Med* 2008, **12**(6A):2189-2204.
 129. Lagos-Quintana M, Rauhut R, Yalcin A, Meyer J, Lendeckel W, Tuschl T: **Identification of tissue-specific microRNAs from mouse.** *Curr Biol* 2002, **12**(9):735-739.
 130. Krutzfeldt J, Rajewsky N, Braich R, Rajeev KG, Tuschl T, Manoharan M, Stoffel M: **Silencing of microRNAs in vivo with 'antagomirs'.** *Nature* 2005, **438**(7068):685-689.
 131. Esau C, Davis S, Murray SF, Yu XX, Pandey SK, Pear M, Watts L, Booten SL, Graham M, McKay R *et al*: **miR-122 regulation of lipid metabolism revealed by in vivo antisense targeting.** *Cell Metab* 2006, **3**(2):87-98.
 132. Jopling CL, Norman KL, Sarnow P: **Positive and negative modulation of viral and cellular mRNAs by liver-specific microRNA miR-122.** *Cold Spring Harb Symp Quant Biol* 2006, **71**:369-376.
 133. Lanford RE, Hildebrandt-Eriksen ES, Petri A, Persson R, Lindow M, Munk ME, Kauppinen S, Orum H: **Therapeutic silencing of microRNA-122 in primates with chronic hepatitis C virus infection.** *Science* 2010, **327**(5962):198-201.

134. El-Serag HB, Rudolph KL: **Hepatocellular carcinoma: epidemiology and molecular carcinogenesis.** *Gastroenterology* 2007, **132**(7):2557-2576.
135. Cheung O, Puri P, Eicken C, Contos MJ, Mirshahi F, Maher JW, Kellum JM, Min H, Luketic VA, Sanyal AJ: **Nonalcoholic steatohepatitis is associated with altered hepatic MicroRNA expression.** *Hepatology* 2008, **48**(6):1810-1820.
136. Filipowicz W, Grosshans H: **The liver-specific microRNA miR-122: biology and therapeutic potential.** *Prog Drug Res* 2011, **67**:221-238.
137. Kojima K, Takata A, Vadnais C, Otsuka M, Yoshikawa T, Akanuma M, Kondo Y, Kang YJ, Kishikawa T, Kato N *et al*: **MicroRNA122 is a key regulator of alpha-fetoprotein expression and influences the aggressiveness of hepatocellular carcinoma.** *Nat Commun* 2011, **2**:338.
138. Sekine S, Ogawa R, Ito R, Hiraoka N, McManus MT, Kanai Y, Hebrok M: **Disruption of Dicer1 induces dysregulated fetal gene expression and promotes hepatocarcinogenesis.** *Gastroenterology* 2009, **136**(7):2304-2315 e2301-2304.
139. Trimboli AJ, Cantemir-Stone CZ, Li F, Wallace JA, Merchant A, Creasap N, Thompson JC, Caserta E, Wang H, Chong JL *et al*: **Pten in stromal fibroblasts suppresses mammary epithelial tumours.** *Nature* 2009, **461**(7267):1084-1091.
140. Adams GM, Norton SJ: **Lipid metabolism. I. Effects of pressure and gas composition on acetate-C14 incorporation into liver lipids.** *Aerosp Med* 1971, **42**(2):146-148.
141. Ntambi JM, Bene H: **Polyunsaturated fatty acid regulation of gene expression.** *J Mol Neurosci* 2001, **16**(2-3):273-278; discussion 279-284.
142. Uchiyama S, Shimizu T, Shirasawa T: **CuZn-SOD deficiency causes ApoB degradation and induces hepatic lipid accumulation by impaired lipoprotein secretion in mice.** *J Biol Chem* 2006, **281**(42):31713-31719.
143. Livak KJ, Schmittgen TD: **Analysis of relative gene expression data using real-time quantitative PCR and the 2(-Delta Delta C(T)) Method.** *Methods* 2001, **25**(4):402-408.
144. Hill JR: **In Vitro Drug Metabolism Using Liver Microsomes.** *Current Protocols in Pharmacology* 2004, **7**(Chapter 8):1-11.
145. Wang B, Majumder S, Nuovo G, Kutay H, Volinia S, Patel T, Schmittgen TD, Croce C, Ghoshal K, Jacob ST: **Role of microRNA-155 at early stages of hepatocarcinogenesis induced by choline-deficient and amino acid-defined diet in C57BL/6 mice.** *Hepatology* 2009, **50**(4):1152-1161.
146. Yu J, Mitsui T, Wei M, Mao H, Butchar JP, Shah MV, Zhang J, Mishra A, Alvarez-Breckenridge C, Liu X *et al*: **NKp46 identifies an NKT cell**

- subset susceptible to leukemic transformation in mouse and human. *J Clin Invest*, **121**(4):1456-1470.
147. Shui JW, Hu MC, Tan TH: **Conditional knockout mice reveal an essential role of protein phosphatase 4 in thymocyte development and pre-T-cell receptor signaling.** *Mol Cell Biol* 2007, **27**(1):79-91.
 148. Wang B, Hsu SH, Majumder S, Kutay H, Huang W, Jacob ST, Ghoshal K: **TGFbeta-mediated upregulation of hepatic miR-181b promotes hepatocarcinogenesis by targeting TIMP3.** *Oncogene* 2009.
 149. Irizarry RA, Hobbs B, Collin F, Beazer-Barclay YD, Antonellis KJ, Scherf U, Speed TP: **Exploration, normalization, and summaries of high density oligonucleotide array probe level data.** *Biostatistics* 2003, **4**(2):249-264.
 150. Smyth GK: **Linear models and empirical bayes methods for assessing differential expression in microarray experiments.** *Stat Appl Genet Mol Biol* 2004, **3**:Article3.
 151. Gordon D, Haynes C, Yang Y, Kramer PL, Finch SJ: **Linear trend tests for case-control genetic association that incorporate random phenotype and genotype misclassification error.** *Genet Epidemiol* 2007, **31**(8):853-870.
 152. Chang J, Nicolas E, Marks D, Sander C, Lerro A, Buendia MA, Xu C, Mason WS, Moloshok T, Bort R *et al*: **miR-122, a mammalian liver-specific microRNA, is processed from hcr mRNA and may downregulate the high affinity cationic amino acid transporter CAT-1.** *RNA Biol* 2004, **1**(2):106-113.
 153. Gatfield D, Le Martelot G, Vejnar CE, Gerlach D, Schaad O, Fleury-Olela F, Ruskeepaa AL, Oresic M, Esau CC, Zdobnov EM *et al*: **Integration of microRNA miR-122 in hepatic circadian gene expression.** *Genes Dev* 2009, **23**(11):1313-1326.
 154. van Dongen S, Abreu-Goodger C, Enright AJ: **Detecting microRNA binding and siRNA off-target effects from expression data.** *Nat Methods* 2008, **5**(12):1023-1025.
 155. Coleman RA, Lee DP: **Enzymes of triacylglycerol synthesis and their regulation.** *Prog Lipid Res* 2004, **43**(2):134-176.
 156. Matsusue K, Kusakabe T, Noguchi T, Takiguchi S, Suzuki T, Yamano S, Gonzalez FJ: **Hepatic steatosis in leptin-deficient mice is promoted by the PPARgamma target gene Fsp27.** *Cell Metab* 2008, **7**(4):302-311.
 157. Bartel DP: **MicroRNAs: target recognition and regulatory functions.** *Cell* 2009, **136**(2):215-233.
 158. Yamashita T, Ji J, Budhu A, Forgues M, Yang W, Wang HY, Jia H, Ye Q, Qin LX, Wauthier E *et al*: **EpCAM-positive hepatocellular carcinoma cells are tumor-initiating cells with stem/progenitor cell features.** *Gastroenterology* 2009, **136**(3):1012-1024.
 159. Thorgeirsson SS, Lee JS, Grisham JW: **Molecular prognostication of liver cancer: end of the beginning.** *J Hepatol* 2006, **44**(4):798-805.

160. Orimo T, Ojima H, Hiraoka N, Saito S, Kosuge T, Kakisaka T, Yokoo H, Nakanishi K, Kamiyama T, Todo S *et al*: **Proteomic profiling reveals the prognostic value of adenomatous polyposis coli-end-binding protein 1 in hepatocellular carcinoma.** *Hepatology* 2008, **48**(6):1851-1863.
161. Man JH, Liang B, Gu YX, Zhou T, Li AL, Li T, Jin BF, Bai B, Zhang HY, Zhang WN *et al*: **Gankyrin plays an essential role in Ras-induced tumorigenesis through regulation of the Rhoa/ROCK pathway in mammalian cells.** *J Clin Invest*, **120**(8):2829-2841.
162. Karin M: **Nuclear factor-kappaB in cancer development and progression.** *Nature* 2006, **441**(7092):431-436.
163. Grivennikov SI, Karin M: **Inflammatory cytokines in cancer: tumour necrosis factor and interleukin 6 take the stage.** *Ann Rheum Dis*, **70 Suppl 1**:i104-108.
164. Lagasse E, Weissman IL: **Flow cytometric identification of murine neutrophils and monocytes.** *J Immunol Methods* 1996, **197**(1-2):139-150.
165. Karlmark KR, Wasmuth HE, Trautwein C, Tacke F: **Chemokine-directed immune cell infiltration in acute and chronic liver disease.** *Expert Rev Gastroenterol Hepatol* 2008, **2**(2):233-242.
166. Baeck C, Wehr A, Karlmark KR, Heymann F, Vucur M, Gassler N, Huss S, Klussmann S, Eulberg D, Luedde T *et al*: **Pharmacological inhibition of the chemokine CCL2 (MCP-1) diminishes liver macrophage infiltration and steatohepatitis in chronic hepatic injury.** *Gut*.
167. Miranda KC, Huynh T, Tay Y, Ang YS, Tam WL, Thomson AM, Lim B, Rigoutsos I: **A pattern-based method for the identification of MicroRNA binding sites and their corresponding heteroduplexes.** *Cell* 2006, **126**(6):1203-1217.
168. Xiang ZL, Zeng ZC, Tang ZY, Fan J, Zhuang PY, Liang Y, Tan YS, He J: **Chemokine receptor CXCR4 expression in hepatocellular carcinoma patients increases the risk of bone metastases and poor survival.** *BMC Cancer* 2009, **9**:176.
169. Coulouarn C, Factor VM, Conner EA, Thorgeirsson SS: **Genomic modeling of tumor onset and progression in a mouse model of aggressive human liver cancer.** *Carcinogenesis*.
170. Nault JC, Zucman-Rossi J: **Genetics of hepatobiliary carcinogenesis.** *Semin Liver Dis*, **31**(2):173-187.
171. Gou L, Wang W, Tong A, Yao Y, Zhou Y, Yi C, Yang J: **Proteomic identification of Rhoa as a potential biomarker for proliferation and metastasis in hepatocellular carcinoma.** *J Mol Med (Berl)*, **89**(8):817-827.
172. Wang W, Wu F, Fang F, Tao Y, Yang L: **Inhibition of invasion and metastasis of hepatocellular carcinoma cells via targeting Rhoc in vitro and in vivo.** *Clin Cancer Res* 2008, **14**(21):6804-6812.

173. Lee JS, Thorgeirsson SS: **Comparative and integrative functional genomics of HCC.** *Oncogene* 2006, **25**(27):3801-3809.
174. Anderson N, Borlak J: **Molecular mechanisms and therapeutic targets in steatosis and steatohepatitis.** *Pharmacol Rev* 2008, **60**(3):311-357.
175. El-Serag HB: **Hepatocellular carcinoma.** *N Engl J Med* 2011, **365**(12):1118-1127.
176. Naugler WE, Sakurai T, Kim S, Maeda S, Kim K, Elsharkawy AM, Karin M: **Gender disparity in liver cancer due to sex differences in MyD88-dependent IL-6 production.** *Science* 2007, **317**(5834):121-124.
177. Jopling CL: **Regulation of hepatitis C virus by microRNA-122.** *Biochem Soc Trans* 2008, **36**(Pt 6):1220-1223.
178. Wang B, Hsu SH, Majumder S, Kutay H, Huang W, Jacob ST, Ghoshal K: **TGFbeta-mediated upregulation of hepatic miR-181b promotes hepatocarcinogenesis by targeting TIMP3.** *Oncogene* 2010, **29**(12):1787-1797.
179. Linhart HG, Troen A, Bell GW, Cantu E, Chao WH, Moran E, Steine E, He T, Jaenisch R: **Folate deficiency induces genomic uracil misincorporation and hypomethylation but does not increase DNA point mutations.** *Gastroenterology* 2009, **136**(1):227-235 e223.
180. Bruix J, Boix L, Sala M, Llovet JM: **Focus on hepatocellular carcinoma.** *Cancer Cell* 2004, **5**(3):215-219.
181. Seeff LB, Hoofnagle JH: **Epidemiology of hepatocellular carcinoma in areas of low hepatitis B and hepatitis C endemicity.** *Oncogene* 2006, **25**(27):3771-3777.
182. Altekruse SF, McGlynn KA, Reichman ME: **Hepatocellular carcinoma incidence, mortality, and survival trends in the United States from 1975 to 2005.** *J Clin Oncol* 2009, **27**(9):1485-1491.
183. Tang ZY: **Hepatocellular carcinoma--cause, treatment and metastasis.** *World J Gastroenterol* 2001, **7**(4):445-454.
184. Ambros V: **The functions of animal microRNAs.** *Nature* 2004, **431**(7006):350-355.
185. Bartel DP: **MicroRNAs: genomics, biogenesis, mechanism, and function.** *Cell* 2004, **116**(2):281-297.
186. Aravalli RN, Steer CJ, Cressman EN: **Molecular mechanisms of hepatocellular carcinoma.** *Hepatology* 2008, **48**(6):2047-2063.
187. Huang YS, Dai Y, Yu XF, Bao SY, Yin YB, Tang M, Hu CX: **Microarray analysis of microRNA expression in hepatocellular carcinoma and non-tumorous tissues without viral hepatitis.** *J Gastroenterol Hepatol* 2008, **23**(1):87-94.
188. Mendell JT, Olson EN: **MicroRNAs in Stress Signaling and Human Disease.** *Cell* 2012, **148**(6):1172-1187.
189. Coulouarn C, Factor VM, Andersen JB, Durkin ME, Thorgeirsson SS: **Loss of miR-122 expression in liver cancer correlates with**

- suppression of the hepatic phenotype and gain of metastatic properties.** *Oncogene* 2009, **28**(40):3526-3536.
190. Budhu A, Jia HL, Forgues M, Liu CG, Goldstein D, Lam A, Zanetti KA, Ye QH, Qin LX, Croce CM *et al*: **Identification of metastasis-related microRNAs in hepatocellular carcinoma.** *Hepatology* 2008, **47**(3):897-907.
191. Tsai WC, Hsu PW, Lai TC, Chau GY, Lin CW, Chen CM, Lin CD, Liao YL, Wang JL, Chau YP *et al*: **MicroRNA-122, a tumor suppressor microRNA that regulates intrahepatic metastasis of hepatocellular carcinoma.** *Hepatology* 2009, **49**(5):1571-1582.
192. Lewis DL, Hagstrom JE, Loomis AG, Wolff JA, Herweijer H: **Efficient delivery of siRNA for inhibition of gene expression in postnatal mice.** *Nat Genet* 2002, **32**(1):107-108.
193. McCaffrey AP, Meuse L, Pham TT, Conklin DS, Hannon GJ, Kay MA: **RNA interference in adult mice.** *Nature* 2002, **418**(6893):38-39.
194. Grimm D, Streetz KL, Jopling CL, Storm TA, Pandey K, Davis CR, Marion P, Salazar F, Kay MA: **Fatality in mice due to oversaturation of cellular microRNA/short hairpin RNA pathways.** *Nature* 2006, **441**(7092):537-541.
195. Tiscornia G, Singer O, Ikawa M, Verma IM: **A general method for gene knockdown in mice by using lentiviral vectors expressing small interfering RNA.** *Proc Natl Acad Sci U S A* 2003, **100**(4):1844-1848.
196. Judge AD, Bola G, Lee AC, MacLachlan I: **Design of noninflammatory synthetic siRNA mediating potent gene silencing in vivo.** *Mol Ther* 2006, **13**(3):494-505.
197. de Fougerolles AR: **Delivery vehicles for small interfering RNA in vivo.** *Hum Gene Ther* 2008, **19**(2):125-132.
198. Whitehead KA, Langer R, Anderson DG: **Knocking down barriers: advances in siRNA delivery.** *Nat Rev Drug Discov* 2009, **8**(2):129-138.
199. Cullis PR, Hope MJ, Tilcock CP: **Lipid polymorphism and the roles of lipids in membranes.** *Chem Phys Lipids* 1986, **40**(2-4):127-144.
200. Hafez IM, Maurer N, Cullis PR: **On the mechanism whereby cationic lipids promote intracellular delivery of polynucleic acids.** *Gene Ther* 2001, **8**(15):1188-1196.
201. Akinc A, Zumbuehl A, Goldberg M, Leshchiner ES, Busini V, Hossain N, Bacallado SA, Nguyen DN, Fuller J, Alvarez R *et al*: **A combinatorial library of lipid-like materials for delivery of RNAi therapeutics.** *Nat Biotechnol* 2008, **26**(5):561-569.
202. Frank-Kamenetsky M, Grefhorst A, Anderson NN, Racie TS, Bramlage B, Akinc A, Butler D, Charisse K, Dorkin R, Fan Y *et al*: **Therapeutic RNAi targeting PCSK9 acutely lowers plasma cholesterol in rodents and LDL cholesterol in nonhuman primates.** *Proc Natl Acad Sci U S A* 2008, **105**(33):11915-11920.

203. Wang X, Yu B, Wu Y, Lee RJ, Lee LJ: **Efficient down-regulation of CDK4 by novel lipid nanoparticle-mediated siRNA delivery.** *Anticancer Res* 2011, **31**(5):1619-1626.
204. Acosta D, Affolder T, Ahn MH, Akimoto T, Albrow MG, Ambrose D, Amerio S, Amidei D, Anastassov A, Anikeev K *et al*: **Observation of the narrow state X(3872)-->J/psipi+pi- in pp collisions at square root of s=1.96 TeV.** *Phys Rev Lett* 2004, **93**(7):072001.
205. Goodman TT, Olive PL, Pun SH: **Increased nanoparticle penetration in collagenase-treated multicellular spheroids.** *Int J Nanomedicine* 2007, **2**(2):265-274.
206. Ghosh SS, Takahashi M, Thummala NR, Parashar B, Chowdhury NR, Chowdhury JR: **Liver-directed gene therapy: promises, problems and prospects at the turn of the century.** *J Hepatol* 2000, **32**(1 Suppl):238-252.
207. Jin X, Yang YD, Li YM: **Gene therapy: regulations, ethics and its practicalities in liver disease.** *World J Gastroenterol* 2008, **14**(15):2303-2307.
208. Anderson WF: **Human gene therapy.** *Nature* 1998, **392**(6679 Suppl):25-30.
209. Xia H, Mao Q, Paulson HL, Davidson BL: **siRNA-mediated gene silencing in vitro and in vivo.** *Nat Biotechnol* 2002, **20**(10):1006-1010.
210. Ocker M, Neureiter D, Lueders M, Zopf S, Ganslmayer M, Hahn EG, Herold C, Schuppan D: **Variants of bcl-2 specific siRNA for silencing antiapoptotic bcl-2 in pancreatic cancer.** *Gut* 2005, **54**(9):1298-1308.
211. Landen CN, Jr., Chavez-Reyes A, Bucana C, Schmandt R, Deavers MT, Lopez-Berestein G, Sood AK: **Therapeutic EphA2 gene targeting in vivo using neutral liposomal small interfering RNA delivery.** *Cancer Res* 2005, **65**(15):6910-6918.
212. Peer D, Lieberman J: **Special delivery: targeted therapy with small RNAs.** *Gene Ther* 2011, **18**(12):1127-1133.
213. Li S, Ma Z: **Nonviral gene therapy.** *Curr Gene Ther* 2001, **1**(2):201-226.
214. Heyes J, Palmer L, Bremner K, MacLachlan I: **Cationic lipid saturation influences intracellular delivery of encapsulated nucleic acids.** *J Control Release* 2005, **107**(2):276-287.
215. Lievens J, Snoeys J, Vekemans K, Van Linthout S, de Zanger R, Collen D, Wisse E, De Geest B: **The size of sinusoidal fenestrae is a critical determinant of hepatocyte transduction after adenoviral gene transfer.** *Gene Ther* 2004, **11**(20):1523-1531.
216. Wisse E, Jacobs F, Topal B, Frederik P, De Geest B: **The size of endothelial fenestrae in human liver sinusoids: implications for hepatocyte-directed gene transfer.** *Gene Ther* 2008, **15**(17):1193-1199.

217. Akinc A, Querbes W, De S, Qin J, Frank-Kamenetsky M, Jayaprakash KN, Jayaraman M, Rajeev KG, Cantley WL, Dorkin JR *et al*: **Targeted delivery of RNAi therapeutics with endogenous and exogenous ligand-based mechanisms.** *Mol Ther*, **18**(7):1357-1364.
218. Jopling CL, Schutz S, Sarnow P: **Position-dependent function for a tandem microRNA miR-122-binding site located in the hepatitis C virus RNA genome.** *Cell host & microbe* 2008, **4**(1):77-85.
219. Jopling CL, Yi M, Lancaster AM, Lemon SM, Sarnow P: **Modulation of hepatitis C virus RNA abundance by a liver-specific MicroRNA.** *Science* 2005, **309**(5740):1577-1581.
220. Dorner M, Horwitz JA, Robbins JB, Barry WT, Feng Q, Mu K, Jones CT, Schoggins JW, Catanese MT, Burton DR *et al*: **A genetically humanized mouse model for hepatitis C virus infection.** *Nature* 2011, **474**(7350):208-211.
221. Burns DM, D'Ambrogio A, Nottrott S, Richter JD: **CPEB and two poly(A) polymerases control miR-122 stability and p53 mRNA translation.** *Nature* 2011, **473**(7345):105-108.